

Workshop summary

Anzivino, G.; Cuendis, Sergio Arguedas; Bernard, V.; Bijnens, J.; Bloch-Devaux, B.; Bordone, M.; Brizioli, F.; Brod, J.; Camalich, J. M.; Ceccucci, A.; Cenci, P.; Christ, N. H.; Colangelo, G.; Cornella, C.; Crivellin, A.; D'Ambrosio, G.; Deppisch, F. F.; Dery, A.; Dettori, F.; Di Carlo, M.

DOI:

[10.1140/epjc/s10052-024-12565-4](https://doi.org/10.1140/epjc/s10052-024-12565-4)

License:

Creative Commons: Attribution (CC BY)

Document Version

Publisher's PDF, also known as Version of record

Citation for published version (Harvard):

Anzivino, G, Cuendis, SA, Bernard, V, Bijnens, J, Bloch-Devaux, B, Bordone, M, Brizioli, F, Brod, J, Camalich, JM, Ceccucci, A, Cenci, P, Christ, NH, Colangelo, G, Cornella, C, Crivellin, A, D'Ambrosio, G, Deppisch, FF, Dery, A, Dettori, F, Di Carlo, M, Döbrich, B, Engelfried, J, Fantechi, R, González-Alonso, M, Gorbahn, M, Goudzovski, E, Grossman, Y, Hermansson-Truedsson, N, Hives, Z, Hoferichter, M, Hoid, B-L, Husek, T, Isidori, G, Jüttner, A, Kampf, K, Kholodenko, S, Knecht, M, Kolesár, M, Koval, M, Lazzeroni, C, Ligeti, Z, Mahmoudi, F, Marchevski, R, Santos, DM, Massri, K, Mombächer, T, Nanjo, H, Neshatpour, S, Nomura, T, Passemar, E, Peruzzo, L, Piccini, M, Pich, A, Sachrajda, CT, Schacht, S, Shiomi, K, Stangl, P, Stoffer, P, Swallow, J, Tsang, JT, Valencia, G, Wanke, R & Zupan, J 2024, 'Workshop summary: Kaons@CERN 2023', *The European Physical Journal C*, vol. 84, no. 4, 377. <https://doi.org/10.1140/epjc/s10052-024-12565-4>

[Link to publication on Research at Birmingham portal](#)

General rights

Unless a licence is specified above, all rights (including copyright and moral rights) in this document are retained by the authors and/or the copyright holders. The express permission of the copyright holder must be obtained for any use of this material other than for purposes permitted by law.

- Users may freely distribute the URL that is used to identify this publication.
- Users may download and/or print one copy of the publication from the University of Birmingham research portal for the purpose of private study or non-commercial research.
- User may use extracts from the document in line with the concept of 'fair dealing' under the Copyright, Designs and Patents Act 1988 (?)
- Users may not further distribute the material nor use it for the purposes of commercial gain.

Where a licence is displayed above, please note the terms and conditions of the licence govern your use of this document.

When citing, please reference the published version.


Take down policy

While the University of Birmingham exercises care and attention in making items available there are rare occasions when an item has been uploaded in error or has been deemed to be commercially or otherwise sensitive.

If you believe that this is the case for this document, please contact UBIRA@lists.bham.ac.uk providing details and we will remove access to the work immediately and investigate.



Workshop summary: Kaons@CERN 2023

G. Anzivino^{1,2}, Sergio Arguedas Cuendis³, V. Bernard⁴, J. Bijmans⁵, B. Bloch-Devaux⁶, M. Bordone⁷, F. Brizioli^{2,8}, J. Brod⁹, J. M. Camalich^{10,11}, A. Ceccucci⁸, P. Cenci², N. H. Christ¹², G. Colangelo¹³, C. Cornella¹⁴, A. Crivellin¹⁵, G. D'Ambrosio¹⁶, F. F. Deppisch¹⁷, A. Dery¹⁸, F. Dettori¹⁹, M. Di Carlo⁷, B. Döbrich²⁰, J. Engelfried²¹ , R. Fantechi²², M. González-Alonso²³, M. Gorbahn²⁴, E. Goudzovski²⁵, Y. Grossman¹⁸, N. Hermansson-Truedsson²⁶, Z. Hives²⁷, M. Hoferichter¹³, B.-L. Hoid¹³, T. Husek^{25,27}, G. Isidori¹⁵, A. Jüttner^{7,28,29,a}, K. Kampf²⁷, S. Kholodenko²², M. Knecht³⁰, M. Kolesár²⁷, M. Koval²⁷, C. Lazzeroni²⁵, Z. Ligeti³¹, F. Mahmoudi^{7,32,33}, R. Marchevski³⁴, Diego Martínez Santos^{35,36}, K. Massri^{8,37}, T. Mombächer⁸, H. Nanjo³⁸, S. Neshatpour³², T. Nomura^{39,40}, E. Passemar^{23,41,42,43}, L. Peruzzo⁴⁴, M. Piccini², A. Pich²³, C. T. Sachrajda²⁸, S. Schacht⁴⁵, K. Shiomu^{39,40}, P. Stangl⁷, P. Stoffer^{15,46}, J. Swallow^{8,47}, J. T. Tsang⁷, G. Valencia⁴⁸, R. Wanke⁴⁴, J. Zupan^{9,49,50}

¹ Dipartimento di Fisica e Geologia dell'Università di Perugia, Via A. Pascoli, 06123 Perugia, Italy

² INFN Sezione di Perugia, Via A. Pascoli, 06123 Perugia, Italy

³ Universidad Estatal a Distancia, San José, Costa Rica

⁴ IJCLab, Univ. Paris-Saclay, CNRS/IN2P3, 91405 Orsay, France

⁵ Division of Particle and Nuclear Physics, Department of Physics, Lund University, Box 118, 221 00 Lund, Sweden

⁶ Dipartimento di Fisica dell'Università di Torino, 10125 Turin, Italy

⁷ Theoretical Physics Department, CERN, Geneva, Switzerland

⁸ CERN, European Organization for Nuclear Research, 1211 Geneva 23, Switzerland

⁹ Department of Physics, University of Cincinnati, Cincinnati, OH 45221, USA

¹⁰ Instituto de Astrofísica de Canarias, C/ Vía Láctea, s/n, 38205 La Laguna, Tenerife, Spain

¹¹ Departamento de Astrofísica, Universidad de La Laguna, La Laguna, Tenerife, Spain

¹² Department of Physics, Columbia University, New York, NY 10027, USA

¹³ Albert Einstein Center for Fundamental Physics, Institute for Theoretical Physics, University of Bern, Sidlerstrasse 5, 3012 Bern, Switzerland

¹⁴ PRISMA+ Cluster of Excellence and MITP, Johannes Gutenberg University, Mainz, Germany

¹⁵ Physik-Institut, Universität Zürich, Winterthurerstrasse 190, 8057 Zürich, Switzerland

¹⁶ INFN Sezione di Napoli, Complesso Universitario di Monte S. Angelo, ed. 6 via Cintia, 80126 Naples, Italy

¹⁷ Department of Physics and Astronomy, University College London, London WC1E 6BT, UK

¹⁸ Department of Physics, LEPP, Cornell University, Ithaca, NY 14853, USA

¹⁹ Università degli Studi di Cagliari and INFN Sezione di Cagliari, Cagliari, Italy

²⁰ Max-Planck-Institut für Physik, Boltzmannstrasse 8, 85748 Garching bei München, Germany

²¹ Instituto de Física, Universidad Autónoma de San Luis Potosí, San Luis Potosí 78000, Mexico

²² INFN Sezione di Pisa, Largo B. Pontecorvo 3, 56127 Pisa, Italy

²³ Department of Theoretical Physics, IFIC, University of Valencia-CSIC, 46071 Valencia, Spain

²⁴ Department of Mathematical Sciences, University of Liverpool, Liverpool L69 7ZL, UK

²⁵ School of Physics and Astronomy, University of Birmingham, Edgbaston, Birmingham B15 2TT, UK

²⁶ The Higgs Centre for Theoretical Physics, School of Physics and Astronomy, The University of Edinburgh, Mayfield Rd, Edinburgh EH9 3JZ, UK

²⁷ Institute of Particle and Nuclear Physics, Charles University, Prague, Czech Republic

²⁸ School of Physics and Astronomy, University of Southampton, Southampton SO17 1BJ, UK

²⁹ STAG Research Centre, University of Southampton, Southampton SO17 1BJ, UK

³⁰ Centre de Physique Théorique, CNRS/Aix-Marseille Univ./Univ. de Toulon (UMR7332), CNRS-Luminy Case 907, 13288 Marseille Cedex 9, France

³¹ Lawrence Berkeley National Laboratory, University of California, Berkeley, CA 94720, USA

³² Université de Lyon, Université Claude Bernard Lyon 1, CNRS/IN2P3, Institut de Physique des 2 Infinis de Lyon, UMR 5822, 69622 Villeurbanne, France

³³ Institut Universitaire de France (IUF), Paris, France

³⁴ École Polytechnique Fédérale de Lausanne (EPFL), 1015 Lausanne, Switzerland

³⁵ Axencia Galega de Innovación, Consellería de Economía e Industria, Xunta de Galicia, Santiago de Compostela, A Coruña, Spain

³⁶ Instituto Galego de Física de Altas Enerxías, 15705 Santiago de Compostela, A Coruña, Spain

- ³⁷ Physics Department, Lancaster University, Lancaster LA1 4YW, UK
³⁸ Department of Physics, Osaka University, Toyonaka, Osaka 560-0043, Japan
³⁹ High Energy Accelerator Research Organization (KEK), Institute of Particle and Nuclear Studies, Tsukuba, Ibaraki 305-0801, Japan
⁴⁰ J-PARC Center, Tokai, Ibaraki 319-1195, Japan
⁴¹ Department of Physics, Indiana University, Bloomington, IN 47405, USA
⁴² Center for Exploration of Energy and Matter, Indiana University, Bloomington, IN 47408, USA
⁴³ Theory Center, Thomas Jefferson National Accelerator Facility, Newport News, VA 23606, USA
⁴⁴ Johannes Gutenberg Universität Mainz, 55099 Mainz, Germany
⁴⁵ Department of Physics and Astronomy, University of Manchester, Manchester M13 9PL, UK
⁴⁶ Paul Scherrer Institut, 5232 Villigen PSI, Switzerland
⁴⁷ INFN Laboratori Nazionali di Frascati, 00044 Frascati, Italy
⁴⁸ School of Physics and Astronomy, Monash University, Wellington Road, Clayton, VIC 3800, Australia
⁴⁹ Berkeley Center for Theoretical Physics, University of California, Berkeley, CA 94720, USA
⁵⁰ Theoretical Physics Group, Lawrence Berkeley National Laboratory, Berkeley, CA 94720, USA

Received: 14 November 2023 / Accepted: 15 February 2024

© The Author(s) 2024

Abstract Kaon physics is at a turning point – while the rare-kaon experiments NA62 and KOTO are in full swing, the end of their lifetime is approaching and the future experimental landscape needs to be defined. With HIKE, KOTO-II and LHCb-Phase-II on the table and under scrutiny, it is a very good moment in time to take stock and contemplate about the opportunities these experiments and theoretical developments provide for particle physics in the coming decade and beyond. This paper provides a compact summary of talks and discussions from the Kaons@CERN 2023 workshop, held in September 2023 at CERN.

Contents

1	Introduction
2	Experimental kaon physics
2.1	Dedicated kaon experiments at CERN
2.1.1	The NA62 experiment: present status
2.1.2	HIKE phase 1 and 2: experimental design and physics reach
2.2	Dedicated kaon experiments at J-PARC
2.2.1	The KOTO experiment: present status
2.2.2	KOTO II prospects and plans
2.3	Kaon physics from other experiments: LHCb and its upgrade 2
2.4	Discussion: current and future experiments
	HIKE
	KOTO and KOTO II
	LHCb and its upgrade 2
2.5	Discussion: complementarity between experiments
2.6	Monte Carlo/QED contributions to the simulation and measurements of kaon physics
3	Kaon physics in the Standard Model

3.1	Theory calculations for the gold-plated modes in the SM
3.2	Lattice QCD for non-perturbative contributions in kaon decays
3.2.1	Theory and general methodology
3.2.2	$K \rightarrow \pi \nu \bar{\nu}$ decays
3.2.3	$K_L \rightarrow \pi^0 \mu^+ \mu^-$ decays
3.2.4	$K^+ \rightarrow \pi^+ \ell^+ \ell^-$ decays
3.2.5	$K_{L,S} \rightarrow \ell^+ \ell^-$ decays
3.2.6	Lattice QCD+QED
3.3	ChPT, short-distance constraints, and large N_c	..
3.4	ChPT and dispersion relations
3.5	Kaon experiments as π^0 factories: a theory point of view
3.6	The time dependent rate $K(t) \rightarrow \mu \mu$
3.7	Discussion: SM predictions – continuum
4	Kaon physics beyond the Standard Model
4.1	The BSM potential of rare kaon decays
4.2	Exotica from kaon decays: theory and experiment
4.2.1	Theory overview
4.2.2	Principal experimental signatures
4.3	Discussion: (B)SM constraints from kaon physics
4.4	Discussion: complementarity of B - and K -decays
5	Outlook and conclusions
	References

1 Introduction

The NA62 experiment at CERN and KOTO at J-PARC Japan are the only two experiments worldwide fully dedicated to the study of rare kaon decays. NA62 is planned to conclude its efforts in 2025, and both experiments are aiming to meet important milestones on that time scale. The future experimental landscape for kaon physics beyond this date has not taken shape yet, but there is a strong and engaged community

^ae-mail: Andreas.Juttner@cern.ch (corresponding author)

committed to continuing these investigations in the coming years. Proposals for next-generation experimental facilities HIKE [1] at CERN and KOTO-II [2] at J-PARC are on the table and under scrutiny. With this background, the aim of this workshop was to bring together theoretical and experimental kaon physicists to reflect on the present situation, future challenges and the main goals of the community.

Kaons, the mesons containing one strange and either a lighter up or down quark, have historically played a central role in developing and establishing the Standard Model (SM) of elementary particle physics. Many of the SM's salient features were discovered through the study of kaons. For example, parity violation was hinted at in kaon decays [3], kaons were central to the development of the Cabibbo theory of flavour [4], and the absence of flavour-changing neutral currents (FCNCs) at tree level led to the postulation of a fourth (the charm) quark [5]. CP violation, one of the three necessary ingredients to justify the baryon asymmetry of the Universe, was discovered in its direct and indirect incarnations in kaon decays [6–8]. It was incorporated in the “new” SM by Kobayashi and Maskawa [9] by introducing a third generation of quarks before its experimental discovery [10]. The Cabibbo–Kobayashi–Maskawa (CKM) quark-mixing matrix describes all quark decays and is the subject of a major particle physics experimental programme.

The full particle content of the SM was later experimentally established at CERN with the Higgs discovery [11, 12] in 2012. Since then, the outlook for particle physics has changed considerably. While the observed baryon asymmetry, the question about the origin of neutrino masses and the patterns of quark and lepton masses and mixings, or the presence of dark matter in the universe, are still lacking a microscopic and confirmed understanding within or beyond the SM (BSM), clear indications of the direction of journey, like hitherto the Higgs particle, are also currently lacking.

Kaon physics plays a very special role in this context. The study of rare kaon decays provides a unique sensitivity to New Physics (NP), than reached by collider experiments. In the SM, the rare decay of a charged or neutral kaon into a pion plus a pair of charged or neutral leptons is hugely suppressed. This is due to the absence of tree-level FCNC interactions (e.g., $s \rightarrow d$) in the SM. Such a transition can only proceed at loop level involving the creation of at least one very heavy (virtual) electroweak (EW) gauge boson. Two ingredients lead to a massive suppression of the decay rate: the Glashow–Iliopoulos–Maiani (GIM) mechanism, which leads to a suppression of the transition by the heavy-mass scale of the gauge bosons, and the smallness of the involved combination of CKM-matrix elements. Both make rare kaon decays even more suppressed than the rare B -meson decays currently studied at LHCb and Belle-II.

While this suppression constitutes a formidable experimental challenge in identifying the decay products amongst

a variety of background signals, NP, with mass scales much heavier than the EW scale, could leave a significantly measurable imprint through tree-level or loop contributions. Despite these challenges, nature has been kind to us: rare kaon decays are one of the theoretically cleanest places to search for the effects of NP – one could even say that they constitute a standard candle of the SM. This is on the one hand due to the limited number of possible decay channels of kaons and pions and, as a result, the relatively clean experimental environment. More importantly, and very much in contrast to rare B -meson decays, there are “gold-plated” rare decay modes amongst the rare-kaon decays, which are purely short-distance dominated and therefore allow for very precise theory predictions. These are the rare decays of charged and neutral kaons into pions and a pair of neutrinos, $K^+ \rightarrow \pi^+ \nu \bar{\nu}$ and $K_L \rightarrow \pi^0 \nu \bar{\nu}$.

The charged-kaon decay is currently being studied at the NA62 experiment at CERN, and a measurement of its branching ratio with a precision of 15% is expected by 2025. However, to substantially improve this measurement, thereby substantially increasing the likelihood of a discovery, the experimental precision will need to be reduced further to the level of the theory prediction, i.e., 5%. This can only be achieved with a next-generation experiment. The HIKE experiment, a future high-intensity kaon factory at CERN currently under approval, will reach the 5% precision goal on the measurement of K^+ during its first phase of operation. Afterwards, a second phase with a neutral K_L beam aiming at the first observation of the very rare decays $K_L \rightarrow \pi^0 \ell^+ \ell^-$ is foreseen. KOTO-II, a planned but not yet funded evolution of KOTO, aims to measure the branching ratio of $K_L \rightarrow \pi^0 \nu \bar{\nu}$ with a precision of 25%.

With the setup and detectors optimised for the measurement of the most challenging rare-decay processes, HIKE phase 1 and 2 as well as KOTO-II will be able to reach unprecedented precision on many other K^+ and K_L decays as well, many of which are also extremely interesting in view of the possibility to provide a window on NP contributions. The LHCb experiment will also contribute to kaon physics, especially with studies of K_S decays. What makes them now less appealing than the golden modes, is the fact that long-distance effects are more relevant or in some cases even dominating, so that NP effects may be hidden behind poorly understood hadronic effects. But significant progress is happening on that front too. For instance, the communities working on lattice QCD, effective field theory and dispersive approaches have, over the last decades, continued sharpening their tools motivated in part by the wealth of experimental information on kaon decays, which calls for a deep and precise theoretical understanding of the hadronic contributions. The prospects for further improving our control over non-perturbative effects on the same time scale as the planned

new experiments are very good, as presentations and discussions during the workshop have made clear.

This workshop summary aims to present a concise overview of the current status of experimental and theoretical kaon physics, to discuss opportunities and expectations for future developments and improvements in precision and to provide entry points into the vast literature on the subject, and is structured as follows. Section 2 is dedicated to experimental aspects and provides an overview of current experiments and of planned future ones. Section 3 summarises the current situation and prospects for improvement of our understanding of kaon decays within the SM. It briefly touches upon the remarkably broad spectrum of quantum field theory tools which have been developed and have to be used in connection with kaon decays. Section 4 is dedicated to a discussion of the huge potential of rare kaon decays for the discovery of NP, in light of the current situation and the future prospects of indirect searches at B factories and direct searches at the energy frontier. The complementarity with these searches provides a strong motivation for carrying out this programme. In Sect. 5, general conclusions and an outlook are provided.

2 Experimental kaon physics

The three major experiments performing kaon physics are: the NA62 fixed-target decay-in-flight experiment at the CERN north area working with a K^+ beam, the KOTO experiment at the J-PARC Hadron Experimental Facility (HEF) working with a K_L beam, and the LHCb experiment at the Large Hadron Collider at CERN with particular sensitivity to K_S and hyperons.

At the CERN north area the HIKE programme is proposed to continue fixed-target decay-in-flight experiments, with much increased beam intensity and a new detector setup, with both K^+ and then K_L beams in a multi-phase project.

At J-PARC, KOTO-II, the evolution of KOTO, is being discussed as a part of the HEF extension project, to reach the sensitivity required to detect tens of $K_L \rightarrow \pi^0 \nu \bar{\nu}$ decays.

The LHCb experiment has already undergone a major upgrade, which includes a paradigm shift to using a software trigger. This is crucial for the K_S and hyperon programme since previously hardware triggers, not designed for kaon studies, were highly inefficient, while now software triggers can be developed to fully exploit the high luminosity available.

2.1 Dedicated kaon experiments at CERN

2.1.1 The NA62 experiment: present status

The main aim of the NA62 experiment is the precise measurement of the ultra-rare decay $K^+ \rightarrow \pi^+ \nu \bar{\nu}$ using a decay-in-

flight technique. NA62 exploits the CERN SPS 400 GeV/c primary proton beam, that impinges on a beryllium target and produces a 75 GeV/c secondary beam made of positively charged particles of which approximately 6% are K^+ . The experimental signature of a $K^+ \rightarrow \pi^+ \nu \bar{\nu}$ decay is an incoming K^+ and an outgoing π^+ with missing energy in the final state. The signal is kinematically discriminated from other kaon decays using the squared missing mass $m_{\text{miss}} = (p_K - p_\pi)^2$ variable, where p_K and p_π are the 4-momenta of the kaon and of the downstream charged particle respectively, in the pion mass hypothesis.

The experiment has taken data in 2016–2018 (Run 1) [13]. NA62 recorded about 3×10^{18} protons on target in Run 1, and at least twice this value is expected in Run 2. The analysis of Run 1 data led to the observation of 20 $K^+ \rightarrow \pi^+ \nu \bar{\nu}$ signal candidates (with about 10 SM signal and $7.03_{-0.85}^{+1.05}$ background events expected). The measured branching ratio $\mathcal{B}(K^+ \rightarrow \pi^+ \nu \bar{\nu}) = (10.6_{-3.4}^{+4.0})_{\text{stat}} \pm 0.9_{\text{syst}} \times 10^{-11}$ is compatible with the SM prediction within one standard deviation, and corresponds to an observational significance of 3.4σ [14]. This is the most precise measurement of the $K^+ \rightarrow \pi^+ \nu \bar{\nu}$ branching ratio to date and provides the strongest evidence so far for the existence of this extremely rare process.

Data taking has resumed with Run 2 in 2021, and is approved until long shutdown 3 (LS3). Several detector upgrades have been implemented during LS2. A first preliminary analysis of the data collected in 2022 exhibits a sensitivity similar to that of the whole Run 1. A measurement of $\mathcal{B}(K^+ \rightarrow \pi^+ \nu \bar{\nu})$ with a precision of 15% is achievable by LS3, assuming a beam delivery similar to that of 2022 in the upcoming years [15].

2.1.2 HIKE phase 1 and 2: experimental design and physics reach

HIKE is a world-leading comprehensive programme of kaon-decay experiments, which follows a staged approach and includes several phases [1]. The programme focuses on several ultra-rare “golden” kaon-decay modes, which are very clean from the theory point of view (providing unique closure tests of the CKM paradigm), and are exceptionally difficult to measure. The primary goal of Phase 1 is a measurement of the $K^+ \rightarrow \pi^+ \nu \bar{\nu}$ branching ratio to a 5% precision (matching the precision of the SM calculation), while the main goal of Phase 2 is the first observation of the $K_L \rightarrow \pi^0 \ell^+ \ell^-$ decays with a significance above 5σ . The experimental layout for both phases is shown in Fig. 1. HIKE will use K^+ and K_L beams of record intensity, and will therefore collect the world’s largest samples of K^+ and K_L decays using a flexible software trigger and detectors with higher performance than those of NA62 and other previous experiments. As a result, HIKE will significantly improve the precision of measure-

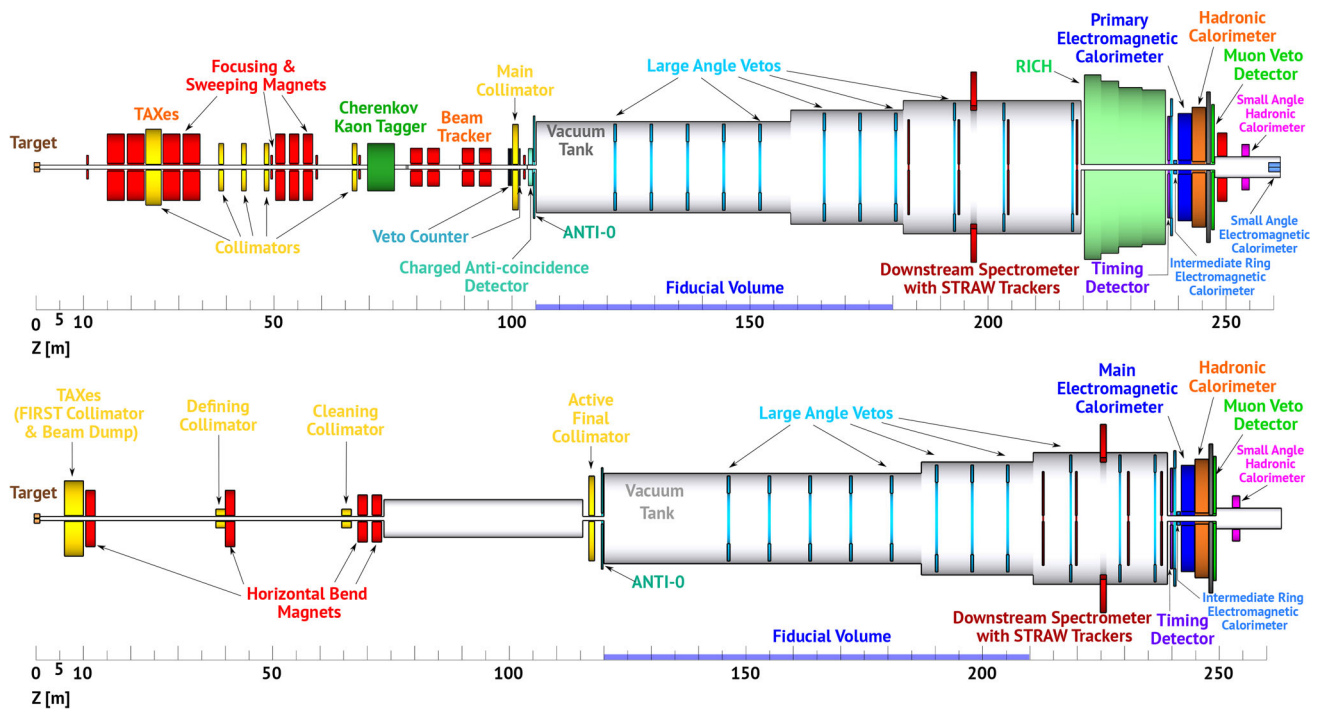


Fig. 1 HIKE phase 1 (top) and phase 2 (bottom) layouts, with an aspect ratio of 1:10

ments over a wide range of kaon decay channels, providing unique results of long-lasting scientific value. Table 1 lists a selection of the many unique measurements that HIKE can perform. The challenges to be addressed in the HIKE detectors are in synergy with or go beyond to current efforts for LHC-experiment upgrades after Long Shutdown 4, and will help in making a significant step towards the needs for FCC detectors. Further in the future, a third phase would address $K_L \rightarrow \pi^0 \nu \bar{\nu}$.

The primary objective for the first phase of HIKE will be measuring the branching ratio of $K^+ \rightarrow \pi^+ \nu \bar{\nu}$ with about 5% precision, improving by a factor of approximately 3 on the NA62 projected precision of about 15% when using the full NA62 dataset. The statistics required to reach the HIKE Phase 1 goal, which corresponds to about 9 times the NA62 one, will be collected in about 4 years thanks to an increase of a factor 4 in the beam intensity and an increase in the signal acceptance of a factor > 2 thanks to new, more granular/performant detectors. To be able to stand the intensity increase, the timing for all the detectors needs to be improved by at least a factor 4 (see Fig. 2). Despite the higher rate, other key performances such as kinematic rejection, photon rejection, and particle identification efficiency must at least be kept equal to the NA62 ones to maintain background rejection under control. In addition to the precise measurement of its branching ratio, the increased statistics will allow investigating the nature of the $K^+ \rightarrow \pi^+ \nu \bar{\nu}$ decay, i.e., vector

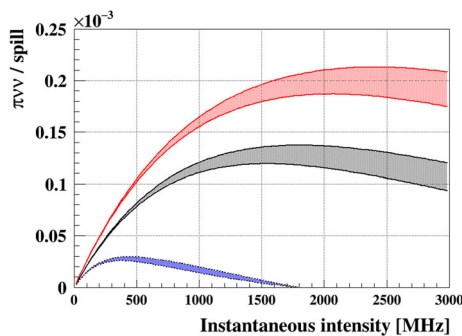
(SM) vs. scalar or tensor (BSM) contributions, that implies testing the fundamental nature of neutrinos.

HIKE precision measurements of other K^+ rare decays will allow studies of the kinematic distributions and form factors with unprecedented precision. For $K^+ \rightarrow \pi^+ \ell^+ \ell^-$ decays at least 5×10^5 events in both the $\ell = \mu$ and $\ell = e$ channels will be collected allowing lepton-flavour-universality tests from total rates, and form factor and angular observables measurements (such as those in the equivalent B -physics channel, with a complementary physics reach). For $K^+ \rightarrow \pi^+ \gamma \gamma$ a branching-ratio precision of a few per-mille will be achieved, to match a similar theory expected precision. In addition, precision studies of chiral perturbation theory (ChPT) predictions can be performed investigating the details of the $\gamma \gamma$ spectrum, including the near-the-cusp effect, to extract low-energy constants (LECs) (cf. Sects. 3.3 and 3.4).

HIKE Phase 2 will use a K_L beam and will allow a general-purpose investigation of K_L decays, especially those with charged particles in the final state - exploiting precision tracking and particle identification systems, which will mostly be maintained from HIKE Phase 1. The primary goal of HIKE Phase 2 will be $K_L \rightarrow \pi^0 \ell^+ \ell^-$, with $l = e, \mu$. The study of $K_L \rightarrow \pi^0 e^+ e^-, \pi^0 \mu^+ \mu^-$ will allow their observation for the first time, and then their measurement with at least 20% precision. This decay gives unique access to short-distance BSM effects in the photon coupling via the tau loop [16], as

Table 1 Summary of HIKE sensitivity for flavour observables. The K^+ decay measurements will be made in phase 1, and the K_L decay measurements in phase 2. The symbol \mathcal{B} denotes the decay branching ratios

$K^+ \rightarrow \pi^+ \nu \bar{\nu}$	$\sigma_{\mathcal{B}}/\mathcal{B} \sim 5\%$	BSM physics, LFUV
$K^+ \rightarrow \pi^+ \ell^+ \ell^-$	Sub-% precision on form-factors	LFUV
$K^+ \rightarrow \pi^- \ell^+ \ell^+, K^+ \rightarrow \pi \mu e$	Sensitivity $\mathcal{O}(10^{-13})$	LFV / LNV
Semileptonic K^+ decays	$\sigma_{\mathcal{B}}/\mathcal{B} \sim 0.1\%$	V_{us} , CKM unitarity
$R_K = \mathcal{B}(K^+ \rightarrow e^+ \nu)/\mathcal{B}(K^+ \rightarrow \mu^+ \nu)$	$\sigma(R_K)/R_K \sim \mathcal{O}(0.1\%)$	LFUV
Ancillary K^+ decays (e.g. $K^+ \rightarrow \pi^+ \gamma \gamma, K^+ \rightarrow \pi^+ \pi^0 e^+ e^-$)	% – % _o	Chiral parameters (LECs)
$K_L \rightarrow \pi^0 \ell^+ \ell^-$	$\sigma_{\mathcal{B}}/\mathcal{B} < 20\%$	$\text{Im}\lambda_t$ to 20% precision, BSM physics, LFUV
$K_L \rightarrow \mu^+ \mu^-$	$\sigma_{\mathcal{B}}/\mathcal{B} \sim 1\%$	Ancillary for $K \rightarrow \mu\mu$ physics
$K_L \rightarrow \pi^0(\pi^0)\mu^\pm e^\mp$	Sensitivity $\mathcal{O}(10^{-12})$	LFV
Semileptonic K_L decays	$\sigma_{\mathcal{B}}/\mathcal{B} \sim 0.1\%$	V_{us} , CKM unitarity
Ancillary K_L decays (e.g. $K_L \rightarrow \gamma\gamma, K_L \rightarrow \pi^0\gamma\gamma$)	% – % _o	Chiral parameters (LECs), SM $K_L \rightarrow \mu\mu, K_L \rightarrow \pi^0 \ell^+ \ell^-$

**Fig. 2** Numbers of selected $K^+ \rightarrow \pi^+ \nu \bar{\nu}$ events per spill as a function of the instantaneous beam intensity. The blue shaded area shows the number of events from a data-driven model of the NA62 signal yield. The black shaded area represents the same model but with detector time resolutions improved by a factor of 4 with respect to NA62, assuming also a software trigger. The red shaded area represents the final HIKE phase 1 signal yield model with all improvements included. The width of the shaded areas illustrates the uncertainty in the intensity dependence model

well as giving access to the CKM CP-violating parameter η . Many other K_L modes will also be measured, that in general can only be studied at HIKE Phase 2. One notable example is $K_L \rightarrow \mu^+ \mu^-$. Its SM prediction exhibits sizable uncertainties due to long-distance contributions, but theoretical efforts are actively ongoing to improve their determination, both in lattice QCD, see Sect. 3.2.5, and with continuum methods, see Sect. 3.7. In view of these developments, an improved measurement of the branching ratio, as expected at HIKE, is highly motivated, and will enhance the sensitivity to BSM scenarios.

Across HIKE Phases 1 and 2, precision measurements of the most common K^+ and K_L decays can allow new global fits to be performed which will help to clarify the current Cabibbo anomaly tensions. Searches for heavy neutral leptons can also be performed at HIKE, in both phases, reaching 1–2 orders of magnitude better sensitivity than NA62, including searches for dark neutrinos, which will reach the see-saw line. Besides, searches for the $K^+ \rightarrow \ell^+ N$ decay can measure the coupling directly: while the analysis of beam-dump data depends on the assumption of decay couplings and needs benchmarks for its interpretation, the production studies are benchmark independent.

A full investigation of a range of feebly interacting particles (FIPs) will be performed at HIKE, during both standard kaon data-taking and dump-mode operation, where all the benchmarks set by the Physics Beyond Colliders initiative will be investigated [1], with the exception of BC3. The most promising channels for FIPs searches in kaon mode are: $K^+ \rightarrow \pi^+ X$, $K_L \rightarrow \pi^0 X$, $K \rightarrow \pi\pi X$, where X can be a dark scalar (e.g., the BC4 model), an axion-like particle (ALP) (BC9, BC10) or, if it is very light, an axiflavor; $K^+ \rightarrow \ell^+ N$ where $\ell = e, \mu$ and N is a heavy neutral lepton; and $K^+ \rightarrow \pi^+ \pi^0$ followed by $\pi^0 \rightarrow \gamma A'$ where A' is a dark photon (BC1, BC2). In addition studies of $K^+ \rightarrow \pi^+ \gamma \gamma$, with a guaranteed SM physics measurement outcome, can also be used to search for BSM physics, in this case scanning the $m_{\gamma\gamma}$ invariant mass spectrum to search for evidence of an ALP decaying to two photons, $X \rightarrow \gamma\gamma$ (see also the theory contributions in Sect. 4.2).

Further details of the physics case and experimental setup can be found here [1].

2.2 Dedicated kaon experiments at J-PARC

2.2.1 The KOTO experiment: present status

The KOTO experiment at the J-PARC 30 GeV Main Ring is dedicated to the search for the rare decay $K_L^0 \rightarrow \pi^0 \nu \bar{\nu}$. This mode directly breaks CP symmetry and is highly suppressed in the SM. In addition, the theoretical uncertainty of this decay is only a few percent. These features make this decay one of the best probes to search for NP beyond the SM. However, due to experimental difficulties, only an upper limit of 3.0×10^{-9} is set by the KOTO experiment with the 2015 data set [17].

In the analysis of data taken in 2016–2018, three signal candidate events were observed with an expected background of 1.22 ± 0.26 events. The number of observed events was statistically consistent with the background expectation [18]. The main contribution was the charged kaon contamination in the neutral beam and halo $K_L^0 \rightarrow 2\pi^0$ events, where K_L mesons are scattered at the surface of the collimators and enter the decay region with a large angle. Those background events were newly revealed in the analysis. A new charged veto counter called UCV was installed in 2021 to detect charged kaons and develop new analysis methods to reduce the halo $K_L^0 \rightarrow 2\pi^0$ background.

The latest analysis is focused on the 2021 data set, because the UCV reduces K^\pm background (BG) events by a factor of 13 with a 97% signal efficiency. The halo background is also reduced by a factor of 8 with 92% signal efficiency by analysis methods newly implemented. Therefore, the numbers of those BG events are reduced to be less than 0.1. Several other analysis methods were implemented to estimate background events more accurately.

The single event sensitivity (SES) of the 2021 data analysis is 8.7×10^{-10} while the SES of the previous analysis was 7.2×10^{-9} . Table 2 summarises the numbers of the background events expected in the signal box. The largest contribution comes from the upstream π^0 background events, where a π^0 is generated by neutrons in the beam halo region in a detector located at the upstream region. The second largest contribution comes from the $K_L^0 \rightarrow 2\pi^0$ background events. The total number of BG events expected in the signal box is estimated to be $0.255 \pm 0.058^{+0.053}_{-0.068}$. Figure 3 shows the scatter plot of reconstructed P_T vs Z_{vtx} for the 2021 data set: the region inside the red line is the signal region. No candidate event was observed in the signal region. An upper limit is therefore set on the branching ratio of the $K_L^0 \rightarrow \pi^0 \nu \bar{\nu}$ decay to be 2.0×10^{-9} at 90% CL with Poisson statistics. This latest result was presented at the workshop.

KOTO still has 2019–2020 data already collected but not yet finalised in the analysis. Measures to reduce the K^\pm background events are needed for this sample, because only a prototype detector of UCV was present in 2020 and there was

Table 2 Preliminary summary of the numbers of background events in the signal region for the 2021 data

Source	Number of events
Upstream- π^0	$0.064 \pm 0.050 \pm 0.006$
$K_L \rightarrow 2\pi^0$	$0.060 \pm 0.022^{+0.051}_{-0.060}$
K^\pm	$0.043 \pm 0.015^{+0.004}_{-0.030}$
Hadron-cluster	$0.024 \pm 0.004 \pm 0.006$
Halo $K_L \rightarrow 2\gamma$	$0.022 \pm 0.005 \pm 0.004$
Scattered $K_L \rightarrow 2\gamma$	$0.018 \pm 0.007 \pm 0.004$
η production in CV	$0.023 \pm 0.010 \pm 0.006$
Total	$0.255 \pm 0.058^{+0.053}_{-0.068}$

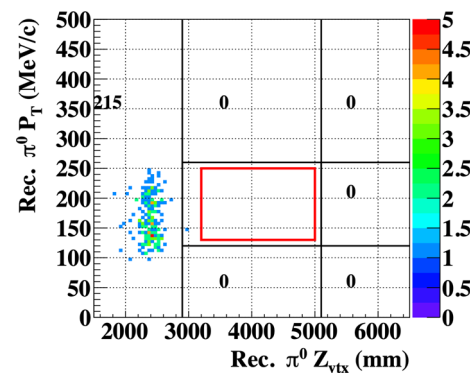


Fig. 3 Scatter plot of reconstructed P_T vs Z_{vtx} for the 2021 data set. The region inside the red line is the signal region

no detector to detect K^\pm in 2019. For the future run, KOTO plans to collect 10 times more protons on target (POT) in 4–5 years to achieve a sensitivity below 10^{-10} .

2.2.2 KOTO II prospects and plans

The KOTO-II experiment, planned at the extended Hadron Experimental Facility of J-PARC, is designed to measure the branching ratio of the decay $K_L \rightarrow \pi^0 \nu \bar{\nu}$ (Fig. 4).

The K_L mesons produced at the T2 target are guided to the KOTO-II detector behind the dump with a 43-m long beamline including two collimators and two magnets. The extraction angle of K_L is 5° with a solid angle of $4.8 \mu\text{sr}$. The K_L production at the target within the same solid angle is 5 times larger in KOTO-II compared to KOTO. The long beamline is designed to reduce short-lived particles; the length of the beamline is 43 m for the KOTO II, and 20 m for the KOTO. The two magnets sweep charged particles out, and the two collimators are designed to suppress beam-halo particles. In total, the K_L flux at the entrance of the detector is 2.4 times larger for KOTO II than for KOTO.

The KOTO II detector (Fig. 5) starts at 44 m from the T2 target, which is the origin of the axis system. The z -axis is along the beam axis pointing downstream. The signal decay

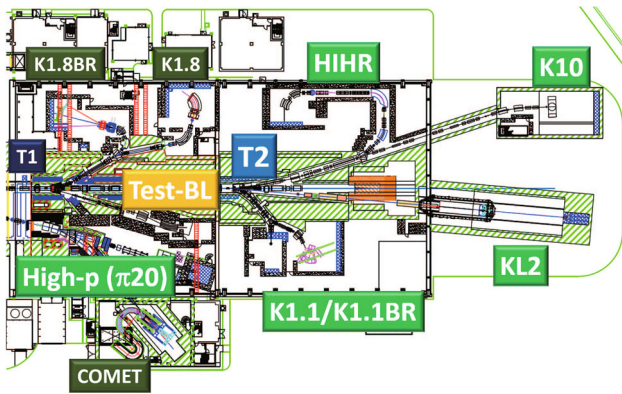


Fig. 4 Layout of the extended Hadron Experimental Facility at J-PARC. The KOTO II detector is behind the dump downstream of the T2 target

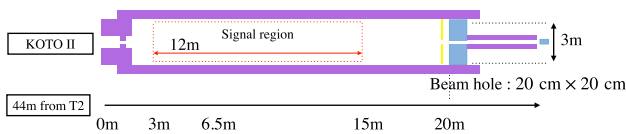


Fig. 5 Conceptual design of the KOTO II detector

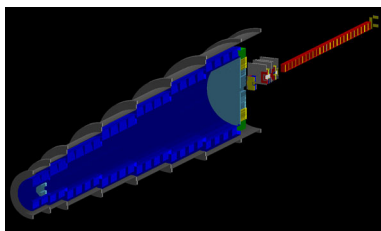


Fig. 6 Cutaway view of realistic KOTO-II detector

region is defined by $3 < z < 15$ m, that is 6 times larger than that in KOTO. An electromagnetic calorimeter is 3 m in diameter (1.5 times larger than in KOTO) and located at $z = 20$ m. Veto counters surround the decay region hermetically. Two photons from the π^0 in the signal $K_L \rightarrow \pi^0 \nu \bar{\nu}$ process are detected with the calorimeter. The decay vertex of the π^0 is reconstructed on the z -axis assuming the invariant mass of the two photons to be the nominal π^0 mass. The transverse momentum of the π^0 (p_T) is reconstructed using the vertex position. Events are vetoed if extra particles are detected other than the two photons from the π^0 in the calorimeter.

Including kinematic event selections, the expected number of signal events is 35 if the SM value for the branching ratio is assumed, with a running time of 3×10^7 s with a 100-kW beam incident in the T2 target. The expected number of total background events is 40. Distributions of the signal and background simulated events in the z - p_T plane are shown in Fig. 7. The signal can be observed with 5.6σ significance. The branching ratio can therefore be measured with a statistical error of 25%, resulting in a precision of the CKM

parameter η of 12%. Deviations of the branching ratio by 40% from the SM value would indicate NP at 90% CL.

The design of the KOTO-II detector is progressing towards a realistic geometry, see Fig. 6. Based on the size and the weight from the realistic geometry, and a radiation shielding simulation, the surrounding detector area is under design. Prototyping of a modular barrel detector and of a calorimeter with photon incident angle determination capabilities are ongoing. A shashlyk counter is considered for the outer region of the calorimeter. A low-gain avalanche photodiode detector is being considered for the in-beam charged veto counter. The option of a straw-tube tracker behind the charged veto detector to measure charged tracks is being evaluated. The Collaboration plans to submit a proposal for KOTO II in JFY 2024, in order to realise the KOTO II experiment in the 2030s.

2.3 Kaon physics from other experiments: LHCb and its upgrade 2

The LHCb experiment [19] at the LHC is optimised primarily for the study of decays of the short-lived beauty and charm hadrons. In addition to its primary objectives, LHCb has proven to be suitable to investigate strange physics, despite the very low $\mathcal{O}(100 \text{ MeV}/c)$ transverse momentum (p_T) of the decay products of kaons and hyperons. In the past, the main bottleneck for strange physics at LHCb was the trigger system, which was selecting only events with $p_T > \mathcal{O}(\text{GeV})$ at the hardware level, resulting in a trigger efficiency of $\epsilon_{\text{trig}} \sim 1\%$ in Run 1 (2010–2012). In Run 2 (2015–2018), a significantly modified software trigger enabled an improvement of the trigger efficiency, especially for channels with muons in the final state, by about an order of magnitude $\epsilon_{\text{trig}} \sim 18\%$ with further improvements limited by the hardware trigger system. In Run 3, which started in 2022, the upgraded LHCb detector is equipped with an entirely software-based trigger system which will boost the sensitivity to kaon and hyperon decays with trigger efficiencies close to 100%. The possibility of fully exploiting the data will therefore rely only on the capability of strange hadrons triggers to cope with the allowed rates, which for most of the channels mentioned here should be feasible. The large improvement in trigger efficiency will enable LHCb to fully profit from the large data sets that will become available in the coming years. The data collected so far by LHCb in Run 1 and 2 correspond to 10 fb^{-1} . About 50 fb^{-1} are expected to be collected after LHCb Run 3 and 4 and there is interest in continuing the experiment at high luminosity with a future Upgrade, possibly reaching 300 fb^{-1} [20] after Run 5 and 6. Furthermore, the huge strangeness production cross section at the LHC, two to three orders of magnitude larger than that of heavy flavours, makes strange-hadron physics an increasingly strong research line at LHCb [21], with several results already published and more in the pipeline. LHCb has

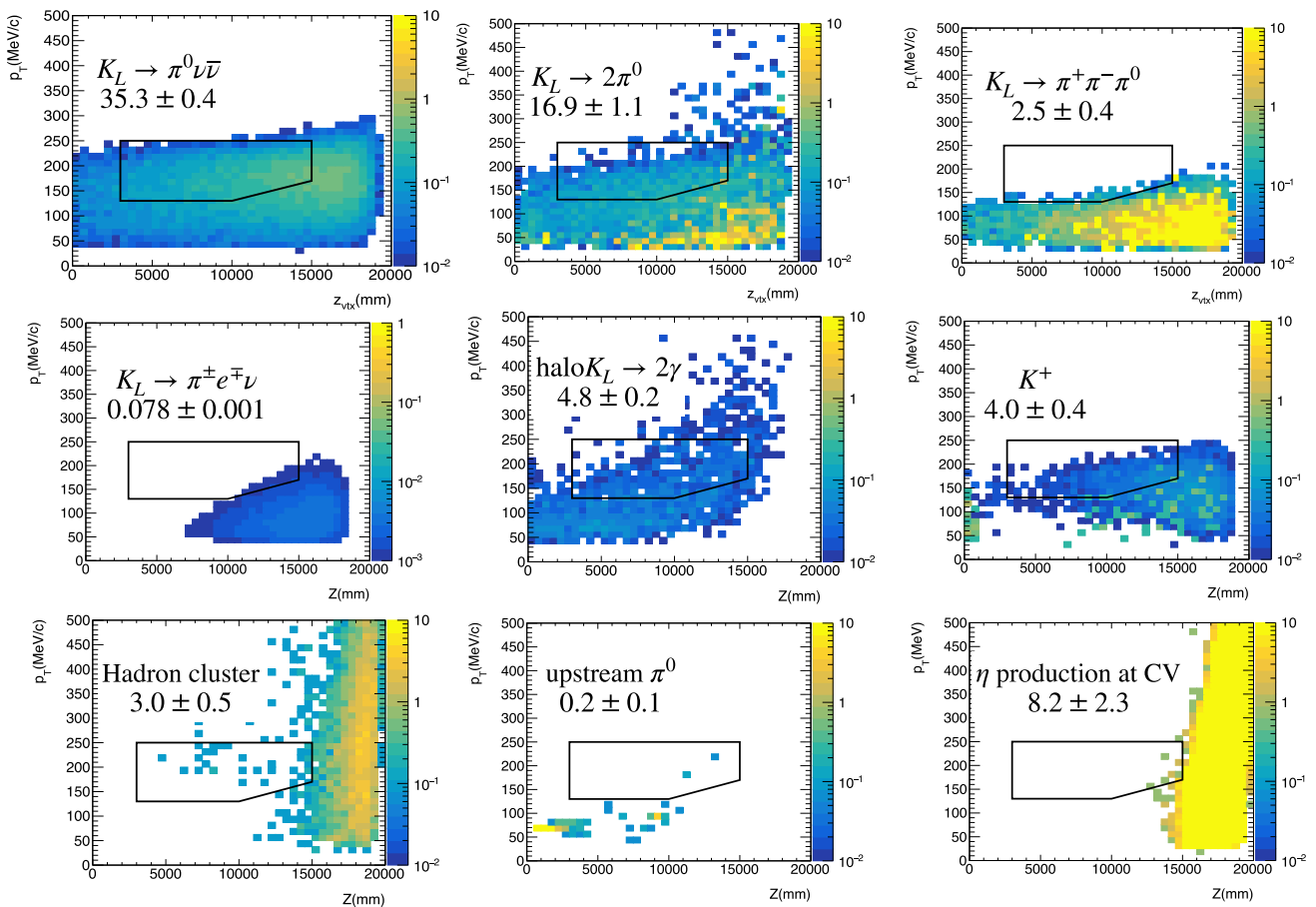


Fig. 7 KOTO-II distributions of the signal and backgrounds in the z - p_T plane (simulation)

published the strongest bound on the branching fraction of $K_S^0 \rightarrow \mu^+ \mu^-$ decays [22], the first 4.1σ evidence for the rare $\Sigma^+ \rightarrow p \mu^+ \mu^-$ decay [23], and the best upper limit on the branching fraction of $K_{S(L)}^0 \rightarrow \mu^+ \mu^- \mu^+ \mu^-$ reaching $\mathcal{O}(10^{-12})$ level for the K_S^0 mode [24].

Detailed sensitivity studies show that improvements of at least an order of magnitude are possible with LHCb Upgrade 2 data [21]. Focusing first on rare decays, the LHCb experiment will be able to constrain the $K_S \rightarrow \mu^+ \mu^-$ branching fraction down to about the SM level of $\sim 5 \times 10^{-12}$. This channel is CP violating and provides access to the CKM parameter η . One of the most interesting decays in the short term will be the $K_S^0 \rightarrow \pi^0 \mu^+ \mu^-$ decay. The form factor a_S , governing the $K_S^0 \rightarrow \pi^0 \mu^+ \mu^-$ process can be extracted from a measurement of the $K_S^0 \rightarrow \pi^0 \mu^+ \mu^-$ branching fraction. A precise measurement of a_S is crucial for the prediction of its long-lived partner $K_L^0 \rightarrow \pi^0 \mu^+ \mu^-$ decay, which is a very sensitive probe of physics beyond the SM. The K_S mode is currently known to only about 50% precision from measurement by the NA48/1 collaboration, $\mathcal{B}_{\text{SM}}(K_S^0 \rightarrow \pi^0 \mu^+ \mu^-) = (2.9^{+1.5}_{-1.2} \pm 0.2) \times 10^{-9}$ [25]. A more precise measurement of this branching fraction will

result in an improved prediction of $K_L^0 \rightarrow \pi^0 \mu^+ \mu^-$ and ultimately in improved BSM constraints that can be derived from it. The sensitivity of LHCb to $K_S^0 \rightarrow \pi^0 \mu^+ \mu^-$ decays has been studied, demonstrating that significant improvements are possible depending on the trigger efficiency already with 10 fb^{-1} of Upgrade data [26]. This puts LHCb in a unique position to provide more information about this decay mode. The analysis of $K_S^0 \rightarrow \pi^0 \mu^+ \mu^-$ decays can also be extended to other decays such as $K_S^0 \rightarrow \gamma \mu^+ \mu^-$, $K_S^0 \rightarrow X \mu^+ \mu^-$, $K_S^0 \rightarrow X \pi \mu$, where X is a scalar or vector particle. The search of lepton-flavour-violating $K_S \rightarrow \mu e$ decays can also be addressed by LHCb providing world-best limits for that mode.

A second group of decays which is gradually becoming more promising is the set of 4-body leptonic decays of the neutral kaon. No experimental constraints are present on the K_S^0 modes except for the recent limit on the $K_S^0 \rightarrow \mu^+ \mu^- \mu^+ \mu^-$ mode provided by LHCb [24]. Even though the rates for these decays are expected to be very low in the SM ($\mathcal{B}(K_S^0 \rightarrow e^+ e^- e^+ e^-) \sim 10^{-10}$, $\mathcal{B}(K_S^0 \rightarrow \mu^+ \mu^- e^+ e^-) \sim 10^{-11}$, $\mathcal{B}(K_S^0 \rightarrow \mu^+ \mu^- \mu^+ \mu^-) \sim 10^{-14}$), any sensitivity approaching the SM rates would be a test of NP, for example

probing dark photons models. The prospects for such decays at LHCb will allow us to scan most of the allowed range in BSM models and get very close to the SM sensitivity if no signal is found.

Semileptonic hyperon decays can also be studied at LHCb. These decays profit from the relatively-high branching fractions, around $\mathcal{B} \sim \mathcal{O}(10^{-4})$, which, coupled with the large strange hyperon production rates at the LHC, results in huge yields at LHCb. More comprehensive studies assessing the prospects for measurements with strange hadrons at LHCb can be found in Ref. [21], using approximate simulations of the LHCb detector. A range of decays have been studied from K_S^0 to hyperons, showing that LHCb will be in a position to give significant contributions to strange-hadron physics in the near future.

2.4 Discussion: current and future experiments

HIKE

The measurement of $\mathcal{B}(K^+ \rightarrow \pi^+ \nu \bar{\nu})$ with a precision matching the core theoretical component of about 5% (cf. Sect. 3.1) is uniquely interesting since it allows access to very high energy scales and can constrain or reveal several BSM models (see Sect. 4). Beyond the branching ratio measurement, the nature of the decay can be established by studying the kinematic distributions of signal candidates. Any BSM (scalar or tensor) contribution would not interfere with the SM contribution and therefore would manifest itself in an additive way. This means the measured kinematic distributions should be a sum of the SM plus BSM contributions. The investigation of the nature of the decay can probe fundamental properties of the SM. For example if the neutrinos are purely left-handed, as predicted by the SM, then the $K^+ \rightarrow \pi^+ \nu \bar{\nu}$ decay should be purely vector in nature, however if there is evidence of a different nature of the decay this indicates the presence of BSM, almost certainly including lepton-number-violating operators (see Sect. 4.3).

Regarding other rare K^+ decays, the measurement of form factors in $K^+ \rightarrow \pi^+ \ell^+ \ell^-$ decays is addressed also by theoreticians, with the foreseen lattice precision on form factors being about 10% (cf. Sect. 3.2) on the timescale of HIKE. The angular distribution analysis of these decays is also of theoretical interest, in relation to the corresponding one in the equivalent B -physics channel. Generally, there is a definite theory interest in the differential studies of decay modes, for example the m_{ee} , $m_{\mu\mu}$ and $m_{\gamma\gamma}$ spectra (the latter from $K^+ \rightarrow \pi^+ \gamma \gamma$) since they, including cusp effects, could give access to BSM including exotica (see Sect. 4.2).

The study of the $K_L \rightarrow \pi^0 \ell^+ \ell^-$ decay is also important since it gives access to short-distance BSM effects in the photon coupling via the tau loop [16] that are not already included in $K \rightarrow \pi \nu \bar{\nu}$, see Sect. 4.1. Besides, the study of

K_L decays will allow HIKE to measure essentially all of the interesting decays. Sensitivity studies will be performed for HIKE Phase 2 for comprehensive set of decays. Similar studies at KOTO II are ongoing to see if some complementary investigations may be performed at J-PARC.

In HIKE, since both kaon and dump modes are foreseen, FIPs can be studied both in production and decay mode and could lead to independent self-contained identification of FIPs (without the need of further experiments). The HIKE programme in particular offers an important opportunity to study FIP signatures since it has precision tracking and PID detectors. In contrast, if a FIP signature were discovered at a dedicated beam dump experiment, in principle a fixed-target experiment with tracking and PID would be needed to characterise it.

Besides, in addition to the most promising channels, very rare decays such as $K^+ \rightarrow \pi^+ \ell^+ \ell^- \gamma$ can be studied at HIKE, with very good possibilities to search for evidence of ALPs, with potentially different couplings. Other relevant channels to look for FIPs are $K_L \rightarrow 2\gamma, 4\gamma, 2e, 4e, \pi\pi ee, \pi\pi\gamma, 2\gamma 2e$ (see Sect. 4.2).

The rare-kaon decays investigated by HIKE offer the possibility to search for BSM physics with a global-fit technique, for example, in the context of lepton flavour universality (LFU) tests [27]. In the SM, the three lepton flavours (e , μ and τ) have exactly the same gauge interactions and are distinguished only through their couplings to the Higgs field and hence the charged lepton masses. BSM models, on the other hand, do not necessarily conform to the lepton-flavour-universality hypothesis and may thereby induce subtle differences between the different generations that cannot be attributed to the different masses. Among the most sensitive probes of these differences are rare kaon decays with electrons, muons or neutrinos in the final state. For BSM scenarios with LFU violating effects, focusing on the case where the NP effects for electrons are different from the those for muons and taus, bounds to Wilson coefficients from individual observables in the kaon sector are shown in Fig. 8 (left). A combined fit of all the decay modes is then performed [27,28]. Projections based on the fits require assumptions for both the possible future measured (central) values as well as the experimental precision. For the latter, the expected long-term experimental precision is considered, while for the central values two scenarios are assumed: projection (A) where predicted central values for observables with only an upper bound available are taken to be the same as the SM prediction while for measured observables the current central values are used; projection (B) where the central values for all of the observables are projected with the best-fit points obtained from the fits with the existing data. The result of a combined fit of all the decay modes [28,29] is shown in Fig. 8 (right). It is evident that the combined measurements foreseen at HIKE, when taken together, have a larger poten-

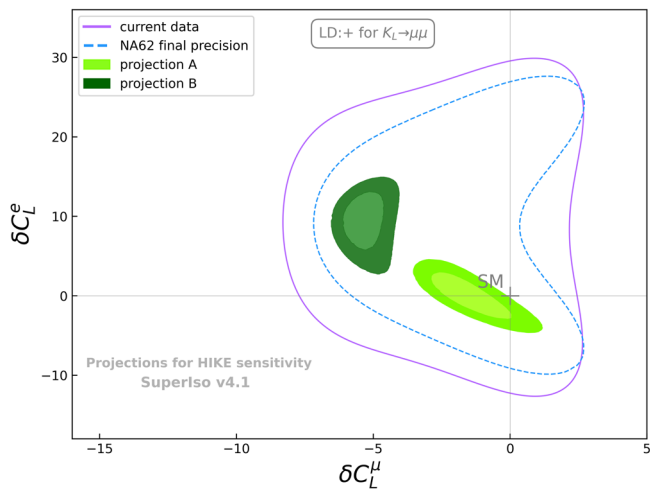
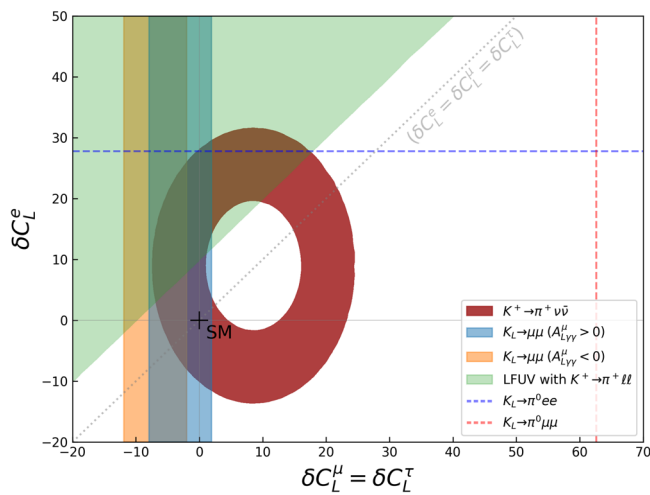


Fig. 8 Bounds on LFU violating new physics contributions to Wilson coefficients from individual observables in the kaon sector (left). See Fig. 7 in Ref. [27] for further information. Global fits in the Wilson coefficients plane with current data (purple contours) and the full projected scenarios (green regions) at the end of HIKE phases 1 and 2

(for one choice of the two possible signs of the LD contributions to $K_L \rightarrow \mu^+ \mu^-$). The blue dotted curve represents the NA62 projection at the end of 2025. For further details of the theory approach, and the full list of inputs, see Refs. [27–29]

tial to show a clear deviation from the SM or to strongly constrain the parameter space available to BSM physics than the single measurements taken in isolation.

KOTO and KOTO II

As mentioned in the KOTO and KOTO II talks, the achievable sensitivities for the $K_L \rightarrow \pi^0 \nu \bar{\nu}$ search will be better than 10^{-10} in KOTO (around $(5-8) \times 10^{-11}$, depending on the running time and the beam power) and 8×10^{-13} with the running time of 3×10^7 s and the beam power of 100 kW in KOTO-II. Although KOTO and KOTO II are designed and optimised for the flagship mode $K_L \rightarrow \pi^0 \nu \bar{\nu}$, the physics programme can be extended to the following channels. It should be noted that the KOTO setup has no tracker and therefore the programme is basically focused on K_L decays into photons. Another feature is the hermetic veto system, which enables one to search for the decay modes including invisible particles.

2 photons + invisible particle(s) A natural extension in KOTO and KOTO II is the $K_L \rightarrow \pi^0 X_{\text{inv}}$ search, where X_{inv} represents any invisible particles. The sensitivity will be almost the same as that of the $K_L \rightarrow \pi^0 \nu \bar{\nu}$ search. Given the reconstruction method and the expected sensitivity, the $K_L \rightarrow \pi^0 X_{\text{inv}}$ search in KOTO II would be limited by the backgrounds coming from $K_L \rightarrow \pi^0 \nu \bar{\nu}$ decays.

4 photons In KOTO, the search for $K_L \rightarrow XX, X \rightarrow \gamma\gamma$ was performed using data taken in 2018 [30]. The upper limit, depending on the X mass (m_X), was set to

be $(1-4) \times 10^{-7}$ for $40 < m_X < 110 \text{ MeV}/c^2$ and $(1-2) \times 10^{-6}$ for $210 < m_X < 240 \text{ MeV}/c^2$ at 90% confidence level.

4 photons + invisible particle(s) A search for $K_L \rightarrow \pi^0 \pi^0 X_{\text{inv}}$ was performed in the KEK E391a experiment, which is the predecessor of KOTO, conducted at the KEK 12 GeV proton synchrotron. The upper limit for the branching ratio of $K_L \rightarrow \pi^0 \pi^0 \nu \bar{\nu}$ was set to be 8.1×10^{-7} at 90% confidence level [31]. The upper limit on $K_L \rightarrow \pi^0 \pi^0 X_{\text{inv}}$ was also set varying from 7.0×10^{-7} to 4.0×10^{-5} for the mass of X ranging from $50 \text{ MeV}/c^2$ to $200 \text{ MeV}/c^2$. In order to improve this limit, a significant reduction of $K_L \rightarrow 3\pi^0$ backgrounds is needed.

6 photons $K_L \rightarrow \pi^0 \pi^0 X, X \rightarrow \gamma\gamma$ corresponds to a peak search in the m_{56} distribution, where m_{56} represents the invariant mass of the photon pair other than $2\pi^0$. Events in the region other than the π^0 mass peak also come from $K_L \rightarrow 3\pi^0$ due to wrong combinations of photons in the event reconstruction. In KEK E391a, the search was done in a particular X mass region, and the upper limit was set to be $(0.2-1) \times 10^{-6}$ at 90% confidence level for $194 < m_X < 219 \text{ MeV}/c^2$ [32]. A feasibility study in KOTO is under way.

3 photons KOTO performed the first search for the $K_L \rightarrow \pi^0 \gamma$ decay, which is forbidden by Lorentz invariance, using data taken in 2016–2018. With a single event sensitivity of 7.1×10^{-8} , the upper limit was set to be 1.7×10^{-7} at 90% confidence level [33]. The number of backgrounds was estimated to be 0.34, dominated by the $K_L \rightarrow 2\pi^0$ contribution, and thus further background reduction is needed to improve the limit.

4 electromagnetic particles

Even though KOTO has neither a tracker nor a spectrometer, there is a possibility that a decay mode whose final state includes only electromagnetic particles can be reconstructed by using the energy and position information measured by the calorimeter. One of the interesting decay modes is $K_L \rightarrow \pi^0 e^+ e^-$. The vertex reconstruction can be done by the same method as used in the $K_L \rightarrow \pi^0 \nu \bar{\nu}$ analysis with an assumption that two photons come from a π^0 decay, four-momentum reconstruction of electron and positrons can be done with the energy and hit position in the calorimeter, and then the invariant mass of two photons and e^+ and e^- can be calculated. KOTO is planning to collect a dataset for a feasibility study. Additional constraints will be needed to reject the $K_L \rightarrow \gamma \gamma e^+ e^-$ background. In KOTO II, a feasibility study to install a straw tracker behind the charged-particle veto detector in front of the calorimeter is under discussion; in this case, the vertex is reconstructed with hits from the straw tracker. The addition of a magnet isn't under consideration at the moment, because of design complications since the bore size of the magnet should be larger than the diameter of the barrel veto in order to avoid dead material in front of the veto detector.

LHCb and its upgrade 2

The LHCb experiment is currently unique in being sensitive to K_S and hyperons [21]. In principle the experiment is sensitive also to K^+ and K_L decays, however their long lifetime reduces their acceptance considerably by three orders of magnitude.

On hyperons, LHCb can probe Σ^+ , Λ , Ξ and Ω decays. LHCb will be able to measure not only the $\Sigma^+ \rightarrow p \mu^+ \mu^-$ integrated and differential branching fraction but also the CP violation asymmetry and the forward backward asymmetry. In a complementary way, the $\Sigma^+ \rightarrow p e^+ e^-$ decay will allow the study of $\Sigma^+ \rightarrow p \gamma$. In addition, all the other $s \rightarrow d \ell \ell$ transitions in the mentioned hyperons will be probed. Besides, $\Delta S = 2$ decays (e.g., $\Xi \rightarrow p \pi$) can be probed and offer sensitivity to models not yet constrained by kaon mixing.

In addition to rare decays, a programme of semileptonic measurements can be performed, starting from $K_S \rightarrow \pi \mu \nu$ and $\Lambda \rightarrow p \mu \nu$, where recent measurements from KLOE and BESIII have significantly improved the precision. Semileptonic hyperon decays can be studied in detail at LHCb and its Upgrades. An improved measurement of these modes will be challenging due to the high levels of contamination from physics backgrounds but will offer high sensitivity to helicity-suppressed NP contributions [34]. Despite the challenges, LHCb is expecting to achieve precision measurements of the branching fraction of $\Lambda \rightarrow p \mu^- \nu_\mu$,

$\Xi^- \rightarrow \Lambda \mu^- \nu_\mu$, and $\Xi^- \rightarrow \Sigma^0 \mu^- \nu_\mu$ decays, as well as to perform sensitive searches for $\Xi^0 \rightarrow \pi^+ \pi^- X$ and $\Xi^0 \rightarrow \mu^+ \mu^- \pi^- X$ decays.

The possibility of studying the interference of the K_S and K_L in dimuon decays seems at the moment out of reach experimentally, but a future dedicated experiment could be thought about.

2.5 Discussion: complementarity between experiments

HIKE and LHCb are complementary, with HIKE studying K^+ and K_L and LHCb being primarily sensitive to K_S and hyperons, and synergic in such that K_S parameters can give input for theory calculations of key K_L decays.

HIKE phase 2 and KOTO II both study K_L decays but with complementary physics goals: the former primarily investigating $K_L \rightarrow \pi^0 \ell^+ \ell^-$ decays using a detector with precise tracking information, and the latter highly optimised to study the $K_L \rightarrow \pi^0 \nu \bar{\nu}$ decay mode. While KOTO II is studying sensitivity to other K_L modes, it is highly likely the specific design of the experiment and the crucial optimisation for the challenging decay $K_L \rightarrow \pi^0 \nu \bar{\nu}$ will make it difficult to reach the precision HIKE Phase 2 can achieve. Nevertheless, in some modes some complementary and competitive measurements may be made to strengthen the cross validation of results in the community. HIKE has a unique advantage for channels with charged particles, in its powerful tracking and PID system which are essential to reach the precision necessary for the observation of $K_L \rightarrow \pi^0 l^+ l^-$ including background suppression. Besides, a possible HIKE Phase 3 for $K_L \rightarrow \pi^0 \nu \bar{\nu}$ in a longer-term future could enhance the complementary to KOTO-II, in the sense that if KOTO-II were to obtain a value in disagreement with the Standard Model HIKE could contribute with further experimental confirmation.

2.6 Monte Carlo/QED contributions to the simulation and measurements of kaon physics

When extracting information on strong or weak interaction dynamics from data, the particle spectra are affected by electromagnetic interactions among the particles involved in the studied process, as well as the real emission of additional photon quanta. These distorted spectra can be corrected by means of the so-called radiative corrections.

The extra photons above the given experimental sensitivity threshold can be simulated in the Monte Carlo (MC), and the effects of the soft photons can be accounted for by using corrections to the spectrum of the non-radiative process. All relevant contributions at the given order should be identified and calculated explicitly since approximate calculations tend to miss delicate cancellations among contributions. The overall size of the QED effects in a given case can

be estimated by integrating over the allowed energy range and emission angles of the additional photon(s), obtaining thus the (one-photon-)inclusive radiative corrections. Needless to say, taking care of the radiative effects (tails) at the MC level leads to a desired agreement between data and MC and stable analyses with respect to the applied cuts.

Although the effect of the QED radiative corrections can seem negligible at first sight, being typically at the intuitive $\sim 1\%$ level in the case of the integral decay width, this is no longer true for invariant-mass spectra or extracted hadronic parameters. By studying one-photon-inclusive corrections to differential decay widths (or, in particular, Dalitz plots), one can easily encounter effects that are $\mathcal{O}(10\%)$. Since the hadronic parameters like form-factor slopes can be comparable in size with the QED effects, corrections $\mathcal{O}(100\%)$ are not rare to occur. The Dalitz decay of the neutral pion ($\pi^0 \rightarrow e^+e^-\gamma$) is a prominent example. One half of the slope of the next-to-leading-order (NLO) QED inclusive radiative corrections (given in terms of the normalized electron–positron invariant mass squared), which gives, in turn, an estimate on the size of the correction to the form-factor slope $a_\pi \simeq M_\pi^2/M_\rho^2 \approx 3\%$, amounts to about twice its size, approximately -6% , and would need to be *subtracted* from the uncorrected measured value [35,36]. One finds corrections of similar size in processes like $\eta \rightarrow e^+e^-\gamma$ [37] or $\Sigma^0 \rightarrow \Lambda e^+e^-$ [38].

Naturally, the above considerations apply also to the kaon sector. With increasing precision in the measurement of $K^+ \rightarrow \pi^+\ell^+\ell^-$ form-factor parameters, lepton-flavour universality can be tested. The QED contribution to the electron channel is expected to be rather large as compared to the muon channel, and ignoring these effects could lead to misinterpretation of the results. Since the difference of the form-factor parameters obtained from respective channels directly relates to the associated LECs [39], the QED part must be subtracted appropriately to obtain correct bounds.

It has been historically proven that similar care should be taken in the case of $K_{\ell 3}$ decays. Particularly, the measurement of $|V_{us}|$ is another example in which the role of radiative corrections has traditionally been very important: These are again $\mathcal{O}(1\%)$ effects and, therefore, comparable in size with the percent precision with which the $K_{\ell 3}$ branching ratios are measured [40]. The unsatisfactory situation regarding the pre-2004 unitarity deficit thus naturally improved once the corrections became available [41–43]. Needless to say, the local significance of radiative effects in certain regions of the $K_{\ell 3}$ Dalitz plots is much greater. And since the consistency of the measurements of form-factor parameters has been historically less than satisfactory, the improper treatment of radiative corrections might have been one of the reasons.

The persisting tension in the $K^+ \rightarrow \pi^0 e^+ \nu \gamma$ ($K_{e3\gamma}$) decay [44] may be also related to the underestimated size of the radiative corrections in the theoretical estimate of

the inclusive ratio $R = \mathcal{B}(K_{e3\gamma(\gamma)}, E_\gamma^* > 30 \text{ MeV}, \theta_{e\gamma}^* > 20^\circ) / \mathcal{B}(K_{e3(\gamma)}) = 0.640(8)\%$ [45–47] since there is no reason to expect that the intuitive $\sim 1\%$ correction would apply for the limited phase space occurring in the numerator, the cuts there being designed to suppress the effects of the dominating inner-bremsstrahlung part. The effects of radiative corrections are expected to be suppressed in the muon mode, which is related to the fact that the structure-dependent part becomes more important compared to the $K_{e3\gamma}$ case [48]. It would be thus interesting to look at the ‘exclusive’ measurement of the $K_{e3\gamma}$ decay or study the $K_{\mu 3\gamma}$ mode. On the experimental side, the MC simulation of the extra photons can be improved by providing the $K_{\ell 3\gamma\gamma}$ generator.

3 Kaon physics in the Standard Model

Rare kaon decays proceed through FCNCs that are suppressed in the SM [5]. They thus offer unique possibilities to discover indirect evidence of degrees of freedom that describe physics beyond the SM, and therefore remain a very active and exciting field of research for both theory and experiment. The neutral- and charged-kaon decay modes $K \rightarrow \pi \nu \bar{\nu}$ stand out among this class of processes, being entirely dominated by the contributions from short-distance scales. This allows for very precise SM predictions as detailed in Sect. 3.1. The situation also looks promising for the class of radiative kaon decays, like $K \rightarrow \gamma^{(*)} \gamma^{(*)}$, $K \rightarrow \pi \gamma^{(*)}$, $K \rightarrow \pi \gamma^{(*)} \gamma^{(*)}, \dots$, where the photon(s) can be either real or virtual, and in which case long-distance hadronic effects represent an important contribution. To predict them in the SM one uses simulations of lattice QCD (Sect. 3.2), ChPT and dispersion theory (Sects. 3.3 and 3.4). A kaon factory naturally also produces a flux of pions and the option of studies of its decay channels is addressed in Sect. 3.5. Strategies for finding observables, e.g., $K_S - K_L$ interferences in the time dependence of the decay probability, that are free from the uncertainties due to hadronic contributions can be devised (cf. Sect. 3.6). Their experimental implementation remains challenging. Section 3.7 summarises some of the reflections made in the discussion session on kaons in the SM, including the interplay between lattice QCD, Sect. 3.2, ChPT, dispersion relations, and short-distance constraints, Sects. 3.3 and 3.4, using as example promising new insights into resolving the long-distance contributions in the rare $K_L \rightarrow \ell^+ \ell^-$ decay.

3.1 Theory calculations for the gold-plated modes in the SM

The rare kaon decays $K^+ \rightarrow \pi^+ \nu \bar{\nu}$ and $K_L \rightarrow \pi^0 \nu \bar{\nu}$ are among the cleanest probes of physics beyond the SM. They

are generated by highly virtual EW box and Z-penguin diagrams that can be calculated to high precision in perturbation theory. The leading decay matrix elements can be extracted from precisely measured semileptonic kaon decays, while GIM suppressed light-quark contributions are tiny and calculable both in ChPT and on the lattice. The leading contribution to the two rare $K \rightarrow \pi \nu \bar{\nu}$ decays is captured by the effective Hamiltonian [49]

$$\mathcal{H}_{\text{eff}} = \frac{4G_F}{\sqrt{2}} \frac{\alpha}{2\pi \sin^2 \theta_w} \sum_{\ell=e,\mu,\tau} (\lambda_c X^\ell + \lambda_t X_t) \times (\bar{s}_L \gamma_\mu d_L)(\bar{\nu}_{\ell L} \gamma^\mu \nu_{\ell L}) + \text{h.c.}, \tag{3.1}$$

where the dependence on the relevant CKM matrix elements appears as the coefficient $\lambda_i = V_{is}^* V_{id}$ in front of the short-distance Wilson coefficients X^ℓ and X_t .

The top-quark contribution X_t is a function of $x_t = m_t(\mu_t)^2/M_W^2$ and has been calculated including two-loop QCD [50,51] and EW [52] corrections. All perturbative corrections to X_t only involve the scale μ_t , where α_s is small. This suggests an excellent convergence of the perturbation series, which is confirmed by the preliminary results of the three-loop calculation [53].

The analytical expressions for X_t , as well as the numerical value of m_t and M_W , depend on the QCD and EW renormalisation schemes. The $\overline{\text{MS}}$ scheme is the natural choice regarding QCD. The numerical value $m_t(m_t) = 162.83(67)$ GeV is obtained from the top-quark pole mass (see Ref. [54] for further details). A numerical value for X_t is obtained by calculating a mean value of the QCD contribution, X_t^{QCD} , by varying $\mu_t \in [60, 320]$ GeV and adding the EW corrections. In total, one finds at NLO in QCD and two-loop EW

$$X_t = 1.462 \pm 0.017_{\text{QCD}} \pm 0.002_{\text{EW}}. \tag{3.2}$$

The theory uncertainty associated with the QCD corrections is given by the difference of the central value and the minimal / maximal value in the μ_t interval. This uncertainty is expected to reduce even further at next-to-next-to-leading order (NNLO) in QCD.

The charm-quark contribution X^ℓ is a function of the neutrino flavour ℓ , while the parameter $P_c = \lambda^{-4}(\frac{2}{3}X^e + \frac{1}{3}X^\tau)$ comprises the charm-quark contribution to $K^+ \rightarrow \pi^+ \nu \bar{\nu}$, which involves a sum over all neutrino flavours. P_c has been calculated at NNLO in QCD [55] and at NLO in the EW interactions [56]. The hard GIM mechanism ensures that it is $x_c = m_c(\mu_c)^2/M_W^2$ suppressed and its numerical value has recently been updated [54] to $P_c = (0.2255/\lambda)^4 \times (0.3604 \pm 0.0087)$. The computation of P_c involves double insertions of charged-current operators that are matched onto the operator of Eq. (3.1). Current conservation ensures that perturbative corrections are absent below the charm scale at this order of the expansion. The effects of dimension-eight operators at the

charm threshold, as well as additional long-distance contributions arising from up- and charm-quarks, have been estimated in Ref. [57], leading to the correction $\delta P_{c,u} = 0.04(2)$. These effects can be computed using lattice QCD in the future, as discussed in Sect. 3.2.2.

The branching ratio of the charged mode is then given by

$$\mathcal{B}(K^+ \rightarrow \pi^+ \nu \bar{\nu}(\gamma)) = \kappa_+(1 + \Delta_{\text{EM}}) \times \left[\left(\frac{\text{Im}\lambda_t}{\lambda^5} X_t \right)^2 + \left(\frac{\text{Re}\lambda_c}{\lambda} (P_c + \delta P_{c,u}) + \frac{\text{Re}\lambda_t}{\lambda^5} X_t \right)^2 \right], \tag{3.3}$$

where the hadronic matrix element is contained in the parameter κ_+ . It is extracted from $K_{\ell 3}$ decay including higher-order chiral corrections [58,59]. The NLO QED corrections [58] are parameterised by $\Delta_{\text{EM}} = -0.003$ in Eq. (3.3).

The remaining parametric input is contained in the CKM factors λ_t and λ_c , defined above. In the numerical evaluation, these parameters are expanded in λ , including the quadratic corrections [54]. The leading order expansion $\text{Im}\lambda_t = A^2 \bar{\eta} \lambda^5$, $\text{Re}\lambda_t = A^2 \lambda^5 (\bar{\rho} - 1)$ and $\text{Re}\lambda_c = -\lambda$ already involves all Wolfenstein parameters. The PDG [40] quotes two different sets of numerical values for these parameters, which are based on the methods of the CKMfitter [60] and UTfit [61] collaboration, respectively. They read

$$\lambda = \begin{cases} 0.22499(67) \\ 0.22500(67) \end{cases} \quad A = \begin{cases} 0.833(11) \\ 0.826^{+0.018}_{-0.015} \end{cases} \quad \bar{\rho} = \begin{cases} 0.159(10) \\ 0.159(10) \end{cases} \\ \bar{\eta} = \begin{cases} 0.348(9) & \text{UTfit} \\ 0.348(10) & \text{CKMfitter.} \end{cases} \tag{3.4}$$

For these CKM parameters the following prediction for the charged mode in the SM are obtained:

$$\mathcal{B}(K^+ \rightarrow \pi^+ \nu \bar{\nu}) = \begin{cases} 8.38(17)(25)(40) \times 10^{-11} & \text{UTfit input} \\ 8.19(17)(25)(53) \times 10^{-11} & \text{CKMfitter input} \end{cases}. \tag{3.5}$$

The errors in parentheses correspond to the remaining short-distance, long-distance, and parametric uncertainties, with all contributions added in quadrature. In more detail, one finds for UTfit CKM input the leading contributions to the uncertainty as

$$10^{11} \times \mathcal{B}(K^+ \rightarrow \pi^+ \nu \bar{\nu}) = 8.38 \pm 0.14_{X_t^{\text{QCD}}} \pm 0.01_{X_t^{\text{EW}}} \pm 0.11_{P_c} \pm 0.25_{\delta P_{c,u}} \pm 0.04_{\kappa_+} \pm 0.14_\lambda \pm 0.31_A \pm 0.12_{\bar{\rho}} \pm 0.03_{\bar{\eta}} \pm 0.05_{m_t} \pm 0.15_{m_c} \pm 0.06_{\alpha_s}, \tag{3.6}$$

where the combined error is 6%. With huge efforts under way on reducing the dominant residual parametric uncertainties, we expect this error to reduce further over the coming years. Theory uncertainties are already smaller and future theoretical calculations will considerably reduce both the short- and

long-distance uncertainties. Here we note the excellent idea to form a ratio of the charged decay mode and ϵ_K [62, 63] that cancels large parts of the parametric uncertainties. This ratio is also theoretically very clean, given recent progress [64–67] in the theory prediction of ϵ_K , and leads to a precision of about 5% for both the charged and neutral kaon decay with consistent central values. The cancellation of CKM uncertainties, in particular for the ratio involving the neutral kaon decay, indicates that $\Delta F = 2$ processes have a crucial impact on the determination of CKM parameters in global fits.

The branching ratio of the neutral mode is computed from

$$\mathcal{B}(K_L \rightarrow \pi^0 \nu \bar{\nu}) = \kappa_L r_{\epsilon_K} \left(\frac{\text{Im}\lambda_t}{\lambda^5} X_t \right)^2, \tag{3.7}$$

and it depends to a good approximation only on the top-quark function X_t discussed above. The hadronic matrix element is again extracted from $K_{\ell 3}$ decay including higher-order chiral corrections [58], while r_{ϵ_K} parameterises the small impact of indirect CP violation [68]. X_t and all remaining parametric input have been discussed above in the context of the charged mode. The SM prediction for the neutral mode then reads

$$\begin{aligned} \mathcal{B}(K_L \rightarrow \pi^0 \nu \bar{\nu}) &= \begin{cases} 2.87(7)(2)(23) \times 10^{-11} & \text{UTfit input} \\ 2.78(6)(2)(29) \times 10^{-11} & \text{CKMfitter input} \end{cases}. \end{aligned} \tag{3.8}$$

Again, the errors in parentheses correspond to the remaining short-distance, long-distance, and parametric uncertainties, with all contributions added in quadrature. In more detail, the leading contributions to the uncertainty for UTfit CKM parameters are

$$\begin{aligned} 10^{11} \times \mathcal{B}(K_L \rightarrow \pi^0 \nu \bar{\nu}) &= 2.87 \pm 0.07_{X_t^{\text{QCD}}} \pm 0.01_{X_t^{\text{EW}}} \pm 0.02_{\kappa_L} \\ &\pm 0.15_{\bar{\eta}} \pm 0.15_A \pm 0.07_{\lambda} \pm 0.03_{m_t}. \end{aligned} \tag{3.9}$$

3.2 Lattice QCD for non-perturbative contributions in kaon decays

As experimental uncertainties decrease, improving the precision of theoretical calculations becomes crucial to perform reliable tests of the SM. Lattice QCD provides a powerful means for non-perturbative, first-principle determinations of several hadronic observables through extensive Monte Carlo simulations.

3.2.1 Theory and general methodology

As the community plans the next generation of studies of rare kaon decays, it may be interesting to reflect on the long timescales required, not only to perform the experiments but also to develop the theoretical methods and carry out the computations. In the history of kaon physics this is nicely

illustrated by $K \rightarrow \pi\pi$ decays, processes in which both indirect and direct CP violation were first discovered. It is only within the last decade that quantitative results for the amplitudes in lattice computations have been obtained [69–72], and in particular for the $\Delta I = 1/2$ rule (after more than half a century) and the direct CP-violation parameter ϵ'/ϵ (after more than two decades). The latest lattice QCD result for the $\Delta I = 1/2$ rule is $\text{Re } A_0/\text{Re } A_2 = 19.9(2.3)(4.4)$, where the values in parentheses give the statistical and systematic errors respectively, to be compared to the experimental value of $\text{Re } A_0/\text{Re } A_2 = 22.45(6)$. As we now understand thanks to the lattice results, the surprisingly large value results from a variety of QCD effects including a suppression of $\text{Re } A_2$ as well as an enhancement of $\text{Re } A_0$ [72]. Here A_0 and A_2 are the decay amplitudes for decays into two-pions with total isospin 0 and 2, respectively. For ϵ'/ϵ the lattice result is $\text{Re}(\epsilon'/\epsilon) = 0.00217(26)(62)(50)_{\text{IB}}$ [72] to be compared to the experimental value of $0.00166(23)$ [40, 73, 74]. For the lattice result the first and second error are again statistical and systematic, respectively, and the error with the subscript IB corresponds to the uncertainty due to isospin-breaking effects which are amplified because of the $\Delta I = 1/2$ rule, for which the central value of the result obtained using ChPT was taken [75]. The emphasis now is on reducing the computational and theoretical uncertainties. We note that the authors of Ref. [76], using the dual QCD approach had also found an enhancement of $\text{Re } A_0$ and the suppression of $\text{Re } A_2$ (see also Ref. [77] for an updated analysis). The dual QCD approach gives a value for ϵ'/ϵ of $0.0005(2)$ [78, 79], below both the experimental result of $0.00166(23)$ and the above lattice result of $0.00217(26)(62)(50)$ [72]. A recently updated estimate, based on analytical techniques for both short- as well as long-distance effects, gives $0.0014(5)$ [80].

In the last decade or so the range of physical quantities and processes for which the non-perturbative hadronic effects can be computed using lattice QCD has been extended very significantly. This includes the possibility of evaluating matrix elements of bi-local operators of the form

$$\int d^4x \langle f | O_1(x) O_2(0) | K \rangle, \tag{3.10}$$

where $O_{1,2}$ are weak or electromagnetic local operators. Applications include the $K_L - K_S$ mass difference $\Delta M_K \equiv M_{K_L} - M_{K_S}$ [81–83], the long-distance contributions to the indirect CP-violating parameter ϵ_K [84, 85], the rare kaon decays $K \rightarrow \pi \ell^+ \ell^-$, where $\ell = e$ or μ [86–89], and the long-distance contribution to the golden mode $K^+ \rightarrow \pi^+ \nu \bar{\nu}$ [90–93]. By “long-distance” we mean a separation between the operators greater than the inverse charm-quark mass and the lattice computations are therefore performed in four-flavour QCD. This allows us to exploit the GIM mechanism where appropriate to reduce, or even avoid, the additional ultraviolet divergences which potentially arise when $x \rightarrow 0$.

In addition, the precision of the perturbative matching calculation relating the matrix element of operators renormalised non-perturbatively to the Wilson coefficients calculated in the $\overline{\text{MS}}$ scheme is improved at larger momentum scales, in this case above m_c .

For $\Delta M_K = 3.483(6)$ MeV and $\epsilon_K = 2.228(11) \times 10^{-3}$ [40], for which O_1 and O_2 are the $\Delta S = 1$ effective weak Hamiltonians, it is likely not possible for lattice QCD computations to reach the experimental precision in the next decade. Nevertheless errors of $\mathcal{O}(5\%)$, or perhaps smaller, can be achieved on ΔM_K and the long-distance contribution to ϵ_K with adequate computing resources (and in the latter case with improved determinations of V_{cb}). At this level of precision, a comparison of the theoretical and experimental results for these very small FCNC quantities will provide significant tests of the SM and constraints on its extensions.

3.2.2 $K \rightarrow \pi \nu \bar{\nu}$ decays

While these decays are short-distance dominated, lattice QCD computations can provide a first principles determination of the long-distance effects in $K^+ \rightarrow \pi^+ \nu \bar{\nu}$ decays with controlled errors. The contribution of these effects to the branching ratio is expected to be $\mathcal{O}(5\%)$ (they are negligible for $K_L \rightarrow \pi^0 \nu \bar{\nu}$ decays). For these decays, one of the operators in Eq. (3.10) is a $\Delta S = 1$ weak operator from the effective Hamiltonian and the other is a $\Delta S = 0$ weak operator corresponding to the emission of either a virtual W -boson or a virtual Z -boson. The theoretical framework has been developed [90] and been implemented in a number of exploratory numerical studies with unphysical quark masses [91–93]. In the latest study [93] it was found that the momentum dependence of the amplitude was very mild, so that it may be sufficient to compute the amplitude at a limited number of kinematic points, and that the contribution from the two-pion intermediate state can be evaluated but is small (less than 1%). The next step is a computation on a $64^3 \times 128$ lattice with near-physical meson masses ($M_\pi = 135.9(3)$ MeV and $M_K = 496.9(7)$ MeV) with a target uncertainty on the long-distance contribution of 30%. Further reductions in the error, towards one of $\mathcal{O}(10\%)$ or less, will require computations at several lattice spacings and are achievable in the next 5–10 years.

3.2.3 $K_L \rightarrow \pi^0 \mu^+ \mu^-$ decays

Measuring this partially CP-violating decay is a target of the second phase of HIKE and making a SM prediction for this process will be possible with current lattice QCD methods in the same time frame. As explained, for example, in Ref. [94] there are three contributions to this decay of approximately equal size: (i) the rare second-order-weak

short-distance process which is the target of these studies, (ii) indirect CP violation proportional to ϵ_K and the amplitude for the $K_S \rightarrow \pi^0 \mu^+ \mu^-$ decay and (iii) the CP-conserving process in which the final state $\mu^+ \mu^-$ pair is produced by two photons. An accurate result for contribution (ii) will be an automatic outcome of the lattice QCD calculations of the amplitude for $K_S \rightarrow \pi^0 \ell^+ \ell^-$ decays, for which the framework enabling lattice computations of the parameters a_S and b_S has been developed [87] and it is expected that they will be evaluated with uncertainties below the 10% level within the next 5–10 years. In particular the sign of a_S will be determined. While not yet thoroughly studied, contribution (iii) should also be calculable in lattice QCD, using the methods being developed for the $K_{L,S} \rightarrow \mu^+ \mu^-$ decays discussed in Sect. 3.2.5, with 10% accuracy – a plausible objective in 5–10 years.

3.2.4 $K^+ \rightarrow \pi^+ \ell^+ \ell^-$ decays

The framework for lattice calculations of the amplitude for $K^+ \rightarrow \pi^+ \ell^+ \ell^-$ decays ($\ell = e, \mu$) has been developed [87] and exploratory numerical studies have been performed [88, 89]. For these decays, one of the operators in Eq. (3.10) is the $\Delta S = 1$ weak Hamiltonian and the other is an electromagnetic current. The emphasis will now be on a reduction of both the statistical and systematic errors with the expectation that the parameters a_+ and b_+ will be determined with uncertainties below the 10% level within the next 5–10 years.

3.2.5 $K_{L,S} \rightarrow \ell^+ \ell^-$ decays

The framework for the computation of the contribution from the two-photon intermediate state to the complex amplitudes of $K_L \rightarrow \mu^+ \mu^-$ and $K_S \rightarrow \mu^+ \mu^-$ decays is being developed [95]. An important first step was a full computation of the complex amplitude of the related decay $\pi^0 \rightarrow e^+ e^-$ [96]. This calculation was performed on 5 gauge ensembles with inverse lattice spacing ranging from 1.015 GeV to 2.36 GeV, so that the continuum limit can be taken, resulting in a result with a precision better than 10% for both the real and imaginary parts of the amplitude. A second step has been the exploratory numerical study of the decay $K_L \rightarrow \gamma \gamma$ with the aim of controlling the subtraction of unphysical exponentially growing terms in the time separation between the weak Hamiltonian and the emission of the first photon [97]. The focus now is on the calculation of $K_L \rightarrow \mu^+ \mu^-$ and a first result for the quark-line connected part of this process was presented in Ref. [98]. A result with 10% accuracy is expected within 5 years. The presence of the $\pi \pi \gamma$ intermediate state introduces a systematic error believed to be below 5% that will require new 3-body methods to remove.

3.2.6 Lattice QCD+QED

Over the past decade, the precision of lattice calculations has advanced to a point where previously neglected subleading effects now demand careful consideration [99]. These effects include the corrections due to electromagnetic interactions and those related to the up and down quark mass difference, which are both expected to be of $\mathcal{O}(1\%)$. The inclusion of such isospin-breaking effects in lattice simulations is conceptually and computationally challenging, mainly due to the difficulty of defining QED in a finite volume with periodic boundary conditions. Many prescriptions have been formulated over the years [100–105] and applied to the calculation of many different observables. The currently observed 3σ tensions with unitarity in the first row of the CKM matrix [40, 99, 106] motivated lattice calculations of isospin-breaking corrections to leptonic decay rates of light mesons, with the aim of determining $|V_{us}|$ and the ratio $|V_{us}/V_{ud}|$ with sub-percent precision. A theoretical framework for lattice QCD+QED calculations of leptonic decay rates has been first developed by the RM123+Soton collaboration in Ref. [107]. This has been successfully applied to the decay rates of pions and kaons into muon-neutrino pairs by the RM123+Soton group [108, 109] and more recently by the RBC/UKQCD collaboration [110], providing results in agreement with each other and with previous ChPT calculations [111]. The results of Ref. [110] highlighted the relevant role of finite-volume effects in this kind of calculations, which scale only as inverse powers of the lattice size and can be potentially sizeable. Work is in progress to tame such systematic uncertainty [112, 113], with the goal of reaching a precision on $|V_{us}/V_{ud}|$ below half percent in the next couple of years. This sets a milestone in precision calculations on the lattice and further progress is expected in the near future. A third lattice calculation is in fact currently ongoing, following an alternative method recently proposed in Ref. [105]. This method differs in the treatment of long-distance QED corrections to the decay amplitudes: as a consequence finite-volume effects are expected to be exponentially suppressed, rather than power-like.

Applications of lattice QCD+QED are not limited to kaon leptonic decays though, but extensions of this framework to processes with hadrons in the final state are currently under study. This new frontier of calculations includes kaon semileptonic decays, $K \rightarrow \pi \ell \nu$, which can provide an independent estimate of $|V_{us}|$, and hadronic kaon decays like $K \rightarrow \pi \pi$, which is crucial for the study of CP violation in the SM. In both cases a new issue arises, which is related to the analytic continuation from Euclidean to Minkowski space-time of those correlation functions where a photon is exchanged between two particles in the final state. A first theoretical study of QED corrections to $K \rightarrow \pi \ell \nu$ on the lattice has been done in Ref. [114], and more recently in

Ref. [105]. Given the current interest in the topic and the impressive recent progress in the field, first lattice results could appear in the next few years. The inclusion of QED corrections in $K \rightarrow \pi \pi$, and hence $\text{Re}(\epsilon'/\epsilon)$, is even more complicated because of the possible mixing of the final-state $\pi \pi$ channels with total isospin 0 and 2. Initial studies on this have been done in Refs. [115–117], marking the start of a challenging research avenue that will extend over the next decade.

3.3 ChPT, short-distance constraints, and large N_c

Besides ab initio calculations provided by numerical simulations of QCD on a discretised space-time (cf. Sect. 3.2), ChPT remains a fundamental tool to study kaon decays in general [94]. In this section, we focus on radiative kaon decays such as $K \rightarrow \gamma^{(*)} \gamma^{(*)}$, $K \rightarrow \pi \gamma^{(*)}$, $K \rightarrow \pi \gamma^{(*)} \gamma^{(*)}$, \dots , where the photon(s) can be either real or virtual. In the latter case it materialises as a lepton–antilepton pair, $\gamma^* \rightarrow \ell^+ \ell^-$, $\ell = e, \mu$. The presence of a real or virtual photon generates a contribution to the decay amplitude from long-distance physics, i.e., from QCD in the non-perturbative regime, which dominates over the short-distance part where NP could potentially hide.

This class of radiative decays displays specific features that makes the interplay with large- N_c arguments and short-distance constraints particularly important. That is, due to electromagnetic gauge invariance, the lowest-order contribution to the amplitude often starts only at NLO in the low-energy expansion [118, 119]. Moreover, the full structure of the amplitude and/or its dependence with respect to the kinematic variables is then only revealed at NNLO. Making predictions for these processes thus requires a theoretical understanding and a numerical evaluation of the corresponding LECs. Unfortunately, this knowledge is lacking at present and this makes predictions difficult.

In the strong sector of ChPT the LECs can be estimated by resonance saturation [120–122], which finds its justification in the 't Hooft large- N_c limit of QCD, $N_c \rightarrow \infty$, $\alpha_s N_c \rightarrow \text{const.}$ [123]. In the weak sector, the limit $N_c \rightarrow \infty$ has been proposed quite some time ago [124] for non-leptonic decays. But a systematic study of the large- N_c limit applied to the case of rare kaon decays has not been undertaken yet. It is important to stress here that the large- N_c limit is not being considered in order to provide an adequate description of the whole amplitude. It would certainly fail to do so, since chiral loops, whose contribution to the decay distribution is clearly visible in the experimental decay distribution in, for instance, $K^\pm \rightarrow \pi^\pm e^+ e^-$, are suppressed in this limit. Rather, it is only meant to be used to get a possible handle on the values of the LECs that contribute to a given amplitude [75, 125–127].

In this respect, there are two main differences between the situation in the strong sector and the one in the weak sec-

tor. First, in the former, the large- N_c limit can be applied to three-flavour QCD, immediately before integrating out also the light quarks and reaching an effective theory where the only surviving degrees of freedom are the light pseudo-scalar states. In the weak sector, the last step before reaching this low-energy description is also provided by three-flavour QCD, but now supplemented by a set of four-fermion operators Q_I modulated by coupling constants C_I , usually called Wilson coefficients. These additional pieces are the low-energy manifestation of the SM degrees of freedom that populate the spectrum from the EW scale down to the hadronic scale around 1 GeV, where only the three lightest quarks remain as active degrees of freedom. The only input that is required from the SM at this ~ 1 GeV scale is therefore the list of four-fermion operators Q_I and the values of the corresponding couplings C_I at this same scale. The second difference is due to the existence, in the weak sector and in the particular case of radiative kaon decays, of short-distance singularities that do not show up in the strong sector. These short-distance singularities arise in QCD correlators involving the time-ordered product of the electromagnetic current with the four-fermion operators Q_I , which are relevant for radiative kaon decays. This time-ordered product is singular at short distances [86, 128], and it is mandatory to understand and correctly address this feature before attempting a determination of the LECs.

This second aspect shows up quite clearly in the large- N_c limit, for instance in the $K \rightarrow \gamma^* \gamma^*$ transition form factor. It manifests itself in the form of a contribution involving a vacuum-polarisation function, which is divergent in QCD. This divergence actually disappears when the two photons are real, so that there is no problem in defining the amplitude for $K \rightarrow \gamma \gamma$ in the usual way, in terms of a kaon-to-two-photon transition form factor. But it is present as soon as at least one of the photons is off-shell, i.e., in the amplitudes for $K \rightarrow \gamma \ell^+ \ell^-$ or for $K \rightarrow \ell_1^+ \ell_1^- \ell_2^+ \ell_2^-$. In these cases this divergence is taken care of by a local contact contribution provided by the operator Q_{7V} , the product of the quark current $(\bar{s}d)_{V-A}$ with the leptonic vector current, the divergence being absorbed by the renormalisation of the corresponding coupling C_{7V} . The renormalised vacuum-polarisation function has an asymptotic behaviour proportional to $\log(Q^2/v^2)$. This differs markedly from the strong sector, where the correlators involved behave asymptotically as inverse powers of Q^2 . As a consequence, the usual picture of saturation by a single resonance – or even a finite number of resonances – does not work, and one needs to consider an infinite tower of narrow resonances [129]. However, while the addition of the local contribution from Q_{7V} allows one to define a finite transition form factor for a neutral kaon into two virtual photons, its insertion into the loop integral that leads to the amplitude for the $K \rightarrow \ell^+ \ell^-$ decay is now divergent. Actually, if CP is conserved, this divergence only appears in the amplitude for

$K_L \rightarrow \ell^+ \ell^-$, and, once minimally subtracted, is of the form $\sim (\log v) C_{7V}(v) \alpha G_F (\bar{s} \gamma^\mu (1 - \gamma_5) d) (\bar{\ell} \gamma_\mu \ell)$. This structure is reminiscent of a two-loop short-distance contribution, also of order $\mathcal{O}(\alpha^2 G_F)$, discussed in Ref. [130].

The large- N_c limit also offers some interesting insight into the amplitudes for the CP-conserving processes $K \rightarrow \pi \gamma^* \rightarrow \pi \ell^+ \ell^-$ [131]. In the charged-kaon channel, the amplitude in the large- N_c limit is dominated by the contributions from the current–current operators Q_1 and Q_2 , whose Wilson coefficients are of similar size, and much larger than those of the QCD penguin operators, but with opposite signs. The LEC a_+ thus results, in the large- N_c limit, from a large cancellation between these two contributions, making a stable prediction difficult without some knowledge of $1/N_c$ suppressed corrections. Since Q_2 does not contribute to the form factor for $K_S \rightarrow \pi^0 \gamma^*$ in the large- N_c limit, this cancellation does not occur and one obtains an unambiguous answer for the LEC a_S . Although its value can only be determined with a relative uncertainty of about $1/N_c \sim 30\%$, its sign is fixed without ambiguity, and corresponds to a positive interference between the direct and indirect CP-violating components of the amplitude for $K_L \rightarrow \pi^0 \ell^+ \ell^-$, which is rather good news in view of the possibility to measure this interference in the future, see Sect. 2.

A systematic investigation of all radiative kaon decay modes from the perspective of the large- N_c limit of QCD remains to be done, but is under way. Although it may not lead to predictions in all possible cases, it may nevertheless provide a useful guide to implementing phenomenological approaches that take some known properties from QCD, in particular at short distances, into better account.

3.4 ChPT and dispersion relations

Besides large- N_c considerations and matching to short-distance constraints, the purview of ChPT can also be extended in combination with dispersion relations, which allow one to implement the constraints from analyticity, unitarity, and crossing symmetry, and thereby unitarise the chiral expansion. This section is focused on $K_{\ell 4}$ decays ($K \rightarrow \pi \pi \ell \nu_\ell$), a prominent example in which the dispersive evaluation of $\pi \pi$ rescattering corrections is particularly important.

Leptonic and semileptonic kaon decays play a crucial role in the determination of CKM matrix elements. On the one hand, the ratio of $K_{\ell 2(\gamma)}$ (i.e., $K \rightarrow \ell \nu_\ell(\gamma)$) to $\pi_{\ell 2(\gamma)}$ decay widths provides access to the ratio $|V_{us}/V_{ud}|$ [106, 133, 134]. On the other hand, photon-inclusive $K_{\ell 3(\gamma)}$ decays ($K \rightarrow \pi \ell \nu_\ell(\gamma)$) are used to determine $|V_{us}|$ directly, ideally using a dispersive representation of the form factors [135, 136], together with input on the form-factor normalisation from lattice QCD [99] and isospin-breaking corrections [41, 43, 59, 137–139]. In contrast, semileptonic $K_{\ell 4}$ decays offer a

Table 3 Results for the LECs at $\mu = 770$ MeV, obtained from matching a dispersive representation of $K_{\ell 4}$ form factors to ChPT

	$10^3 \times L_1^r$	$10^3 \times L_2^r$	$10^3 \times L_3^r$	χ^2/dof
Dispersive treatment, NLO matching [132]	0.51(6)	0.89(9)	-2.82(12)	141/116 = 1.2
Dispersive treatment, NNLO matching [132]	0.69(18)	0.63(13)	-2.63(46)	122/122 = 1.0
BE14 global fit [122]	0.53(6)	0.81(4)	-3.07(20)	

unique opportunity to probe strong dynamics at low energies: since the final state contains two pions, they are ideal to study $\pi\pi$ interaction [140–142]. In particular, the determination of $\pi\pi$ S -wave scattering lengths from $K_{\ell 4}$ decays can be compared to very precise theoretical predictions based on Roy equations matched to two-loop ChPT [143, 144] and taking into account important isospin-breaking corrections [145, 146]. Furthermore, $K_{\ell 4}$ decays are the best source of information about some of the $\mathcal{O}(p^4)$ LECs of $SU(3)$ ChPT.

On the experimental side, impressive precision was reached by the high-statistics measurements of the E865 experiment at BNL [147, 148] and the NA48/2 experiment at CERN [142, 149]. The statistical errors of the S -wave of one form factor reached in both experiments the sub-percent level. Matching this precision requires a theoretical treatment beyond one-loop order in the chiral expansion [150]. Even at two loops [151], ChPT is not able to predict the observed curvature of one of the form factors.

For the dispersive treatment of the $K_{\ell 4}$ form factors of Ref. [132], a model-independent parametrisation valid up to and including $\mathcal{O}(p^6)$ was employed, known as reconstruction theorem [152, 153]. This framework is based on unitarity, analyticity, and crossing, and it includes a resummation of $\pi\pi$ - and $K\pi$ -rescattering effects. The dispersion relation leads to a coupled system of integral equations, which can be solved numerically using input on the elastic $\pi\pi$ - and $K\pi$ scattering phase shifts [143, 154–156]. The system is parameterised by a few subtraction constants, which are fit to the experimental form-factor data, together with a constraint from the soft-pion theorem [157, 158]. Isospin-breaking and radiative corrections beyond the ones included in the experimental analyses were computed in Ref. [159] at one loop in ChPT including photons and leptons.

The resummed rescattering effects are expected to give the most important contributions beyond $\mathcal{O}(p^6)$ and indeed it turns out that the dispersive description is able to reproduce the experimentally measured form-factor curvature. The dispersion relation enables an analytic continuation of the form factors beyond the physical region and the matching to ChPT can be performed at zero energy, where the chiral expansion should converge best. The matching to one-loop and two-loop ChPT leads to the results for the LECs L_1^r , L_2^r , and L_3^r shown in Table 3. The LECs are universal parameters of $SU(3)$

ChPT and enter the description of many mesonic processes at low energies, e.g., (in the case of L_3^r) $\eta \rightarrow 3\pi$ [160].

Future experimental improvement on the form factors could reduce further the uncertainties on the LECs L_1^r , L_2^r , and L_3^r . More information on the dependence on the dilepton invariant mass could be used to determine L_9^r . Better data could also give access to valuable information on $K\pi$ scattering, and in particular data on the muonic mode $K_{\mu 4}$ would provide access to a third form factor that is helicity suppressed and invisible in K_{e4} decays.

3.5 Kaon experiments as π^0 factories: a theory point of view

Having a primary beam of protons hitting the target, one can get not only kaon flux but naturally also pions. Thus, any typical kaon facility (as today's NA62) would also represent a pion factory. Even if the secondary beam were composed only of kaons (at NA62 the charged kaons represent 6%), due to the hadronic decay modes of kaons to pions, one would have again a clean source of the lightest mesons. For the charged kaons, the dominant hadronic mode is $K^+ \rightarrow \pi^+\pi^0$ (its branching ratio is approximately 20.7%). Due to the very different lifetime of pions (3×10^{-8} and 8×10^{-17} s for the charged and neutral pion, respectively), it is unlikely that one can measure both secondary pions by the same detectors. Here, the focus is on the neutral pion decay modes. The π^0 meson is in some sense unique as it represents the lightest hadron. It plays a crucial role in the study of low-energy properties of the strong interaction and is also important in various scenarios of BSM. There are two fundamental parameters connected with the π^0 decays – the pion decay constant F_π and the lifetime. F_π represents the fundamental order parameter of the spontaneous chiral symmetry breaking. Its standard determination from the pion weak decay relies on the validity of the SM. A tension between its determination from the weak decay π_{l2} and the direct π^0 decay would strongly indicate NP [135, 161], although in this comparison the role of isospin-breaking effects, especially the definition of F_π in the presence of electromagnetic interactions, becomes critical [162]. The second parameter, the π^0 lifetime is important for the normalisation of other processes (including kaons).

Let us briefly summarise all observed decay modes with their corresponding branching fractions: $\pi^0 \rightarrow \gamma\gamma$

($98.823(34) \times 10^{-2}$), $\pi^0 \rightarrow \gamma e^+ e^-$ ($1.174(35) \times 10^{-2}$), $\pi^0 \rightarrow e^+ e^+ e^- e^-$ ($3.34(16) \times 10^{-5}$), $\pi^0 \rightarrow e^+ e^-$ ($6.85(35) \times 10^{-8}$) and $\pi^0 \rightarrow \gamma$ positronium ($1.82(29) \times 10^{-9}$). Within the SM (including massive neutrinos), there are further possible decay modes. The pure $\pi^0 \rightarrow \nu \bar{\nu}$ is helicity suppressed and, similarly, $\pi^0 \rightarrow \gamma \nu \bar{\nu}$ seems to be very far from being measured in present or next-generation experiments. Within the SM, the first process that might be also seen is $\pi^0 \rightarrow 4\gamma$ (being roughly 3 orders below the theoretical prediction [163]). It might be a very important process as it goes via the anomalous $\pi^0 \gamma \gamma$ -vertex and the interesting light-by-light scattering. Besides, π^0 decays are also ideal for studying BSM physics [164], in searches for dark photons [165], for C-parity violation [163, 166], or by a precision measurement of $\pi^0 \rightarrow e^+ e^-$.

The observed decay modes of neutral pions are governed mainly by the above mentioned $\pi^0 \rightarrow \gamma^* \gamma^*$ transition form factor $F_{\pi \gamma^* \gamma^*}$, including the dilepton decay $\pi^0 \rightarrow e^+ e^-$ via a loop process. Its knowledge is also important for the anomalous magnetic moment of the muon a_μ as it enters hadronic light-by-light (HLbL) scattering via the pion-pole contribution. The uncertainty of HLbL scattering is subdominant with respect to hadronic vacuum polarisation, but still relevant, and efforts to reduce the theoretical uncertainty are ongoing [167, 168].

It is therefore interesting to study and improve our present knowledge of the above π^0 decay modes. Starting with the dominant $\pi^0 \rightarrow \gamma \gamma$, one can compare the most precise theoretical estimate based on the EM corrections and the two-loop ChPT calculation [161], with the most recent experimental measurement:

$$\begin{aligned} \text{theory: } \Gamma(\pi^0 \rightarrow \gamma \gamma) &= 8.09(11) \text{ eV}, \\ \text{PrimEx: } \Gamma(\pi^0 \rightarrow \gamma \gamma) &= 7.80(12) \text{ eV} \end{aligned} \quad (3.11)$$

leading to almost 2σ difference. The substantial improvement in recent years from an error of 10% down to 1.5% is solely due to the Primakoff-type measurements at JLab [169]. Given the difference with the theory, it is desirable to verify the measurement by a different method, e.g., at a kaon facility.

An even bigger tension was reported for the $\pi^0 \rightarrow e^+ e^-$ decay by the KTeV E799-II experiment [170]. This rare process is important for BSM studies as its long-range SM contribution is loop-induced and chirally suppressed, in such a way that potential BSM effects could compete. Further, a discrepancy could have implications for our understanding of $F_{\pi \gamma^* \gamma^*}$ and $g - 2$, while at the same time providing valuable BSM constraints. However, the original more than 3σ discrepancy is shifted down to 1.7σ if radiative corrections are correctly incorporated [171, 172]. The problem with the radiative corrections lies in the fact that the extra radiative photon is experimentally indistinguishable from a

Dalitz decay $\pi^0 \rightarrow \gamma e^+ e^-$. Its dedicated study [36, 173] is thus important in the complete understanding of the two-lepton decay mode and the pion transition form factor. With radiative corrections now directly included in the experimental analyses, cf. Sect. 2.6, a precision measurement of $\pi^0 \rightarrow e^+ e^-$ can then be confronted with the most recent theoretical study, $\mathcal{B}(\pi^0 \rightarrow e^+ e^-) = 6.25(3) \times 10^{-8}$ [174], including Z exchange and relying on detailed dispersive analyses of $F_{\pi \gamma^* \gamma^*}$ in the context of HLbL scattering [175–177], cf. Sect. 3.7, providing a precision test of the SM in analogy to the rare kaon decay $K_L \rightarrow \ell^+ \ell^-$.

In summary, the π^0 decay modes represent a complex and interrelated system important for our understanding of the fundamental interactions that can be studied naturally in future kaon experiments.

3.6 The time dependent rate $K(t) \rightarrow \mu \mu$

While improvements for the SM predictions for the $K_{L,S} \rightarrow \mu^+ \mu^-$ modes are under way (see Sects. 3.2.5 and 3.7), bringing in particular the long-distance effects under good control, it is also worthwhile to imagine measuring the time dependent rate, $\Gamma(K \rightarrow \mu^+ \mu^-)(t)$, from which the theoretically-clean, pure short-distance contribution can be extracted, proportional to the Wolfenstein parameter $\bar{\eta}$.

The time dependent decay rate of an initial neutral kaon beam is given in terms of the following function of time [40]

$$\begin{aligned} \frac{1}{\mathcal{N}} \left(\frac{d\Gamma}{dt} \right) &= f(t) \equiv C_L e^{-\Gamma_L t} + C_S e^{-\Gamma_S t} \\ &+ 2 C_{\text{Int.}} \cos(\Delta M_K t - \varphi_0) e^{-(\Gamma_L + \Gamma_S)t/2}, \end{aligned} \quad (3.12)$$

where \mathcal{N} is a normalisation factor, $\Gamma_L(\Gamma_S)$ is the $K_L(K_S)$ decay width, and ΔM_K is the $K_L - K_S$ mass difference. The four *experimental parameters*, $\{C_L, C_S, C_{\text{Int.}}, \varphi_0\}$, are directly related to the four *theory parameters* describing the system [178],

$$\begin{aligned} \{ &|A(K_S)_{\ell=0}|, |A(K_L)_{\ell=0}|, |A(K_S)_{\ell=1}|, \\ &\arg [A(K_S)_{\ell=0}^* A(K_L)_{\ell=0}] \}, \end{aligned} \quad (3.13)$$

where $\ell = 0$ (*S*-wave symmetric wave function) and $\ell = 1$ (*P*-wave anti-symmetric wave function) correspond to the CP-odd and -even ($\mu^+ \mu^-$) final states, respectively.

Under the following assumptions, all fulfilled to an excellent approximation within the SM – (i) CP violation in mixing is negligible, (ii) no scalar leptonic operators are relevant, and (iii) CP violation in the long-distance physics is negligible – the $\ell = 1$ amplitude for K_L vanishes (since it is a CP-odd transition which cannot be induced by vectorial short-distance operators), $|A(K_L)_{\ell=1}| = 0$. Moreover, under the above assumptions the CP-odd amplitude, $|A(K_S)_{\ell=0}|$, is a pure short-distance parameter.

The relations between the experimental and theory parameters can be written as

$$\begin{aligned}
 C_L &= |A(K_L)_{\ell=0}|^2, \\
 C_S &= |A(K_S)_{\ell=0}|^2 + \beta_\mu^2 |A(K_S)_{\ell=1}|^2, \\
 C_{\text{Int.}} &= D |A(K_S)_{\ell=0}| |A(K_L)_{\ell=0}|, \\
 \varphi_0 &= \arg [A(K_S)_{\ell=0}^* A(K_L)_{\ell=0}], \tag{3.14}
 \end{aligned}$$

where

$$\beta_\mu = \sqrt{1 - \frac{4m_\mu^2}{M_K^2}}, \quad D = \frac{N_{K^0} - N_{\bar{K}^0}}{N_{K^0} + N_{\bar{K}^0}}. \tag{3.15}$$

From Eq. (3.14), one can extract the pure short-distance parameter, $|A(K_S)_{\ell=0}|$, using a fit to the experimental parameters (together with knowledge of the dilution factor, D),

$$\frac{1}{D} \frac{C_{\text{Int.}}^2}{C_L} = |A(K_S)_{\ell=0}|^2. \tag{3.16}$$

In terms of SM CKM parameters, the branching ratio, $\mathcal{B}(K_S \rightarrow \mu^+ \mu^-)_{\ell=0}$, is related to the amplitude of interest via

$$\mathcal{B}(K_S \rightarrow \mu^+ \mu^-)_{\ell=0} = \frac{\tau_S \beta_\mu}{16\pi M_K} |A(K_S)_{\ell=0}|^2, \tag{3.17}$$

and is predicted to an excellent precision. The prediction, in terms of Wolfenstein parameters, is given by [178, 179]

$$\begin{aligned}
 \mathcal{B}(K_S \rightarrow \mu^+ \mu^-)_{\ell=0}^{\text{SM}} &= \frac{\tau_S \beta_\mu}{16\pi M_K} \\
 &\times \left| \frac{2G_F^2 M_W^2}{\pi^2} f_K M_K m_\mu Y_t \times A^2 \lambda^5 \bar{\eta} \right|^2, \tag{3.18}
 \end{aligned}$$

where Y_t is a loop function, dependent on $x_t = m_t^2/M_W^2$, that is known, and the only hadronic parameter is f_K , known to a very high accuracy. The current numeric SM prediction reads [179]

$$\begin{aligned}
 \mathcal{B}(K_S \rightarrow \mu^+ \mu^-)_{\ell=0}^{\text{SM}} &= 1.70(02)_{\text{QCD/EW}}(01)_{f_K} (19)_{\text{param.}} \times 10^{-13}, \tag{3.19}
 \end{aligned}$$

where the non-parametric uncertainties are of the order of $\sim 1\%$.

This demonstrates the potential of a future measurement of $\Gamma(K \rightarrow \mu^+ \mu^-)(t)$, marking it a *third kaon golden mode*. To summarise recent theory progress:

1. A measurement sensitive to interference effects in the time dependent $K \rightarrow \mu^+ \mu^-$ rate can be used to extract the CP-violating short-distance mode, $\mathcal{B}(K_S \rightarrow \mu^+ \mu^-)_{\ell=0}$, which provides a clean measurement of $|V_{ts} V_{td} \sin(\beta + \beta_s)| \approx |A^2 \lambda^5 \bar{\eta}|$, with theory uncertainty of $\mathcal{O}(1\%)$ [178–180].

2. The combination of a measurement of $\mathcal{B}(K_S \rightarrow \mu^+ \mu^-)_{\ell=0}$ with a measurement of $\mathcal{B}(K_L \rightarrow \pi^0 \nu \bar{\nu})$ results in a ratio that is a very clean test of the SM, in particular avoiding $|V_{cb}|$ -related uncertainties [62].
3. The same $\mathcal{B}(K_S \rightarrow \mu^+ \mu^-)_{\ell=0}$ observable is a potent probe of NP scenarios affecting the kaon sector, complementary to the sensitivity of $K_L \rightarrow \pi^0 \nu \bar{\nu}$ [181].
4. The phase shift characterising the K_L - K_S oscillations in the $K(t) \rightarrow \mu^+ \mu^-$ rate is also cleanly predicted within the SM, up to a fourfold discrete ambiguity [182].

These recent results are an example for novel experimental and theoretical ideas that are developing, driven by the prospect of the realisation of future kaon factories.

3.7 Discussion: SM predictions – continuum

Theoretical uncertainties in SM predictions for kaon decays can be roughly separated into (i) parametric uncertainties, which can be reduced by improving the precision of CKM input parameters, (ii) perturbative corrections, which can be improved by higher-order loop corrections, see Sect. 3.1, and (iii) long-distance contributions, which are traditionally calculated in ChPT [94]. Limitations concern the energy range in which predictions apply and the knowledge of LECs. The latter one is particularly severe for many radiative channels, since, due to gauge invariance, some form factors may receive contributions only at high orders, when LECs parameterising unknown high-energy contributions proliferate, or be dominated by resonance contributions that are only poorly reproduced by the chiral expansion. As discussed in Sect. 3.3, a promising strategy in this case concerns the interplay with large- N_c considerations and matching to short-distance constraints.

Moreover, in recent years lattice QCD has made remarkable progress in calculating the respective matrix elements (cf. Sect. 3.2), but also improved continuum strategies have been developed that allow one to extend the scope and predictive power of ChPT. One such strategy concerns the use of dispersion relations to unitarise amplitudes, capturing rescattering effects that are known to impede a rapid convergence of ChPT, e.g., for S -wave $\pi\pi$ scattering (cf. Sect. 3.4). In addition, dispersive techniques can be used to constrain LECs directly, e.g., in many cases elastic contributions can be calculated unambiguously in terms of known form factors. Recent examples of such ideas include radiative corrections to $K_{\ell 3}$ decays [137–139] (including input from lattice QCD), the kaon mass difference [183], and even matrix elements for neutrinoless double- β decay [184, 185]. In general, further constraints arise from the short-distance behaviour, where both perturbative calculations and large- N_c arguments may prove useful. In many cases, the different methods are com-

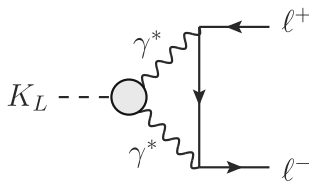


Fig. 9 Long-distance contribution to $K_L \rightarrow \ell^+ \ell^-$. The $K_L \rightarrow \gamma^* \gamma^*$ form factor is indicated by the gray blob

plementary, in such a way that combined analyses can help further improve the precision.

As a concrete example, some of these techniques have been used to improve the long-distance contribution to $K_L \rightarrow \ell^+ \ell^-$, which arises from the $K_L \rightarrow \gamma^* \gamma^*$ form factor as shown in Fig. 9 and needs to be controlled if constraints on the short-distance amplitude [186, 187] are to be extracted. In one-loop ChPT, the point-like form factor in the diagram generates a UV divergence, which becomes absorbed by a LEC with unknown finite part [188]. Moreover, the full dynamics of the $K_L \rightarrow \gamma^* \gamma^*$ form factor are only resolved at subleading orders, at which yet new parameters appear. However, similar form factors have been studied with dispersive techniques in great detail in the context of the HLbL contribution to the anomalous magnetic moment of the muon [167], in the case of π^0 [174, 176, 177], $\eta^{(\prime)}$ [189] and f_1 [190, 191], and similar strategies apply to the K_L [192]. Including data from both leptonic ($K_L \rightarrow \ell^+ \ell^- \gamma$) and hadronic ($K_L \rightarrow \pi^+ \pi^- \gamma$) processes and matching to the asymptotic contribution [193] in terms of a dispersive integral indeed allows one to reduce the uncertainty of the resulting prediction for the long-distance part of the $K_L \rightarrow \ell^+ \ell^-$ amplitude. Further improvements, including a definite statement on the relative sign between long-distance and short-distance contributions, should become possible in combination with input from lattice QCD [97, 98, 194], see Sect. 3.2.5. Finally, continuum, data-driven techniques profit from data on related processes, e.g., in the case of $K_L \rightarrow \ell^+ \ell^-$ a significant part of the error budget in Ref. [192] derives from experimental uncertainties in the spectra of $K_L \rightarrow \ell^+ \ell^- \gamma$ and $K_L \rightarrow \pi^+ \pi^- \gamma$, which could thus be reduced with improved measurements at future kaon facilities.

4 Kaon physics beyond the Standard Model

The SM provides a successful and economical description of particle physics up to energies of about 1 TeV. However, there are various phenomenological and theoretical reasons that motivate an extension of this theory at higher energies. The EW hierarchy problem (i.e., the instability of the Higgs potential under quantum corrections) and the unexplained hierarchies of the SM Yukawa coupling (the so-called flavour

problem) are among the most compelling theoretical arguments in favour of new (heavy) degrees of freedom. In this perspective, the SM can be viewed as the renormalisable part of an effective field theory valid up to some still undetermined cutoff scale Λ . There are no direct indications about the value of Λ ; however, natural solutions of the hierarchy problem suggest that it should not exceed a few TeV.

4.1 The BSM potential of rare kaon decays

Indirect NP searches, such as those conducted via FCNC processes, aim at probing the SM cutoff by looking at suppressed SM processes, where the relative impact of new degrees of freedom can be larger. In this perspective, rare K decays, and in particular the theoretically clean $K \rightarrow \pi \nu \bar{\nu}$ modes, play a unique role, since they could allow us to probe, for the first time and with high precision, the short-distance structure of the $s \rightarrow d$ FCNC amplitude.

The $s \rightarrow d$ transition is very interesting since it experiences a twofold suppression within the SM: (1) it is forbidden at the tree-level, and (2) it is further strongly suppressed by the hierarchy of the SM Yukawa couplings. In all kaon decays measured so far it is impossible to get precise short-distance information about the $s \rightarrow d$ transition (i.e., determining the strength of this transition at the EW scale): the interesting short-distance dynamics is obscured by large long-distance effects. This does not happen only in $K \rightarrow \pi \nu \bar{\nu}$ decays. This is the reason why these processes are (i) very interesting, (ii) very suppressed, and (iii) can be predicted with high accuracy in the SM.

$\mathcal{B}(K^+ \rightarrow \pi^+ \nu \bar{\nu})$ and $\mathcal{B}(K_L \rightarrow \pi^0 \nu \bar{\nu})$ are conceptually comparable to clean precise EW observables, such as the W mass or the Higgs self-coupling. Similarly to those, rare K decays probe EW dynamics. However, rare K decays probe it in a different and less tested sector connected to the flavour problem, which is one of the main reasons why the SM needs to be extended. Not surprisingly, there are plenty of examples in the literature of well motivated BSM models, perfectly consistent with present high-energy data, which would give rise to large deviations from the SM in both decay modes (see, e.g., Refs. [195–202]). A further unique aspect of $K \rightarrow \pi \nu \bar{\nu}$ decays is that they are sensitive to the interaction of light quarks (s and d) with third-generation leptons (the τ neutrinos). This additional unique aspect enhances their sensitivity to motivated BSM models shedding light on the origin of the flavour hierarchies (see, e.g., Refs. [198, 202, 203]). Note that, besides being particularly motivated, such models are also favoured by present data that indicates an excess, over the SM predictions, in $b \rightarrow c \tau \nu$ decays. An illustration of the potential impact of a future precise measurement of $\mathcal{B}(K^+ \rightarrow \pi^+ \nu \bar{\nu})$ in this context, also in connection with the expected precision on $\mathcal{B}(B \rightarrow K^{(*)} \nu \bar{\nu})$, is shown in Fig. 10.

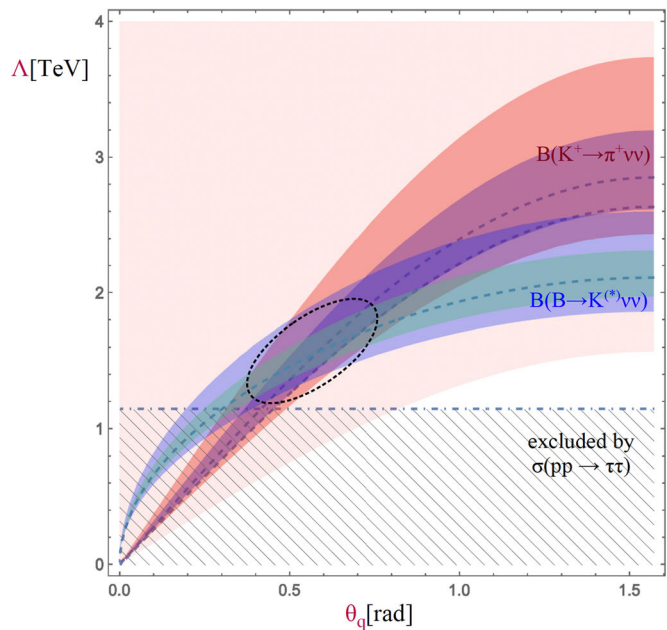
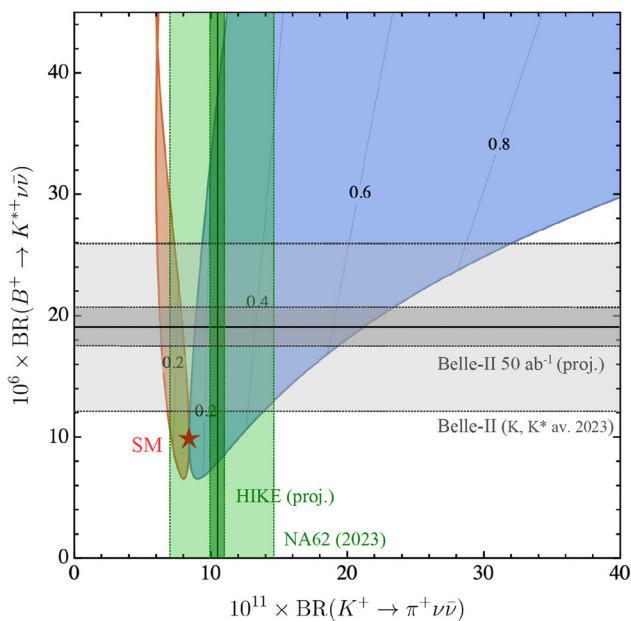


Fig. 10 $\mathcal{B}(K^+ \rightarrow \pi^+ \nu \bar{\nu})$ vs. $\mathcal{B}(B \rightarrow K^{(*)} \nu \bar{\nu})$ in extensions of the SM with NP coupled dominantly to the 3rd family leading to an effective interaction of the type $(\bar{q}_L^3 \gamma^\mu T q_L^3)(\bar{\ell}_L^3 \gamma_\mu T \ell_L^3)$, with $T = \sigma^a$ (triplet) or $T = 1$ (singlet). Left: Allowed values for the two modes, setting $R_D = 1.25$, and assuming a triplet interaction (red) or triplet – 2 singlet (blue); the bands denote present errors and future projections [198]. Right: Scale of the effective operator (singlet case) vs. the parameter

θ_q describing the flavour alignment [$q_L^3 \equiv \cos(\theta_q)b_L + \sin(\theta_q)t_L$]; the coloured bands denote 1σ and 2σ regions assuming a 5% [10%] measurement of $\mathcal{B}(K^+ \rightarrow \pi^+ \nu \bar{\nu})$ [$\mathcal{B}(B \rightarrow K^{(*)} \nu \bar{\nu})$] around the present central value; the pink area indicates the present allowed region. These plots highlight the importance of combining precise data on the two modes in determining not only the effective scale of NP, but also its EW and flavour structure

Loosely speaking, the motivated BSM theories that can be tested by means of $K \rightarrow \pi \nu \bar{\nu}$ decays fall into the same category as those researched at HL-LHC, i.e., theories with new heavy particles in the few TeV regime. An explicit example of the complementarity of $K \rightarrow \pi \nu \bar{\nu}$ with collider and electroweak observables in this context has recently been shown in [204]. In this respect, it is worth emphasising that NP around the TeV scale is perfectly compatible with current data, and still represents the most natural option to address the EW hierarchy problem [204]. Limits on specific exotic particles, or new contact interactions, can even exceed 100 TeV, but this fact should not be over-interpreted: these strong limits only apply to exotic states that badly violate some of the accidental symmetries of the SM. Low-scale NP models compatible with current data imply small deviations from the SM and can only be searched for via dedicated precision measurements.

As with all precision tests, also in the case of $\mathcal{B}(K \rightarrow \pi \nu \bar{\nu})$ the impact of the result depends both on the experimental and on the theoretical accuracy. Right now, the experimental precision on $\mathcal{B}(K^+ \rightarrow \pi^+ \nu \bar{\nu})$ is around 40%, well above the theoretical one. Reaching the few-percent level on this mode would represent major progress. If, as predicted in motivated NP models, a significant deviation from the SM were observed, this would be a major breakthrough. How-

ever, the value of this observable is such that a precision measurement would have far-reaching implications even in case of a result compatible with the SM. This would allow us to rule out (or further constrain) a class of well motivated BSM theories in the TeV-energy domain addressing the origin of the flavour hierarchies.

4.2 Exotica from kaon decays: theory and experiment

The question of how to rank searches for exotics or forbidden decays inevitably runs into theoretical prejudices. One can for instance order NP models in terms of their simplicity such as the minimal field content that is added to the existing SM structure. One can see that this may not be the best criterion by considering that before the discovery of the muon or even charm, simplicity would not have guided one to the complex structure of the SM. The other option is to ask for interesting experimental signatures, so that no stone is left unturned. This can easily lead to rather complicated model building (“signature building”), and also runs against the problem of limited resources.

An option that is quite appealing is to give priority to the models that already solve some of the outstanding problems in particle physics. An example of such a model is the QCD axion, which solves both the strong CP problem and is a cold

dark matter candidate. In this case HIKE is in a very advantageous position that it will probe very interesting parameter space. Assuming sizeable flavour-violating couplings, such as in the case of axiflavor [205], HIKE will probe values of axion decay constant, f_a , that result in the correct DM abundance in minimal scenarios.

4.2.1 Theory overview

Heavy NP with flavour-violating couplings is very efficiently probed via classic FCNC probes such as $K-\bar{K}$ mixing, $\mu \rightarrow e$ conversion, rare B decays, etc. The effects of such heavy NP are encoded in the values of the Wilson coefficients, for instance $C_{ds}(\bar{d}\gamma^{\mu}s)(\bar{d}\gamma_{\mu}s)$ for $K-\bar{K}$ mixing. The tree level exchanges of heavy NP mediators will result in $C_{ds} \propto g^2/M^2$, where g is the flavour-violating coupling of the heavy mediator to the quark current, M the mediator mass, and we are omitting $\mathcal{O}(1)$ factors. That is, the classic FCNC probes with SM particles as asymptotic states can probe very heavy mediators that have $\mathcal{O}(1)$ flavour-violating couplings, or much lighter NP that is proportionally more weakly coupled.

There is a qualitative change in the sensitivity, if one searches for rare decays to light NP states. For instance, if light NP state ϕ couples through dimension 5 operators that are suppressed by $1/f_a$, the branching ratio for $K \rightarrow \pi\phi$ is parametrically given by $\mathcal{B}(K \rightarrow \pi\phi) \propto (M_W^2/f_a M_K)^2$. That is, the sensitivity to the UV scale f_a is parametrically enhanced because the kaons are light. The underlying reason is that the kaon decay width is suppressed by the off-shellness of the W , so that $\Gamma_K \propto M_K^5/M_W^4$. This same heuristic argument applies to other light mesons and leptons: which one wins depends on flavour and CP structure of NP.

The other open question is how “exotic” are such light NP states. Here, an important comment is that any global $U(1)$ that is spontaneously broken will result in a light (pseudo-)Nambu–Goldstone boson. The perhaps most celebrated example is the QCD axion, while in general such light pseudoscalars a go under the term axion-like particles or ALPs. These can have flavour-violating couplings [206–211]. If these are already present in the UV then $K \rightarrow \pi a$ decays probe very high scales, $f_a \sim 10^{13}$ GeV, while if the flavour violation is due to the SM CKM, generated at 1-loop, then the reach is correspondingly lower, at $f_a \sim 10^6$ GeV [212,213]. Beyond ALPs, there are many other well motivated models of light NP to which kaon decays are sensitive, such as light Higgs-mixed scalar, heavy neutral leptons, dark photon, etc. Even seemingly exotic signatures could in fact be due to relatively simple extensions of the SM. One such example, is for instance the decay $K \rightarrow \pi 2(e^+e^-)$ that would be generated within a dark Higgsed $U(1)_d$, where both the Higgs and the dark photon are light. A more complete list can be found in Ref. [213].

4.2.2 Principal experimental signatures

Discussed below are the principal K^+ decay channels that have been exploited by NA62, and will be exploited at HIKE, to address the Physics Beyond Collider (PBC) benchmark scenarios (BC) in the classification of Ref. [214]. The updated HIKE sensitivity is published in the HIKE proposal [1].

Kaon decays also provide sensitivity to a large number of non-minimal scenarios that evade detection in beam-dump experiments [215–217], which have been studied experimentally only to a minimal extent so far. Examples of non-minimal scenarios accessible in kaon experiments are: short-lived Majorana heavy neutral leptons (HNLs) decaying via a displaced-vertex topology $K^+ \rightarrow \ell_1^+ N$, $N \rightarrow \pi^- \ell_2^+$ [218]; dark neutrino produced and decaying via the $K^+ \rightarrow \ell^+ N$, $N \rightarrow \nu Z'$, $Z' \rightarrow e^+e^-$ chain [217]; a muonphilic force scenario leading to $K^+ \rightarrow \mu^+ \nu X$ decays [219].

$K^+ \rightarrow \pi^+ X_{\text{inv}}$ decays: The search for the $K^+ \rightarrow \pi^+ X_{\text{inv}}$ decay, where X_{inv} is an invisible particle, provides sensitivity to the benchmark scenarios BC4 (dark scalar), BC10 (ALP with fermion coupling) and BC11 (ALP with gluon coupling). The accessible m_X ranges are approximately 0–110 MeV/ c^2 and 150–260 MeV/ c^2 , corresponding to the $K^+ \rightarrow \pi^+ \nu \bar{\nu}$ signal regions. The principal background comes from the $K^+ \rightarrow \pi^+ \nu \bar{\nu}$ decay itself. The search strategy based on the peak search in the spectrum of the reconstructed missing mass $m_{\text{miss}}^2 = (P_{K^+} - P_{\pi^+})^2$ has been established by the NA62 experiment [220], and the full NA62 Run 1 (2016–2018) dataset has been analysed [14]. The search at HIKE Phase 1 will be performed by direct extension of the $K^+ \rightarrow \pi^+ \nu \bar{\nu}$ measurement. The HIKE Phase 1 sensitivity projection has been performed by extension of the NA62 analysis, assuming a 40-fold increase in the size of the data sample with respect to NA62 Run 1.

The above scenarios are also addressed by a dedicated search for the $\pi^0 \rightarrow X_{\text{inv}}$ decay using a technique established by NA62 [221]. This search covers the m_X region in the vicinity of the π^0 mass. The region $m_X > 260$ MeV/ c for the scenarios BC4 and BC11 is addressed experimentally by searches for $K^+ \rightarrow \pi^+ X$ decays followed by displaced $X \rightarrow \mu^+ \mu^-$ or $X \rightarrow \gamma\gamma$ decays, respectively.

$K^+ \rightarrow \ell^+ N$ decays: Searches for the $K^+ \rightarrow \ell^+ N$ decays ($\ell = e, \mu$), where N is an invisible particle, provide sensitivity to the benchmark scenarios BC6 (HNL with electron coupling) and BC7 (HNL with muon coupling). The technique has been established by the NA62 experiment, which has obtained world-leading exclusion limits on the HNL mixing parameters $|U_{\ell 4}|^2$ over much of the accessible mass range of 144–462 MeV/ c^2 with the Run 1 dataset [222,223]. Both searches are limited by background. In particular, the $K^+ \rightarrow \mu^+ \nu$ decay followed by $\mu^+ \rightarrow e^+ \nu \bar{\nu}$ decay in flight, and the $\pi^+ \rightarrow e^+ \nu$ decay of the pions

in the unseparated beam, represent irreducible backgrounds to the $K^+ \rightarrow e^+N$ process.

The HIKE sensitivity projection is obtained by extension of the NA62 analysis assuming the similar resolution and background. In the $K^+ \rightarrow \mu^+N$ case, it is assumed additionally that, unlike NA62, the trigger line is not down-scaled, which is possible for a fully software trigger. HIKE sensitivity to $|U_{e4}|^2$ in the mass range 144–462 MeV/ c^2 approaches the seesaw neutrino mass models [224]. For $m_N < 140$ MeV/ c^2 , HIKE will improve the PIENU limits [225] on $|U_{e4}|^2$ via the $\pi^+ \rightarrow e^+N$ decays of pions in the unseparated beam, and has a further potential via the $K^+ \rightarrow \pi^0 e^+N$ decay [226]. HIKE will also approach the seesaw neutrino mass models for $|U_{\mu 4}|^2$.

$\pi^0 \rightarrow \gamma A'$ decay: A search for the $K^+ \rightarrow \pi^+ \pi^0, \pi^0 \rightarrow \gamma A', A' \rightarrow e^+ e^-$ prompt decay chain had been performed by the NA48/2 experiment [227], addressing the benchmark dark photon scenario BC1. The case of invisible dark photon (scenario BC2) has been addressed by the NA62 experiment [165]. The HIKE experiment will be able to improve on both searches. Of particular interest for the future experimental programme are the displaced $A' \rightarrow e^+ e^-$ vertex analysis which potentially provides sensitivity for lower dark photon couplings, and a study of an alternative dark photon production channel $K^+ \rightarrow \mu^+ \nu A'$, followed by either prompt or displaced $A' \rightarrow e^+ e^-$ decays, extending the search region above the π^0 mass.

Other processes: Other exotic processes studied recently using the NA62 Run 1 dataset include searches for lepton-flavour and -number violating decays, including $K^+ \rightarrow \pi^- \mu^+ \mu^+$ and $K^+ \rightarrow \pi^- e^+ e^+$ [228], $K^+ \rightarrow \pi^\pm \mu^\mp e^+$ and $\pi^0 \rightarrow \mu^- e^+$ [229], $K^+ \rightarrow \pi^- (\pi^0) e^+ e^+$ [230], and $K^+ \rightarrow \mu^- \nu e^+ e^+$ [231]. These searches are almost background-free, and typically reach sensitivities to the decay branching ratios of $\mathcal{O}(10^{-11})$. The sensitivities will be improved significantly with NA62 Run 2 and HIKE datasets.

The NA62 experiment has recently reported the first search for pair-production of hidden-sector mediators in the prompt $K^+ \rightarrow \pi^+ aa, a \rightarrow e^+ e^-$ and $K^+ \rightarrow \pi^+ S, S \rightarrow A' A', A' \rightarrow e^+ e^-$ decay chains leading to a five-track final state [232].

4.3 Discussion: (B)SM constraints from kaon physics

In this section the impact of kaon observables as constraints on the SM and beyond is discussed.

The interplay of kaon physics with other areas of particle physics can be nicely illustrated by the example of anomalous couplings of the Z boson to top quarks. These couplings can be measured directly at the LHC via $t\bar{t} + Z$ production [233]. It turns out, however, that indirect constraints are more powerful [234]. In particular, rare B and K meson decays are sensitive probes of such couplings. Moreover, anomalous

$t\bar{t}Z$ couplings are related, via gauge invariance, to anomalous couplings of W bosons, which leads to a rich interplay between rare decays, EW precision observables, and collider signals.

This interplay can be discussed in a transparent way in the context of SM effective field theory (SMEFT) [235, 236]. At mass dimension six, there are three operators that induce anomalous $t\bar{t} + Z$ couplings at tree level, namely, $Q_{\phi q, 33}^{(3)}, Q_{\phi q, 33}^{(1)}, Q_{\phi u, 33}$. Strong constraints from B meson decays require the combination $C_{\phi q, 33}^{(3)} + C_{\phi q, 33}^{(1)}$ to be very small. In certain models with vector-like quarks, this combination vanishes identically [237], which is assumed in the following. In this case, rare K and B meson decays put strong bounds on non-standard $t\bar{t}Z$ couplings. Currently, the $B_s \rightarrow \mu^+ \mu^-$ mode is clearly dominant (Fig. 11, left panel), but precise measurements of the $K \rightarrow \pi \nu \bar{\nu}$ will lead to comparable (and complementary) constraints in the future. The single other most important constraint arises from the measurement of the T parameter, while the modification of the left-handed $b\bar{b}Z$ (i.e., δg_b^L) leads to weaker constraints. The modification of the charged current affects the t -channel single top production cross section which has been measured by both ATLAS [238] and CMS [239]; however, rare decays are expected to give stronger bounds even in the future with a larger LHC data sample.

Rare kaon decays are also sensitive probes of light new particles that can appear in the final state. For instance, the measurement of the $K^+ \rightarrow \pi^+ \nu \bar{\nu}$ branching ratio can set stringent bounds on well-motivated models of axion dark matter if the axions have flavour off-diagonal couplings, see the discussion in Sect. 4.2 for details.

The expected $K^+ \rightarrow \pi^+ \nu \bar{\nu}$ event rate at HIKE will result in a measurement of the invariant mass spectrum of the final-state neutrino pair and test fundamental properties of neutrinos. If we consider only lepton-number-conserving interactions of SMEFT, the resulting three light Majorana neutrinos can only couple through an axial vector current with the quark sector in the limit of small neutrino masses. The resulting missing mass spectrum would be a rescaled SM spectrum. Dimension seven operators, that violate lepton number, can generate scalar interactions and (neutrino flavour-changing) tensor interactions. Neutrino flavour-conserving scalar interactions were studied in Ref. [240] and a sensitivity to energy scales in the multi TeV range was found. The neutrino spectrum peaks at higher invariant masses if compared with the SM expectation. The situation changes if we go beyond the three light Majorana neutrino scenario. Three extra neutrinos can potentially form Dirac neutrinos, together with the lepton doublets of the SM. In this scenario, scalar and tensor interactions are already generated at dimension six in ν SMEFT without the need for lepton number violation. Preliminary results [241, 242] for this scenario and extra sterile Majorana

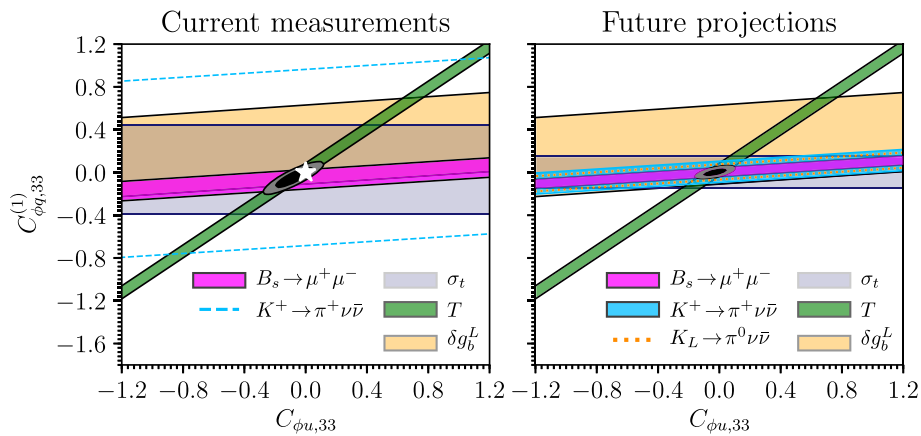


Fig. 11 Constraints on anomalous $t\bar{t}Z$ couplings. The left panel shows current constraints on the two independent coefficients $C_{\phi q,33}^{(1)}$ and $C_{\phi u,33}$, arising from the rare decays $B_s \rightarrow \mu^+\mu^-$ and $K^+ \rightarrow \pi^+\nu\bar{\nu}$, t -channel single top production (σ_t), as well as the EW precision parameters T and δg_b^L . The white star indicates the SM expectation. The

right panel shows future projections, assuming 5% measurements of the rare-decay modes and a naive rescaling of the uncertainty in single top production with 300/fb of data. The EW precision parameters were measured at LEP and are not expected to change significantly. See text for discussion

rana neutrinos were discussed. Both scenarios are sensitive to NP in the 100 TeV range. Dirac neutrinos also allow for lepton-flavour-conserving tensor interactions. The scenario with extra massive sterile neutrinos can lead to unique modifications of the spectrum through the modified phase space.

4.4 Discussion: complementarity of B - and K -decays

Flavour physics is a traditional source of correlation among B - and K -physics: are there observables and models correlating B - and K -physics? What about lepton-flavour-universality violation (LFUV)? Which models? What about model independent tests? CP violation? Which LFUV scale can be tested? What about lepton-flavour-violating (LFV) decays like $K \rightarrow \pi\mu e$?

Based on the stronger constraints of FCNCs of the first two families compared to the third family, the traditional Minimal Flavour Violation (MFV) protection of FCNCs based on $U(3)$ flavour symmetry was already challenged by a less protective $U(2)$: indeed Isidori and collaborators have recently applied this $U(2)$ to interesting B - and K -correlations [201,243], in particular $B \rightarrow \pi\nu\bar{\nu}$ and $K \rightarrow \pi\nu\bar{\nu}$. Also a typical NP scale of $\sim 1-2$ TeV was indicated.

Since a SMEFT approach generically predicts LFV in higher dimensional operators, it is interesting to question LFUV and LFV in kaon physics independently, and also address which kaon observable could be more interesting; for instance, LFUV was tested in $K^\pm \rightarrow \pi^\pm\ell^+\ell^-$ [39]: in the presence of LFUV in higher dimensional operators, for instance Q_{7V} , affecting differently $K^\pm \rightarrow \pi^\pm e^+e^-$ and $K^\pm \rightarrow \pi^\pm\mu^+\mu^-$, experiment could test LFUV by measuring the form factors of the different final states.

However, if NP affects left-handed currents also neutrinos of different flavours are affected in $K \rightarrow \pi\nu\bar{\nu}$. Moreover, $K_L \rightarrow \mu^+\mu^-$ and $K_L \rightarrow \pi^0\ell^+\ell^-$ experiments may give relevant constraints to LFUV (dimension-six $V - A \otimes V - A$ operators) coefficients [27]. In this research all kaon decays potentially constraining LFUV interactions ($K_L \rightarrow \pi^0\nu\bar{\nu}$, $K^+ \rightarrow \pi^+\nu\bar{\nu}$, $K_L \rightarrow \mu^+\mu^-$ and $K_L \rightarrow \pi^0\ell^+\ell^-$) are limiting the supposed different couplings to the first and second left-handed family. Also the projections for the future programmes of KOTO and NA62, i.e. KOTO-II and HIKE Phases 1 and 2, are studied.

One of the questions of this workshop was how to quantify the impact of BSM reach, through dimension-6 operators, in flavour and collider experiments (kaons, beauty, $\Delta F = 2, 1$, muon decays, dipole moments, Higgs decays, ...): one can parameterise the limits in terms of the scale appearing in the Wilson coefficients of dimension-6 operators, but it was also argued that specific models could be more useful to show the experimental reach. For instance there are specific models that might be more effective to address B - and K -physics and the possible $g - 2$ muon anomaly. Other studies have shown that the explanation of $B \rightarrow D^{(*)}\tau\bar{\nu}$ decay would generate, through W -box diagrams, effects in $K \rightarrow \pi\nu\bar{\nu}$ [244].

Several theoretical and experimental studies have explored the possibility of lepton number violation manifesting itself in rare kaon decays. Also NA62, KOTO, KOTO-II and HIKE have studied this, see Sect. 2. Several models have been discussed at the workshop: (i) using SMEFT its detection would put high-scale leptogenesis under tension and would hint to small radiatively generated neutrino masses [240], (ii) German Valencia and collaborators [245] compare constraints on pairs of light scalars or vectors from their contribution to $K \rightarrow \pi\nu\bar{\nu}$ and $B \rightarrow M\nu\bar{\nu}$ ($M = K, \pi$ etc.).

One interesting question in the workshop was the possible connection between the strong CP problem and the flavour problem: it was discussed the possibility that solving the flavour problem of the SM with a simple $U(1)_H$ flavour symmetry naturally leads to an axion that solves the strong CP problem and constitutes a viable Dark Matter candidate. This framework is very predictive and experimentally testable by future axion and precision flavour experiments [205].

The interplay between kaon physics and other areas is also evident in precision measurements of charged-current decays of K^+ and K_L . These decays serve as a robust BSM probe through the testing of first-row CKM unitarity and the exploration for nonstandard currents. They are sensitive to effective TeV scales, complementing EW precision data and direct LHC searches, as can be seen in the SMEFT framework [134,246–248]. The current discrepancies observed across various modes provide further motivation to delve into these processes and resolve the existing uncertainties.

5 Outlook and conclusions

This document provides a compact summary of talks and discussions from the workshop Kaons@CERN 23 [249]. Over 100 leaders in experiment and theory participated in the workshop to take stock, discuss and contemplate about the opportunities that current and future kaon-physics experiments, as well as anticipated theoretical developments, provide for particle physics in the coming decade and beyond. A few outcomes are worth highlighting:

- The rare-decay channels $K^+ \rightarrow \pi^+ \nu \bar{\nu}$ and $K_L \rightarrow \pi^0 \nu \bar{\nu}$ are among the theoretically cleanest standard candles of the SM. Being essentially free of hadronic uncertainties they allow for accurate and precise tests of the SM. Their suppression in the SM leads to sensitivity to NP at the highest scales.
- The theoretical precision matching the projections of future experiments HIKE and KOTO-II does already exist.
- Generic NP models show complementarity of searches in B and K decays. Results from a future kaon factory will uniquely impact the constraining or understanding of the microscopic structure of NP.
- Besides the gold-plated rare modes, HIKE and KOTO-II will measure a plethora of other K^+ and K_L decays (rare, less rare and radiative) with unprecedented precision. For some of these decays the improved measurements will help the community of SM theorists working in ChPT, dispersion theory and lattice QCD+QED to test their predictions and sharpen their tools.
- For several other decays not belonging to the gold-plated class, the improved measurements will help put further

constraints on NP models, in particular if one analyses them in combined fits. Moreover their effectiveness can increase if theoretical calculations of long-distance contributions improve, even at a later stage. Precision HIKE measurements of the dominant K^+ and K_L decay modes can also provide important NP input.

- While the best possible outcome is that NP will be discovered by HIKE and/or KOTO-II, the resulting precision measurement of the SM are guaranteed deliverables and will allow for stronger constraints of NP models, and hence, stronger exclusion limits.

As the workshop has shown – the kaon physics community is diverse, young and vibrant and distributed around the entire world. A clear commitment to a kaon factory in terms of HIKE will give it a further boost and allow it to further develop ideas and projects that are already ongoing. Historically, the study of kaon physics was an important driver for the development of the SM, but it is far from a closed chapter: kaon physics still harbours many fundamental questions. As this workshop has clearly highlighted, through their sensitivity to high-scale physics, kaons could very well be the place where first signs of NP will be discovered. Studying kaons to high precision with a next-generation kaon factory should therefore be a priority for both CERN and J-PARC.

Acknowledgements We acknowledge the kind financial support by LHCb, NA62 and the CERN Department of Theoretical Physics.

Data Availability Statement This manuscript has no associated data or the data will not be deposited. [Authors' comment: This article is a conference summary.]

Code availability My manuscript has no associated code/software. [Author's comment: Code/Software sharing not applicable to this article as no code/software was generated or analysed during the current study.]

Open Access This article is licensed under a Creative Commons Attribution 4.0 International License, which permits use, sharing, adaptation, distribution and reproduction in any medium or format, as long as you give appropriate credit to the original author(s) and the source, provide a link to the Creative Commons licence, and indicate if changes were made. The images or other third party material in this article are included in the article's Creative Commons licence, unless indicated otherwise in a credit line to the material. If material is not included in the article's Creative Commons licence and your intended use is not permitted by statutory regulation or exceeds the permitted use, you will need to obtain permission directly from the copyright holder. To view a copy of this licence, visit <http://creativecommons.org/licenses/by/4.0/>.

Funded by SCOAP³.

References

1. HIKE Collaboration, High Intensity Kaon Experiments (HIKE) at the CERN SPS: proposal for phases 1 and 2. Technical Report.

- CERN-SPSC-2023-031 and SPSC-P-368, CERN (2023). <https://cds.cern.ch/record/2878543>
2. K. Aoki et al., Extension of the J-PARC hadron experimental facility: third white paper. [arXiv:2110.04462](https://arxiv.org/abs/2110.04462)
 3. T.D. Lee, C.-N. Yang, Question of parity conservation in weak interactions. *Phys. Rev.* **104**, 254 (1956). <https://doi.org/10.1103/PhysRev.104.254>
 4. N. Cabibbo, Unitary symmetry and leptonic decays. *Phys. Rev. Lett.* **10**, 531 (1963). <https://doi.org/10.1103/PhysRevLett.10.531>
 5. S.L. Glashow, J. Iliopoulos, L. Maiani, Weak interactions with lepton-hadron symmetry. *Phys. Rev. D* **2**, 1285 (1970). <https://doi.org/10.1103/PhysRevD.2.1285>
 6. J.H. Christenson, J.W. Cronin, V.L. Fitch, R. Turlay, Evidence for the 2π decay of the K_S^0 meson. *Phys. Rev. Lett.* **13**, 138 (1964). <https://doi.org/10.1103/PhysRevLett.13.138>
 7. KTeV Collaboration, Observation of direct CP violation in $K_{S,L} \rightarrow \pi\pi$ decays. *Phys. Rev. Lett.* **83**, 22 (1999). <https://doi.org/10.1103/PhysRevLett.83.22>. [arXiv:hep-ex/9905060](https://arxiv.org/abs/hep-ex/9905060)
 8. NA48 Collaboration, A new measurement of direct CP violation in two pion decays of the neutral kaon. *Phys. Lett. B* **465**, 335 (1999). [https://doi.org/10.1016/S0370-2693\(99\)01030-8](https://doi.org/10.1016/S0370-2693(99)01030-8). [arXiv:hep-ex/9909022](https://arxiv.org/abs/hep-ex/9909022)
 9. M. Kobayashi, T. Maskawa, CP violation in the renormalizable theory of weak interaction. *Prog. Theor. Phys.* **49**, 652 (1973). <https://doi.org/10.1143/PTP.49.652>
 10. E288 Collaboration, Observation of a dimuon resonance at 9.5-GeV in 400-GeV proton-nucleus collisions. *Phys. Rev. Lett.* **39**, 252 (1977). <https://doi.org/10.1103/PhysRevLett.39.252>
 11. CMS Collaboration, Observation of a new boson at a mass of 125 GeV with the CMS experiment at the LHC. *Phys. Lett. B* **716**, 30 (2012). <https://doi.org/10.1016/j.physletb.2012.08.021>. [arXiv:1207.7235](https://arxiv.org/abs/1207.7235)
 12. ATLAS Collaboration, Observation of a new particle in the search for the Standard Model Higgs boson with the ATLAS detector at the LHC. *Phys. Lett. B* **716**, 1 (2012). <https://doi.org/10.1016/j.physletb.2012.08.020>. [arXiv:1207.7214](https://arxiv.org/abs/1207.7214)
 13. NA62 Collaboration, The beam and detector of the NA62 experiment at CERN. *JINST* **P2**, P05025 (2017). <https://doi.org/10.1088/1748-0221/12/05/P05025>. [arXiv:1703.08501](https://arxiv.org/abs/1703.08501)
 14. NA62 Collaboration, Measurement of the very rare $K^+ \rightarrow \pi^+ \nu \bar{\nu}$ decay. *JHEP* **06**, 093 (2021). [https://doi.org/10.1007/JHEP06\(2021\)093](https://doi.org/10.1007/JHEP06(2021)093). [arXiv:2103.15389](https://arxiv.org/abs/2103.15389)
 15. NA62 Collaboration, 2023 NA62 status report to the CERN SPSC. Technical Report. CERN-SPSC-2023-013 and SPSC-SR-326, CERN (2023). <https://cds.cern.ch/record/2856997>
 16. G. Isidori, Decoding flavour hierarchies: an essential key to physics beyond the SM (2013). <https://indico.cern.ch/event/1196830/>
 17. KOTO Collaboration, Search for $K_L \rightarrow \pi^0 \nu \bar{\nu}$ and $K_L \rightarrow \pi^0 X^0$ decays at the J-PARC KOTO experiment. *Phys. Rev. Lett.* **122**, 021802 (2019). <https://doi.org/10.1103/PhysRevLett.122.021802>. [arXiv:1810.09655](https://arxiv.org/abs/1810.09655)
 18. KOTO Collaboration, Study of the $K_L \rightarrow \pi^0 \nu \bar{\nu}$ decay at the J-PARC KOTO experiment. *Phys. Rev. Lett.* **126**, 121801 (2021). <https://doi.org/10.1103/PhysRevLett.126.121801>. [arXiv:2012.07571](https://arxiv.org/abs/2012.07571)
 19. LHCb Collaboration, The LHCb detector at the LHC. *JINST* **3**, S08005 (2008). <https://doi.org/10.1088/1748-0221/3/08/S08005>
 20. LHCb Collaboration, Physics case for an LHCb upgrade II—opportunities in flavour physics, and beyond, in the HL-LHC era. [arXiv:1808.08865](https://arxiv.org/abs/1808.08865)
 21. A.A. Alves Junior et al., Prospects for measurements with strange hadrons at LHCb. *JHEP* **05**, 048 (2019). [https://doi.org/10.1007/JHEP05\(2019\)048](https://doi.org/10.1007/JHEP05(2019)048). [arXiv:1808.03477](https://arxiv.org/abs/1808.03477)
 22. LHCb Collaboration, Constraints on the $K_S^0 \rightarrow \mu^+ \mu^-$ branching fraction. *Phys. Rev. Lett.* **125**, 231801 (2020). <https://doi.org/10.1103/PhysRevLett.125.231801>. [arXiv:2001.10354](https://arxiv.org/abs/2001.10354)
 23. LHCb Collaboration, Evidence for the rare decay $\Sigma^+ \rightarrow p \mu^+ \mu^-$. *Phys. Rev. Lett.* **120**, 221803 (2018). <https://doi.org/10.1103/PhysRevLett.120.221803>. [arXiv:1712.08606](https://arxiv.org/abs/1712.08606)
 24. LHCb Collaboration, Search for $K_{S(L)}^0 \rightarrow \mu^+ \mu^- \mu^+ \mu^-$ decays at LHCb. *Phys. Rev. D* **108**, L031102 (2023). <https://doi.org/10.1103/PhysRevD.108.L031102>. [arXiv:2212.04977](https://arxiv.org/abs/2212.04977)
 25. NA48/1 Collaboration, Observation of the rare decay $K_S \rightarrow \pi^0 \mu^+ \mu^-$. *Phys. Lett. B* **599**, 197 (2004). <https://doi.org/10.1016/j.physletb.2004.08.058>. [arXiv:hep-ex/0409011](https://arxiv.org/abs/hep-ex/0409011)
 26. V.G. Chobanova, X. Cid Vidal, J.P. Dalseno, M. Lucio Martínez, D. Martínez Santos, V. Renaudin, Sensitivity of LHCb and its upgrade in the measurement of $B(K_S^0 \rightarrow \pi^0 \mu^+ \mu^-)$ (2016). <https://cds.cern.ch/record/2195218>
 27. G. D'Ambrosio, A.M. Iyer, F. Mahmoudi, S. Neshatpour, Anatomy of kaon decays and prospects for lepton flavour universality violation. *JHEP* **09**, 148 (2022). [https://doi.org/10.1007/JHEP09\(2022\)148](https://doi.org/10.1007/JHEP09(2022)148). [arXiv:2206.14748](https://arxiv.org/abs/2206.14748)
 28. G. D'Ambrosio, F. Mahmoudi, S. Neshatpour, Beyond the standard model prospects for kaon physics at future experiments. *JHEP* **02**, 166 (2024). [https://doi.org/10.1007/JHEP02\(2024\)166](https://doi.org/10.1007/JHEP02(2024)166). [arXiv:2311.04878](https://arxiv.org/abs/2311.04878)
 29. S. Neshatpour, F. Mahmoudi, Flavour physics phenomenology with SuperIso (2022). <https://doi.org/10.22323/1.409.0010>
 30. KOTO Collaboration, Search for the pair production of dark particles X with $K_L^0 \rightarrow XX$, $X \rightarrow \gamma\gamma$. *Phys. Rev. Lett.* **130**, 111801 (2023). <https://doi.org/10.1103/PhysRevLett.130.111801>. [arXiv:2209.11019](https://arxiv.org/abs/2209.11019)
 31. E391a Collaboration, Study of the $K_L^0 \rightarrow \pi^0 \pi^0 \nu \bar{\nu}$ decay. *Phys. Rev. D* **84**, 052009 (2011). <https://doi.org/10.1103/PhysRevD.84.052009>. [arXiv:1106.3404](https://arxiv.org/abs/1106.3404)
 32. E391a Collaboration, Search for a light pseudoscalar particle in the decay $K_L^0 \rightarrow \pi^0 \pi^0 X$. *Phys. Rev. Lett.* **102**, 051802 (2009). <https://doi.org/10.1103/PhysRevLett.102.051802>. [arXiv:0810.4222](https://arxiv.org/abs/0810.4222)
 33. KOTO Collaboration, First search for $K_L^0 \rightarrow \pi^0 \gamma$. *Phys. Rev. D* **102**, 051103 (2020). <https://doi.org/10.1103/PhysRevD.102.051103>. [arXiv:2006.14918](https://arxiv.org/abs/2006.14918)
 34. H.-M. Chang, M. González-Alonso, J. Martin Camalich, Nonstandard semileptonic hyperon decays. *Phys. Rev. Lett.* **114**, 161802 (2015). <https://doi.org/10.1103/PhysRevLett.114.161802>. [arXiv:1412.8484](https://arxiv.org/abs/1412.8484)
 35. G.B. Tupper, T.R. Grose, M.A. Samuel, Two photon exchange effect in radiative corrections to $\pi^0 \rightarrow \gamma e^- e^+$. *Phys. Rev. D* **28**, 2905 (1983). <https://doi.org/10.1103/PhysRevD.28.2905>
 36. T. Husek, K. Kampf, J. Novotný, Radiative corrections to the Dalitz decay $\pi^0 \rightarrow e^+ e^- \gamma$ revisited. *Phys. Rev. D* **92**, 054027 (2015). <https://doi.org/10.1103/PhysRevD.92.054027>. [arXiv:1504.06178](https://arxiv.org/abs/1504.06178)
 37. T. Husek, K. Kampf, S. Leupold, J. Novotný, Radiative corrections to the $\eta^{(\prime)}$ Dalitz decays. *Phys. Rev. D* **97**, 096013 (2018). <https://doi.org/10.1103/PhysRevD.97.096013>. [arXiv:1711.11001](https://arxiv.org/abs/1711.11001)
 38. T. Husek, S. Leupold, Radiative corrections for the decay $\Sigma^0 \rightarrow L e^+ e^-$. *Eur. Phys. J. C* **80**, 218 (2020). <https://doi.org/10.1140/epjc/s10052-020-7710-7>. [arXiv:1911.02571](https://arxiv.org/abs/1911.02571)
 39. A. Crivellin, G. D'Ambrosio, M. Hoferichter, L.C. Tunstall, Violation of lepton flavor and lepton flavor universality in rare kaon decays. *Phys. Rev. D* **93**, 074038 (2016). <https://doi.org/10.1103/PhysRevD.93.074038>. [arXiv:1601.00970](https://arxiv.org/abs/1601.00970)
 40. Particle Data Group Collaboration, Review of particle physics. *PTEP* **2022**, 083C01 (2022). <https://doi.org/10.1093/ptep/ptac097>

41. V. Cirigliano, M. Knecht, H. Neufeld, H. Rupertsberger, P. Talavera, Radiative corrections to $K_{\ell 3}$ decays. *Eur. Phys. J. C* **23**, 121 (2002). <https://doi.org/10.1007/s100520100825>. [arXiv:hep-ph/0110153](https://arxiv.org/abs/hep-ph/0110153)
42. V. Cirigliano, H. Neufeld, H. Pichl, K_{e3} decays and CKM unitarity. *Eur. Phys. J. C* **35**, 53 (2004). <https://doi.org/10.1140/epjc/s2004-01745-1>. [arXiv:hep-ph/0401173](https://arxiv.org/abs/hep-ph/0401173)
43. V. Cirigliano, M. Giannotti, H. Neufeld, Electromagnetic effects in $K_{\ell 3}$ decays. *JHEP* **11**, 006 (2008). <https://doi.org/10.1088/1126-6708/2008/11/006>. [arXiv:0807.4507](https://arxiv.org/abs/0807.4507)
44. NA62 Collaboration, A study of the $K^+ \rightarrow \pi^0 e^+ \nu \gamma$ decay. *JHEP* **09**, 040 (2023). [https://doi.org/10.1007/JHEP09\(2023\)040](https://doi.org/10.1007/JHEP09(2023)040). [arXiv:2304.12271](https://arxiv.org/abs/2304.12271)
45. H.W. Fearing, E. Fischbach, J. Smith, Soft-photon theorems and radiative K_{l3} decays. *Phys. Rev. Lett.* **24**, 189 (1970). <https://doi.org/10.1103/PhysRevLett.24.189>
46. J. Bijnens, G. Ecker, J. Gasser, Radiative semileptonic kaon decays. *Nucl. Phys. B* **396**, 81 (1993). [https://doi.org/10.1016/0550-3213\(93\)90259-R](https://doi.org/10.1016/0550-3213(93)90259-R). [arXiv:hep-ph/9209261](https://arxiv.org/abs/hep-ph/9209261)
47. B. Kubis, R. Schmidt, Radiative corrections in $K \rightarrow \pi \ell^+ \ell^-$ decays. *Eur. Phys. J. C* **70**, 219 (2010). <https://doi.org/10.1140/epjc/s10052-010-1442-z>. [arXiv:1007.1887](https://arxiv.org/abs/1007.1887)
48. B.R. Holstein, Radiative K_{l3} decays and chiral symmetry. *Phys. Rev. D* **41**, 2829 (1990). <https://doi.org/10.1103/PhysRevD.41.2829>
49. G. Buchalla, A.J. Buras, M.E. Lautenbacher, Weak decays beyond leading logarithms. *Rev. Mod. Phys.* **68**, 1125 (1996). <https://doi.org/10.1103/RevModPhys.68.1125>. [arXiv:hep-ph/9512380](https://arxiv.org/abs/hep-ph/9512380)
50. G. Buchalla, A.J. Buras, The rare decays $K \rightarrow \pi \nu \bar{\nu}$, $B \rightarrow X \nu \bar{\nu}$ and $B \rightarrow l^+ l^-$: an update. *Nucl. Phys. B* **548**, 309 (1999). [https://doi.org/10.1016/S0550-3213\(99\)00149-2](https://doi.org/10.1016/S0550-3213(99)00149-2). [arXiv:hep-ph/9901288](https://arxiv.org/abs/hep-ph/9901288)
51. M. Misiak, J. Urban, QCD corrections to FCNC decays mediated by Z penguins and W boxes. *Phys. Lett. B* **451**, 161 (1999). [https://doi.org/10.1016/S0370-2693\(99\)00150-1](https://doi.org/10.1016/S0370-2693(99)00150-1). [arXiv:hep-ph/9901278](https://arxiv.org/abs/hep-ph/9901278)
52. J. Brod, M. Gorbahn, E. Stamou, Two-loop electroweak corrections for the $K \rightarrow \pi \nu \bar{\nu}$ decays. *Phys. Rev. D* **83**, 034030 (2011). <https://doi.org/10.1103/PhysRevD.83.034030>. [arXiv:1009.0947](https://arxiv.org/abs/1009.0947)
53. M. Gorbahn, E. Stamou, H. Yu et al., $K^+ \rightarrow \pi^+ \nu \bar{\nu}$ at NNLO in QCD (in preparation)
54. J. Brod, M. Gorbahn, E. Stamou, Updated standard model prediction for $K \rightarrow \pi \nu \bar{\nu}$ and ϵ_K . *PoS BEAUTY2020*, 056 (2021). <https://doi.org/10.22323/1.391.0056>. [arXiv:2105.02868](https://arxiv.org/abs/2105.02868)
55. A.J. Buras, M. Gorbahn, U. Haisch, U. Nierste, Charm quark contribution to $K^+ \rightarrow \pi^+ \nu \bar{\nu}$ at next-to-next-to-leading order. *JHEP* **11**, 002 (2006). <https://doi.org/10.1088/1126-6708/2006/11/002>. [arXiv:hep-ph/0603079](https://arxiv.org/abs/hep-ph/0603079)
56. J. Brod, M. Gorbahn, Electroweak corrections to the charm quark contribution to $K^+ \rightarrow \pi^+ \nu \bar{\nu}$. *Phys. Rev. D* **78**, 034006 (2008). <https://doi.org/10.1103/PhysRevD.78.034006>. [arXiv:0805.4119](https://arxiv.org/abs/0805.4119)
57. G. Isidori, F. Mescia, C. Smith, Light-quark loops in $K \rightarrow \pi \nu \bar{\nu}$. *Nucl. Phys. B* **718**, 319 (2005). <https://doi.org/10.1016/j.nuclphysb.2005.04.008>. [arXiv:hep-ph/0503107](https://arxiv.org/abs/hep-ph/0503107)
58. F. Mescia, C. Smith, Improved estimates of rare K decay matrix-elements from K_{l3} decays. *Phys. Rev. D* **76**, 034017 (2007). <https://doi.org/10.1103/PhysRevD.76.034017>. [arXiv:0705.2025](https://arxiv.org/abs/0705.2025)
59. J. Bijnens, K. Ghorbani, Isospin breaking in $K\pi$ vector form-factors for the weak and rare decays $K_{\ell 3}$, $K \rightarrow \pi \nu \bar{\nu}$ and $K \rightarrow \pi \ell^+ \ell^-$. [arXiv:0711.0148](https://arxiv.org/abs/0711.0148)
60. A. Hocker, H. Lacker, S. Laplace, F. Le Diberder, A New approach to a global fit of the CKM matrix. *Eur. Phys. J. C* **21**, 225 (2001). <https://doi.org/10.1007/s100520100729>. [arXiv:hep-ph/0104062](https://arxiv.org/abs/hep-ph/0104062)
61. UTfit Collaboration, The 2004 UTfit collaboration report on the status of the unitarity triangle in the standard model. *JHEP* **07**, 028 (2005). <https://doi.org/10.1088/1126-6708/2005/07/028>. [arXiv:hep-ph/0501199](https://arxiv.org/abs/hep-ph/0501199)
62. A.J. Buras, E. Venturini, Searching for new physics in rare K and B decays without $|V_{cb}|$ and $|V_{ub}|$ uncertainties. *Acta Phys. Pol. B* **53**, 6 (2021). <https://doi.org/10.5506/APhysPolB.53.6-A1>. [arXiv:2109.11032](https://arxiv.org/abs/2109.11032)
63. A.J. Buras, E. Venturini, The exclusive vision of rare K and B decays and of the quark mixing in the standard model. *Eur. Phys. J. C* **82**, 615 (2022). <https://doi.org/10.1140/epjc/s10052-022-10583-8>. [arXiv:2203.11960](https://arxiv.org/abs/2203.11960)
64. J. Brod, M. Gorbahn, E. Stamou, Standard-model prediction of ϵ_K with manifest quark-mixing unitarity. *Phys. Rev. Lett.* **125**, 171803 (2020). <https://doi.org/10.1103/PhysRevLett.125.171803>. [arXiv:1911.06822](https://arxiv.org/abs/1911.06822)
65. J. Brod, S. Kvedaraitė, Z. Polonsky, Two-loop electroweak corrections to the top-quark contribution to ϵ_K . *JHEP* **12**, 198 (2021). [https://doi.org/10.1007/JHEP12\(2021\)198](https://doi.org/10.1007/JHEP12(2021)198). [arXiv:2108.00017](https://arxiv.org/abs/2108.00017)
66. J. Brod, S. Kvedaraitė, Z. Polonsky, A. Youssef, Electroweak corrections to the charm-top-quark contribution to ϵ_K . *JHEP* **12**, 014 (2022). [https://doi.org/10.1007/JHEP12\(2022\)014](https://doi.org/10.1007/JHEP12(2022)014). [arXiv:2207.07669](https://arxiv.org/abs/2207.07669)
67. M. Gorbahn, J. Sebastian, S. Kvedaraitė, B_K in SMOM at NNLO in QCD (in preparation)
68. G. Buchalla, A.J. Buras, $K \rightarrow \pi \nu \bar{\nu}$ and high precision determinations of the CKM matrix. *Phys. Rev. D* **54**, 6782 (1996). <https://doi.org/10.1103/PhysRevD.54.6782>. [arXiv:hep-ph/9607447](https://arxiv.org/abs/hep-ph/9607447)
69. T. Blum et al., $K \rightarrow \pi \pi \Delta I = 3/2$ decay amplitude in the continuum limit. *Phys. Rev. D* **91**, 074502 (2015). <https://doi.org/10.1103/PhysRevD.91.074502>. [arXiv:1502.00263](https://arxiv.org/abs/1502.00263)
70. RBC, UKQCD Collaboration, Standard model prediction for direct CP violation in $K \rightarrow \pi \pi$ decay. *Phys. Rev. Lett.* **115**, 212001 (2015). <https://doi.org/10.1103/PhysRevLett.115.212001>. [arXiv:1505.07863](https://arxiv.org/abs/1505.07863)
71. Z. Bai et al., Erratum: Standard-model prediction for direct CP violation in $K \rightarrow \pi \pi$ decay. [arXiv:1603.03065](https://arxiv.org/abs/1603.03065)
72. RBC, UKQCD Collaboration, Direct CP violation and the $\Delta I = 1/2$ rule in $K \rightarrow \pi \pi$ decay from the standard model. *Phys. Rev. D* **102**, 054509 (2020). <https://doi.org/10.1103/PhysRevD.102.054509>. [arXiv:2004.09440](https://arxiv.org/abs/2004.09440)
73. NA48 Collaboration, A precision measurement of direct CP violation in the decay of neutral kaons into two pions. *Phys. Lett. B* **544**, 97 (2002). [https://doi.org/10.1016/S0370-2693\(02\)02476-0](https://doi.org/10.1016/S0370-2693(02)02476-0). [arXiv:hep-ex/0208009](https://arxiv.org/abs/hep-ex/0208009)
74. KTeV Collaboration, Precise measurements of direct CP violation, CPT symmetry, and other parameters in the neutral kaon system. *Phys. Rev. D* **83**, 092001 (2011). <https://doi.org/10.1103/PhysRevD.83.092001>. [arXiv:1011.0127](https://arxiv.org/abs/1011.0127)
75. V. Cirigliano, H. Gisbert, A. Pich, A. Rodríguez-Sánchez, Isospin-violating contributions to ϵ'/ϵ . *JHEP* **02**, 032 (2020). [https://doi.org/10.1007/JHEP02\(2020\)032](https://doi.org/10.1007/JHEP02(2020)032). [arXiv:1911.01359](https://arxiv.org/abs/1911.01359)
76. W.A. Bardeen, A.J. Buras, J.M. Gérard, A consistent analysis of the Delta I = 1/2 rule for K decays. *Phys. Lett. B* **192**, 138 (1987). [https://doi.org/10.1016/0370-2693\(87\)91156-7](https://doi.org/10.1016/0370-2693(87)91156-7)
77. A.J. Buras, J.-M. Gérard, W.A. Bardeen, Large N approach to kaon decays and mixing 28 years later: $\Delta I = 1/2$ rule, \hat{B}_K and ΔM_K . *Eur. Phys. J. C* **74**, 2871 (2014). <https://doi.org/10.1140/epjc/s10052-014-2871-x>. [arXiv:1401.1385](https://arxiv.org/abs/1401.1385)
78. A.J. Buras, ϵ'/ϵ in the standard model and beyond: 2021, in *11th International Workshop on the CKM Unitarity Triangle* (2022). [arXiv:2203.12632](https://arxiv.org/abs/2203.12632)
79. A.J. Buras, *Kaon Theory: 50 Years Later* (2023). [arXiv:2307.15737](https://arxiv.org/abs/2307.15737)
80. V. Cirigliano, H. Gisbert, A. Pich, A. Rodríguez-Sánchez, Theoretical status of ϵ'/ϵ . *J. Phys. Conf. Ser.* **1526**, 012011 (2020). <https://doi.org/10.1088/1742-6596/1526/1/012011>. [arXiv:1912.04736](https://arxiv.org/abs/1912.04736)

81. RBC, UKQCD Collaboration, Long distance contribution to the K_L - K_S mass difference. *Phys. Rev. D* **88**, 014508 (2013). <https://doi.org/10.1103/PhysRevD.88.014508>. arXiv:1212.5931
82. Z. Bai, N.H. Christ, T. Izubuchi, C.T. Sachrajda, A. Soni, J. Yu, $K_L - K_S$ mass difference from lattice QCD. *Phys. Rev. Lett.* **113**, 112003 (2014). <https://doi.org/10.1103/PhysRevLett.113.112003>. arXiv:1406.0916
83. Z. Bai, N.H. Christ, C.T. Sachrajda, The K_L - K_S mass difference. EPJ Web Conf. **175**, 13017 (2018). <https://doi.org/10.1051/epjconf/201817513017>
84. N.H. Christ, Z. Bai, Computing the long-distance contributions to ϵ_K . PoS **LATTICE2015**, 342 (2016). <https://doi.org/10.22323/1.251.0342>
85. Z. Bai, N.H. Christ, J.M. Karpie, C.T. Sachrajda, A. Soni, B. Wang, Long-distance contribution to ϵ_K from lattice QCD. arXiv:2309.01193
86. G. Isidori, G. Martinelli, P. Turchetti, Rare kaon decays on the lattice. *Phys. Lett. B* **633**, 75 (2006). <https://doi.org/10.1016/j.physletb.2005.11.044>. arXiv:hep-lat/0506026
87. RBC, UKQCD Collaboration, Prospects for a lattice computation of rare kaon decay amplitudes: $K \rightarrow \pi \ell^+ \ell^-$ decays. *Phys. Rev. D* **92**, 094512 (2015). <https://doi.org/10.1103/PhysRevD.92.094512>. arXiv:1507.03094
88. N.H. Christ, X. Feng, A. Jüttner, A. Lawson, A. Portelli, C.T. Sachrajda, First exploratory calculation of the long-distance contributions to the rare kaon decays $K \rightarrow \pi \ell^+ \ell^-$. *Phys. Rev. D* **94**, 114516 (2016). <https://doi.org/10.1103/PhysRevD.94.114516>. arXiv:1608.07585
89. RBC, UKQCD Collaboration, Simulating rare kaon decays $K^+ \rightarrow \pi^+ \ell^+ \ell^-$ using domain wall lattice QCD with physical light quark masses. *Phys. Rev. D* **107**, L011503 (2023). <https://doi.org/10.1103/PhysRevD.107.L011503>. arXiv:2202.08795
90. RBC, UKQCD Collaboration, Prospects for a lattice computation of rare kaon decay amplitudes II $K \rightarrow \pi \nu \bar{\nu}$ decays. *Phys. Rev. D* **93**, 114517 (2016). <https://doi.org/10.1103/PhysRevD.93.114517>. arXiv:1605.04442
91. Z. Bai, N.H. Christ, X. Feng, A. Lawson, A. Portelli, C.T. Sachrajda, Exploratory lattice QCD study of the rare kaon decay $K^+ \rightarrow \pi^+ \nu \bar{\nu}$. *Phys. Rev. Lett.* **118**, 252001 (2017). <https://doi.org/10.1103/PhysRevLett.118.252001>. arXiv:1701.02858
92. Z. Bai, N.H. Christ, X. Feng, A. Lawson, A. Portelli, C.T. Sachrajda, $K^+ \rightarrow \pi^+ \nu \bar{\nu}$ decay amplitude from lattice QCD. *Phys. Rev. D* **98**, 074509 (2018). <https://doi.org/10.1103/PhysRevD.98.074509>. arXiv:1806.11520
93. RBC, UKQCD Collaboration, Lattice QCD study of the rare kaon decay $K^+ \rightarrow \pi^+ \nu \bar{\nu}$ at a near-physical pion mass. *Phys. Rev. D* **100**, 114506 (2019). <https://doi.org/10.1103/PhysRevD.100.114506>. arXiv:1910.10644
94. V. Cirigliano, G. Ecker, H. Neufeld, A. Pich, J. Portolés, Kaon decays in the standard model. *Rev. Mod. Phys.* **84**, 399 (2012). <https://doi.org/10.1103/RevModPhys.84.399>. arXiv:1107.6001
95. N.H. Christ, X. Feng, L. Jin, C. Tu, Y. Zhao, Lattice QCD calculation of the two-photon contributions to $K_L \rightarrow \mu^+ \mu^-$ and $\pi^0 \rightarrow e^+ e^-$ decays. PoS **LATTICE2019**, 128 (2020). <https://doi.org/10.22323/1.363.0128>
96. N. Christ, X. Feng, L. Jin, C. Tu, Y. Zhao, Lattice QCD calculation of $\pi^0 \rightarrow e^+ e^-$ decay. *Phys. Rev. Lett.* **130**, 191901 (2023). <https://doi.org/10.1103/PhysRevLett.130.191901>. arXiv:2208.03834
97. Y. Zhao, N.H. Christ, Calculating $K \rightarrow \gamma \gamma$ using lattice QCD. PoS **LATTICE2021**, 451 (2022). <https://doi.org/10.22323/1.396.0451>
98. E.-H. Chao, N.H. Christ, X. Feng, L. Jin, $K_L \rightarrow \mu^+ \mu^-$ from lattice QCD. PoS **LATTICE2023**, 250 (2024). <https://doi.org/10.22323/1.453.0250>. arXiv:2312.01224
99. Flavour Lattice Averaging Group (FLAG) Collaboration, FLAG review 2021. *Eur. Phys. J. C* **82**, 869 (2022). <https://doi.org/10.1140/epjc/s10052-022-10536-1>. arXiv:2111.09849
100. M. Hayakawa, S. Uno, QED in finite volume and finite size scaling effect on electromagnetic properties of hadrons. *Prog. Theor. Phys.* **120**, 413 (2008). <https://doi.org/10.1143/PTP.120.413>. arXiv:0804.2044
101. M.G. Endres, A. Shindler, B.C. Tiburzi, A. Walker-Loud, Massive photons: an infrared regularization scheme for lattice QCD+QED. *Phys. Rev. Lett.* **117**, 072002 (2016). <https://doi.org/10.1103/PhysRevLett.117.072002>. arXiv:1507.08916
102. A.S. Kronfeld, U.J. Wiese, SU(N) gauge theories with C periodic boundary conditions. I. Topological structure. *Nucl. Phys. B* **357**, 521 (1991). [https://doi.org/10.1016/0550-3213\(91\)90479-H](https://doi.org/10.1016/0550-3213(91)90479-H)
103. B. Lucini, A. Patella, A. Ramos, N. Tantalo, Charged hadrons in local finite-volume QED+QCD with C* boundary conditions. *JHEP* **02**, 076 (2016). [https://doi.org/10.1007/JHEP02\(2016\)076](https://doi.org/10.1007/JHEP02(2016)076). arXiv:1509.01636
104. X. Feng, L. Jin, QED self energies from lattice QCD without power-law finite-volume errors. *Phys. Rev. D* **100**, 094509 (2019). <https://doi.org/10.1103/PhysRevD.100.094509>. arXiv:1812.09817
105. N.H. Christ, X. Feng, L.-C. Jin, C.T. Sachrajda, T. Wang, Radiative corrections to leptonic decays using infinite-volume reconstruction. *Phys. Rev. D* **108**, 014501 (2023). <https://doi.org/10.1103/PhysRevD.108.014501>. arXiv:2304.08026
106. V. Cirigliano, A. Crivellin, M. Hoferichter, M. Moulson, Scrutinizing CKM unitarity with a new measurement of the $K_{\mu 3}/K_{\mu 2}$ branching fraction. *Phys. Lett. B* **838**, 137748 (2023). <https://doi.org/10.1016/j.physletb.2023.137748>. arXiv:2208.11707
107. N. Carrasco, V. Lubicz, G. Martinelli, C.T. Sachrajda, N. Tantalo, C. Tarantino et al., QED corrections to hadronic processes in lattice QCD. *Phys. Rev. D* **91**, 074506 (2015). <https://doi.org/10.1103/PhysRevD.91.074506>. arXiv:1502.00257
108. D. Giusti, V. Lubicz, G. Martinelli, C.T. Sachrajda, F. Sanfilippo, S. Simula et al., First lattice calculation of the QED corrections to leptonic decay rates. *Phys. Rev. Lett.* **120**, 072001 (2018). <https://doi.org/10.1103/PhysRevLett.120.072001>. arXiv:1711.06537
109. M. Di Carlo, D. Giusti, V. Lubicz, G. Martinelli, C.T. Sachrajda, F. Sanfilippo et al., Light-meson leptonic decay rates in lattice QCD+QED. *Phys. Rev. D* **100**, 034514 (2019). <https://doi.org/10.1103/PhysRevD.100.034514>. arXiv:1904.08731
110. P. Boyle et al., Isospin-breaking corrections to light-meson leptonic decays from lattice simulations at physical quark masses. *JHEP* **02**, 242 (2023). [https://doi.org/10.1007/JHEP02\(2023\)242](https://doi.org/10.1007/JHEP02(2023)242). arXiv:2211.12865
111. V. Cirigliano, H. Neufeld, A note on isospin violation in $P_{\ell 2}(\gamma)$ decays. *Phys. Lett. B* **700**, 7 (2011). <https://doi.org/10.1016/j.physletb.2011.04.038>. arXiv:1102.0563
112. M. Di Carlo, Isospin-breaking corrections to weak decays: the current status and a new infrared improvement. PoS **LATTICE2023**, 120 (2024). <https://doi.org/10.22323/1.453.0120>. arXiv:2401.07666
113. M. Di Carlo, M.T. Hansen, N. Hermansson-Truedsson, A. Portelli, Structure-dependent electromagnetic finite-volume effects through order $1/L^3$. PoS **LATTICE2023**, 265 (2023). arXiv:2310.13358
114. C.T. Sachrajda, M. Di Carlo, G. Martinelli, D. Giusti, V. Lubicz, F. Sanfilippo et al., Radiative corrections to semileptonic decay rates. PoS **LATTICE2019**, 162 (2019). <https://doi.org/10.22323/1.363.0162>. arXiv:1910.07342
115. Y. Cai, Z. Davoudi, QED-corrected Lellouch-Lüscher formula for $K \rightarrow \pi \pi$ decay. PoS **LATTICE2018**, 280 (2018). <https://doi.org/10.22323/1.334.0280>. arXiv:1812.11015

116. N. Christ, X. Feng, Including electromagnetism in $K \rightarrow \pi\pi$ decay calculations. EPJ Web Conf. **175**, 13016 (2018). <https://doi.org/10.1051/epjconf/201817513016>. arXiv:1711.09339
117. N. Christ, X. Feng, J. Karpie, T. Nguyen, π - π scattering, QED, and finite-volume quantization. Phys. Rev. D **106**, 014508 (2022). <https://doi.org/10.1103/PhysRevD.106.014508>. arXiv:2111.04668
118. G. Ecker, A. Pich, E. de Rafael, $K \rightarrow \pi\ell^+\ell^-$ decays in the effective chiral Lagrangian of the standard model. Nucl. Phys. B **291**, 692 (1987). [https://doi.org/10.1016/0550-3213\(87\)90491-3](https://doi.org/10.1016/0550-3213(87)90491-3)
119. G. Ecker, A. Pich, E. de Rafael, Radiative kaon decays and CP violation in chiral perturbation theory. Nucl. Phys. B **303**, 665 (1988). [https://doi.org/10.1016/0550-3213\(88\)90425-7](https://doi.org/10.1016/0550-3213(88)90425-7)
120. G. Ecker, J. Gasser, A. Pich, E. de Rafael, The role of resonances in chiral perturbation theory. Nucl. Phys. B **321**, 311 (1989). [https://doi.org/10.1016/0550-3213\(89\)90346-5](https://doi.org/10.1016/0550-3213(89)90346-5)
121. V. Cirigliano, G. Ecker, M. Eidemüller, R. Kaiser, A. Pich, J. Portolés, Towards a consistent estimate of the chiral low-energy constants. Nucl. Phys. B **753**, 139 (2006). <https://doi.org/10.1016/j.nuclphysb.2006.07.010>. arXiv:hep-ph/0603205
122. J. Bijnens, G. Ecker, Mesonic low-energy constants. Annu. Rev. Nucl. Part. Sci. **64**, 149 (2014). <https://doi.org/10.1146/annurev-nucl-102313-025528>. arXiv:1405.6488
123. G. 't Hooft, A planar diagram theory for strong interactions. Nucl. Phys. B **72**, 461 (1974). [https://doi.org/10.1016/0550-3213\(74\)90154-0](https://doi.org/10.1016/0550-3213(74)90154-0)
124. A.J. Buras, J.M. Gérard, $1/N$ expansion for kaons. Nucl. Phys. B **264**, 371 (1986). [https://doi.org/10.1016/0550-3213\(86\)90489-X](https://doi.org/10.1016/0550-3213(86)90489-X)
125. A. Pich, E. de Rafael, Weak K amplitudes in the chiral and $1/N_c$ expansions. Phys. Lett. B **374**, 186 (1996). [https://doi.org/10.1016/0370-2693\(96\)00171-2](https://doi.org/10.1016/0370-2693(96)00171-2). arXiv:hep-ph/9511465
126. M. Knecht, S. Peris, E. de Rafael, The electroweak $\pi^+ - \pi^0$ mass difference and weak matrix elements in the $1/N_c$ expansion. Phys. Lett. B **443**, 255 (1998). [https://doi.org/10.1016/S0370-2693\(98\)01344-6](https://doi.org/10.1016/S0370-2693(98)01344-6). arXiv:hep-ph/9809594
127. J. Bijnens, J. Prades, ϵ'/ϵ in the chiral limit. JHEP **06**, 035 (2000). <https://doi.org/10.1088/1126-6708/2000/06/035>. arXiv:hep-ph/0005189
128. G. D'Ambrosio, D. Greynat, M. Knecht, On the amplitudes for the CP-conserving $K^\pm(K_S) \rightarrow \pi^\pm(\pi^0)\ell^+\ell^-$ rare decay modes. JHEP **02**, 049 (2019). [https://doi.org/10.1007/JHEP02\(2019\)049](https://doi.org/10.1007/JHEP02(2019)049). arXiv:1812.00735
129. G. D'Ambrosio, D. Greynat, M. Knecht, Matching long and short distances at order $\mathcal{O}(\alpha_s)$ in the form factors for $K \rightarrow \pi\ell^+\ell^-$. Phys. Lett. B **797**, 134891 (2019). <https://doi.org/10.1016/j.physletb.2019.134891>. arXiv:1906.03046
130. J.O. Eeg, K. Kumerički, I. Picek, On the short distance dispersive two photon $K_L \rightarrow \mu^+\mu^-$ amplitude. Eur. Phys. J. C **1**, 531 (1998). <https://doi.org/10.1007/s100520050102>. arXiv:hep-ph/9605337
131. G. D'Ambrosio, M. Knecht, S. Neshtapour, Work in progress
132. G. Colangelo, E. Passemar, P. Stoffer, A dispersive treatment of $K_{\ell 4}$ decays. Eur. Phys. J. C **75**, 172 (2015). <https://doi.org/10.1140/epjc/s10052-015-3357-1>. arXiv:1501.05627
133. W.J. Marciano, Precise determination of $|V_{us}|$ from lattice calculations of pseudoscalar decay constants. Phys. Rev. Lett. **93**, 231803 (2004). <https://doi.org/10.1103/PhysRevLett.93.231803>. arXiv:hep-ph/0402299
134. FlaviaNet Working Group on Kaon Decays Collaboration, An evaluation of $|V_{us}|$ and precise tests of the Standard Model from world data on leptonic and semileptonic kaon decays. Eur. Phys. J. C **69**, 399 (2010). <https://doi.org/10.1140/epjc/s10052-010-1406-3>. arXiv:1005.2323
135. V. Bernard, M. Oertel, E. Passemar, J. Stern, Tests of non-standard electroweak couplings of right-handed quarks. JHEP **01**, 015 (2008). <https://doi.org/10.1088/1126-6708/2008/01/015>. arXiv:0707.4194
136. V. Bernard, M. Oertel, E. Passemar, J. Stern, Dispersive representation and shape of the K_{J3} form factors: robustness. Phys. Rev. D **80**, 034034 (2009). <https://doi.org/10.1103/PhysRevD.80.034034>. arXiv:0903.1654
137. C.-Y. Seng, D. Galviz, M. Gorchtein, U.-G. Meißner, High-precision determination of the K_{e3} radiative corrections. Phys. Lett. B **820**, 136522 (2021). <https://doi.org/10.1016/j.physletb.2021.136522>. arXiv:2103.00975
138. C.-Y. Seng, D. Galviz, M. Gorchtein, U.-G. Meißner, Improved K_{e3} radiative corrections sharpen the $K_{\mu 2}-K_{e3}$ discrepancy. JHEP **11**, 172 (2021). [https://doi.org/10.1007/JHEP11\(2021\)172](https://doi.org/10.1007/JHEP11(2021)172). arXiv:2103.04843
139. C.-Y. Seng, D. Galviz, M. Gorchtein, U.-G. Meißner, Complete theory of radiative corrections to $K_{\ell 3}$ decays and the V_{us} update. JHEP **07**, 071 (2022). [https://doi.org/10.1007/JHEP07\(2022\)071](https://doi.org/10.1007/JHEP07(2022)071). arXiv:2203.05217
140. E.P. Shabalin, Possibility of determining $\pi\pi$ -scattering phases from angular correlations in K_{e4} decay. JETP **44**, 765 (1963). <http://jetp.ras.ru/cgi-bin/e/index/e/17/2/p517?a=list>
141. N. Cabibbo, A. Maksymowicz, Angular correlations in K_{e4} decays and determination of low-energy $\pi - \pi$ phase shifts. Phys. Rev. **137**, B438 (1965). <https://doi.org/10.1103/PhysRev.137.B438>
142. NA48/2 Collaboration, Precise tests of low energy QCD from K_{e4} decay properties. Eur. Phys. J. C **70**, 635 (2010). <https://doi.org/10.1140/epjc/s10052-010-1480-6>
143. B. Ananthanarayan, G. Colangelo, J. Gasser, H. Leutwyler, Roy equation analysis of $\pi\pi$ scattering. Phys. Rep. **353**, 207 (2001). [https://doi.org/10.1016/S0370-1573\(01\)00009-6](https://doi.org/10.1016/S0370-1573(01)00009-6). arXiv:hep-ph/0005297
144. G. Colangelo, J. Gasser, H. Leutwyler, The $\pi\pi$ S-wave scattering lengths. Phys. Lett. B **488**, 261 (2000). [https://doi.org/10.1016/S0370-2693\(00\)00898-4](https://doi.org/10.1016/S0370-2693(00)00898-4). arXiv:hep-ph/0007112
145. G. Colangelo, J. Gasser, A. Rusetsky, Isospin breaking in K_{I4} decays. Eur. Phys. J. C **59**, 777 (2009). <https://doi.org/10.1140/epjc/s10052-008-0818-9>. arXiv:0811.0775
146. V. Bernard, S. Descotes-Genon, M. Knecht, Isospin breaking in the phases of the K_{e4} form factors. Eur. Phys. J. C **73**, 2478 (2013). <https://doi.org/10.1140/epjc/s10052-013-2478-7>. arXiv:1305.3843
147. BNL-E865 Collaboration, A new measurement of K_{e4}^+ decay and the s-wave $\pi\pi$ -scattering length a_0^0 . Phys. Rev. Lett. **87**, 221801 (2001). <https://doi.org/10.1103/PhysRevLett.105.019901>. arXiv:hep-ex/0106071
148. S. Pislak et al., High statistics measurement of K_{e4} decay properties. Phys. Rev. D **67**, 072004 (2003). <https://doi.org/10.1103/PhysRevD.67.072004>. arXiv:hep-ex/0301040
149. NA48/2 Collaboration, New measurement of the charged kaon semileptonic $K^\pm \rightarrow \pi^+\pi^-e^\pm\nu$ (K_{e4}) decay branching ratio and hadronic form factors. Phys. Lett. B **715**, 105 (2012). <https://doi.org/10.1016/j.physletb.2012.07.048>. arXiv:1206.7065
150. J. Bijnens, G. Colangelo, J. Gasser, K_{I4} decays beyond one loop. Nucl. Phys. B **427**, 427 (1994). [https://doi.org/10.1016/0550-3213\(94\)90634-3](https://doi.org/10.1016/0550-3213(94)90634-3). arXiv:hep-ph/9403390
151. G. Amoros, J. Bijnens, P. Talavera, $K_{\ell 4}$ form-factors and $\pi - \pi$ scattering. Nucl. Phys. B **585**, 293 (2000). [https://doi.org/10.1016/S0550-3213\(00\)00366-7](https://doi.org/10.1016/S0550-3213(00)00366-7). arXiv:hep-ph/0003258
152. J. Stern, H. Sazdjian, N.H. Fuchs, What $\pi - \pi$ scattering tells us about chiral perturbation theory. Phys. Rev. D **47**, 3814 (1993). <https://doi.org/10.1103/PhysRevD.47.3814>. arXiv:hep-ph/9301244
153. B. Ananthanarayan, P. Büttiker, Comparison of πK scattering in $SU(3)$ chiral perturbation theory and dispersion rela-

- tions. Eur. Phys. J. C **19**, 517 (2001). <https://doi.org/10.1007/s100520100629>. arXiv:hep-ph/0012023
154. I. Caprini, G. Colangelo, H. Leutwyler, Regge analysis of the $\pi\pi$ scattering amplitude. Eur. Phys. J. C **72**, 1860 (2012). <https://doi.org/10.1140/epjc/s10052-012-1860-1>. arXiv:1111.7160
 155. P. Büttiker, S. Descotes-Genon, B. Moussallam, A new analysis of πK scattering from Roy and Steiner type equations. Eur. Phys. J. C **33**, 409 (2004). <https://doi.org/10.1140/epjc/s2004-01591-1>. arXiv:hep-ph/0310283
 156. D.R. Boito, R. Escribano, M. Jamin, $K\pi$ vector form factor constrained by $\tau \rightarrow K\pi\nu_\tau$ and K_{J3} decays. JHEP **09**, 031 (2010). [https://doi.org/10.1007/JHEP09\(2010\)031](https://doi.org/10.1007/JHEP09(2010)031). arXiv:1007.1858
 157. C.G. Callan, S.B. Treiman, Equal time commutators and K meson decays. Phys. Rev. Lett. **16**, 153 (1966). <https://doi.org/10.1103/PhysRevLett.16.153>
 158. S. Weinberg, Current commutator calculation of the $K_{\ell 4}$ form factors. Phys. Rev. Lett. **17**, 336 (1966). <https://doi.org/10.1103/PhysRevLett.17.336>
 159. P. Stoffer, Isospin breaking effects in $K_{\ell 4}$ decays. Eur. Phys. J. C **74**, 2749 (2014). <https://doi.org/10.1140/epjc/s10052-014-2749-y>. arXiv:1312.2066
 160. G. Colangelo, S. Lanz, H. Leutwyler, E. Passemar, Dispersive analysis of $\eta \rightarrow 3\pi$. Eur. Phys. J. C **78**, 947 (2018). <https://doi.org/10.1140/epjc/s10052-018-6377-9>. arXiv:1807.11937
 161. K. Kampf, B. Moussallam, Chiral expansions of the π^0 lifetime. Phys. Rev. D **79**, 076005 (2009). <https://doi.org/10.1103/PhysRevD.79.076005>. arXiv:0901.4688
 162. J. Gasser, G.R.S. Zarnauskas, On the pion decay constant. Phys. Lett. B **693**, 122 (2010). <https://doi.org/10.1016/j.physletb.2010.08.021>. arXiv:1008.3479
 163. J. McDonough et al., New searches for the C noninvariant decay $\pi^0 \rightarrow 3\gamma$ and the rare decay $\pi^0 \rightarrow 4\gamma$. Phys. Rev. D **38**, 2121 (1988). <https://doi.org/10.1103/PhysRevD.38.2121>
 164. NA62 Collaboration, Forbidden kaon and pion decays in NA62. PoS KAON13, 013 (2013). <https://doi.org/10.22323/1.181.0013>. arXiv:1306.3361
 165. NA62 Collaboration, Search for production of an invisible dark photon in π^0 decays. JHEP **05**, 182 (2019). [https://doi.org/10.1007/JHEP05\(2019\)182](https://doi.org/10.1007/JHEP05(2019)182). arXiv:1903.08767
 166. H. Akdag, B. Kubis, A. Wirzba, C and CP violation in effective field theories. JHEP **06**, 154 (2023). [https://doi.org/10.1007/JHEP06\(2023\)154](https://doi.org/10.1007/JHEP06(2023)154). arXiv:2212.07794
 167. T. Aoyama et al., The anomalous magnetic moment of the muon in the Standard Model. Phys. Rep. **887**, 1 (2020). <https://doi.org/10.1016/j.physrep.2020.07.006>. arXiv:2006.04822
 168. G. Colangelo et al., Prospects for precise predictions of a_μ in the Standard Model. arXiv:2203.15810
 169. PrimEx-II Collaboration, Precision measurement of the neutral pion lifetime. Science **368**, 506 (2020). <https://doi.org/10.1126/science.aay6641>
 170. KTeV Collaboration, Measurement of the rare decay $\pi^0 \rightarrow e^+e^-$. Phys. Rev. D **75**, 012004 (2007). <https://doi.org/10.1103/PhysRevD.75.012004>. arXiv:hep-ex/0610072
 171. P. Vařko, J. Novotný, Two-loop QED radiative corrections to the decay $\pi^0 \rightarrow e^+e^-$: the virtual corrections and soft-photon bremsstrahlung. JHEP **10**, 122 (2011). [https://doi.org/10.1007/JHEP10\(2011\)122](https://doi.org/10.1007/JHEP10(2011)122). arXiv:1106.5956
 172. T. Husek, K. Kampf, J. Novotný, Rare decay $\pi^0 \rightarrow e^+e^-$: on corrections beyond the leading order. Eur. Phys. J. C **74**, 3010 (2014). <https://doi.org/10.1140/epjc/s10052-014-3010-4>. arXiv:1405.6927
 173. T. Husek, E. Goudzovski, K. Kampf, Precise determination of the branching ratio of the neutral-pion Dalitz decay. Phys. Rev. Lett. **122**, 022003 (2019). <https://doi.org/10.1103/PhysRevLett.122.022003>. arXiv:1809.01153
 174. M. Hoferichter, B.-L. Hoid, B. Kubis, J. Lüdtke, Improved Standard-Model prediction for $\pi^0 \rightarrow e^+e^-$. Phys. Rev. Lett. **128**, 172004 (2022). <https://doi.org/10.1103/PhysRevLett.128.172004>. arXiv:2105.04563
 175. M. Hoferichter, B. Kubis, S. Leupold, F. Niecknig, S.P. Schneider, Dispersive analysis of the pion transition form factor. Eur. Phys. J. C **74**, 3180 (2014). <https://doi.org/10.1140/epjc/s10052-014-3180-0>. arXiv:1410.4691
 176. M. Hoferichter, B.-L. Hoid, B. Kubis, S. Leupold, S.P. Schneider, Dispersion relation for hadronic light-by-light scattering: pion pole. JHEP **10**, 141 (2018). [https://doi.org/10.1007/JHEP10\(2018\)141](https://doi.org/10.1007/JHEP10(2018)141). arXiv:1808.04823
 177. M. Hoferichter, B.-L. Hoid, B. Kubis, S. Leupold, S.P. Schneider, Pion-pole contribution to hadronic light-by-light scattering in the anomalous magnetic moment of the muon. Phys. Rev. Lett. **121**, 112002 (2018). <https://doi.org/10.1103/PhysRevLett.121.112002>. arXiv:1805.01471
 178. A. Dery, M. Ghosh, Y. Grossman, S. Schacht, $K \rightarrow \mu^+\mu^-$ as a clean probe of short-distance physics. JHEP **07**, 103 (2021). [https://doi.org/10.1007/JHEP07\(2021\)103](https://doi.org/10.1007/JHEP07(2021)103). arXiv:2104.06427
 179. J. Brod, E. Stamou, Impact of indirect CP violation on $\text{Br}(K_S \rightarrow \mu^+\mu^-)_{I=0}$. JHEP **05**, 155 (2023). [https://doi.org/10.1007/JHEP05\(2023\)155](https://doi.org/10.1007/JHEP05(2023)155). arXiv:2209.07445
 180. G. D'Ambrosio, T. Kitahara, Direct CP violation in $K \rightarrow \mu^+\mu^-$. Phys. Rev. Lett. **119**, 201802 (2017). <https://doi.org/10.1103/PhysRevLett.119.201802>. arXiv:1707.06999
 181. A. Dery, M. Ghosh, $K \rightarrow \mu^+\mu^-$ beyond the standard model. JHEP **03**, 048 (2022). [https://doi.org/10.1007/JHEP03\(2022\)048](https://doi.org/10.1007/JHEP03(2022)048). arXiv:2112.05801
 182. A. Dery, M. Ghosh, Y. Grossman, T. Kitahara, S. Schacht, A precision relation between $\Gamma(K \rightarrow \mu^+\mu^-)(t)$ and $\text{B}(K_L \rightarrow \mu^+\mu^-)/\text{B}(K_L \rightarrow \gamma\gamma)$. JHEP **03**, 014 (2023). [https://doi.org/10.1007/JHEP03\(2023\)014](https://doi.org/10.1007/JHEP03(2023)014). arXiv:2211.03804
 183. D. Stamen, D. Hariharan, M. Hoferichter, B. Kubis, P. Stoffer, Kaon electromagnetic form factors in dispersion theory. Eur. Phys. J. C **82**, 432 (2022). <https://doi.org/10.1140/epjc/s10052-022-10348-3>. arXiv:2202.11106
 184. V. Cirigliano, W. Dekens, J. de Vries, M. Hoferichter, E. Mereghetti, Toward complete leading-order predictions for neutrinoless double β decay. Phys. Rev. Lett. **126**, 172002 (2021). <https://doi.org/10.1103/PhysRevLett.126.172002>. arXiv:2012.11602
 185. V. Cirigliano, W. Dekens, J. de Vries, M. Hoferichter, E. Mereghetti, Determining the leading-order contact term in neutrinoless double β decay. JHEP **05**, 289 (2021). [https://doi.org/10.1007/JHEP05\(2021\)289](https://doi.org/10.1007/JHEP05(2021)289). arXiv:2102.03371
 186. G. Buchalla, A.J. Buras, The rare decays $K^+ \rightarrow \pi^+\nu\bar{\nu}$ and $K_L \rightarrow \mu^+\mu^-$ beyond leading logarithms. Nucl. Phys. B **412**, 106 (1994). [https://doi.org/10.1016/0550-3213\(94\)90496-0](https://doi.org/10.1016/0550-3213(94)90496-0). arXiv:hep-ph/9308272
 187. M. Gorbahn, U. Haisch, Charm quark contribution to $K_L \rightarrow \mu^+\mu^-$ at next-to-next-to-leading order. Phys. Rev. Lett. **97**, 122002 (2006). <https://doi.org/10.1103/PhysRevLett.97.122002>. arXiv:hep-ph/0605203
 188. D. Gómez Dumm, A. Pich, Long distance contributions to the $K_L \rightarrow \mu^+\mu^-$ decay width. Phys. Rev. Lett. **80**, 4633 (1998). <https://doi.org/10.1103/PhysRevLett.80.4633>. arXiv:hep-ph/9801298
 189. S. Holz, J. Plenter, C.W. Xiao, T. Dato, C. Hanhart, B. Kubis et al., Towards an improved understanding of $\eta \rightarrow \gamma^*\gamma^*$. Eur. Phys. J. C **81**, 1002 (2021). <https://doi.org/10.1140/epjc/s10052-021-09661-0>. arXiv:1509.02194
 190. M. Zanke, M. Hoferichter, B. Kubis, On the transition form factors of the axial-vector resonance $f_1(1285)$ and its decay into e^+e^- . JHEP **07**, 106 (2021). [https://doi.org/10.1007/JHEP07\(2021\)106](https://doi.org/10.1007/JHEP07(2021)106). arXiv:2103.09829

191. M. Hoferichter, B. Kubis, M. Zanke, Axial-vector transition form factors and $e^+e^- \rightarrow f_1\pi^+\pi^-$. *JHEP* **08**, 209 (2023). [https://doi.org/10.1007/JHEP08\(2023\)209](https://doi.org/10.1007/JHEP08(2023)209). arXiv:2307.14413
192. M. Hoferichter, B.-L. Hoid, J. Ruiz de Elvira, Improved Standard-Model prediction for $K_L \rightarrow \ell^+\ell^-$. arXiv:2310.17689
193. G. Isidori, R. Unterdorfer, On the short distance constraints from $K_{L,S} \rightarrow \mu^+\mu^-$. *JHEP* **01**, 009 (2004). <https://doi.org/10.1088/1126-6708/2004/01/009>. arXiv:hep-ph/0311084
194. B.-L. Hoid, M. Hoferichter, J. Ruiz de Elvira, Comparing phenomenological estimates of dilepton decays of pseudoscalar mesons with lattice QCD. *PoS LATTICE2023*, 244 (2024). <https://doi.org/10.22323/1.453.0244>. arXiv:2312.00520
195. D.M. Straub, Anatomy of flavour-changing Z couplings in models with partial compositeness. *JHEP* **08**, 108 (2013). [https://doi.org/10.1007/JHEP08\(2013\)108](https://doi.org/10.1007/JHEP08(2013)108). arXiv:1302.4651
196. A.J. Buras, D. Buttazzo, R. Kneijens, $K \rightarrow \pi\nu\bar{\nu}$ and ε'/ε in simplified new physics models. *JHEP* **11**, 166 (2015). [https://doi.org/10.1007/JHEP11\(2015\)166](https://doi.org/10.1007/JHEP11(2015)166). arXiv:1507.08672
197. K. Ishiwata, Z. Ligeti, M.B. Wise, New vector-like fermions and flavor physics. *JHEP* **10**, 027 (2015). [https://doi.org/10.1007/JHEP10\(2015\)027](https://doi.org/10.1007/JHEP10(2015)027). arXiv:1506.03484
198. M. Bordone, D. Buttazzo, G. Isidori, J. Monnard, Probing lepton flavour universality with $K \rightarrow \pi\nu\bar{\nu}$ decays. *Eur. Phys. J. C* **77**, 618 (2017). <https://doi.org/10.1140/epjc/s10052-017-5202-1>. arXiv:1705.10729
199. S. Fajfer, N. Košnik, L. Vale Silva, Footprints of leptoquarks: from $R_{K^{(*)}}$ to $K \rightarrow \pi\nu\bar{\nu}$. *Eur. Phys. J. C* **78**, 275 (2018). <https://doi.org/10.1140/epjc/s10052-018-5757-5>. arXiv:1802.00786
200. R. Mandal, A. Pich, Constraints on scalar leptoquarks from lepton and kaon physics. *JHEP* **12**, 089 (2019). [https://doi.org/10.1007/JHEP12\(2019\)089](https://doi.org/10.1007/JHEP12(2019)089). arXiv:1908.11155
201. D. Marzocca, S. Trifinopoulos, E. Venturini, From B-meson anomalies to Kaon physics with scalar leptoquarks. *Eur. Phys. J. C* **82**, 320 (2022). <https://doi.org/10.1140/epjc/s10052-022-10271-7>. arXiv:2106.15630
202. O.L. Crosas, G. Isidori, J.M. Lizana, N. Selimovic, B.A. Stefanek, Flavor non-universal vector leptoquark imprints in $K \rightarrow \pi\nu\bar{\nu}$ and $\Delta F = 2$ transitions. *Phys. Lett. B* **835**, 137525 (2022). <https://doi.org/10.1016/j.physletb.2022.137525>. arXiv:2207.00018
203. J. Davighi, G. Isidori, Non-universal gauge interactions addressing the inescapable link between Higgs and flavour. *JHEP* **07**, 147 (2023). [https://doi.org/10.1007/JHEP07\(2023\)147](https://doi.org/10.1007/JHEP07(2023)147). arXiv:2303.01520
204. L. Allwicher, C. Cornella, B.A. Stefanek, G. Isidori, New physics in the third generation: a comprehensive SMEFT analysis and future prospects. *JHEP* **03**, 049 (2024). [https://doi.org/10.1007/JHEP03\(2024\)049](https://doi.org/10.1007/JHEP03(2024)049). arXiv:2311.00020
205. L. Calibbi, F. Goertz, D. Redigolo, R. Ziegler, J. Zupan, Minimal axion model from flavor. *Phys. Rev. D* **95**, 095009 (2017). <https://doi.org/10.1103/PhysRevD.95.095009>. arXiv:1612.08040
206. F. Wilczek, Axions and family symmetry breaking. *Phys. Rev. Lett.* **49**, 1549 (1982). <https://doi.org/10.1103/PhysRevLett.49.1549>
207. A. Davidson, K.C. Wali, Minimal flavor unification via multigenerational Peccei–Quinn symmetry. *Phys. Rev. Lett.* **48**, 11 (1982). <https://doi.org/10.1103/PhysRevLett.48.11>
208. J.L. Feng, T. Moroi, H. Murayama, E. Schnapka, Third generation familons, b factories, and neutrino cosmology. *Phys. Rev. D* **57**, 5875 (1998). <https://doi.org/10.1103/PhysRevD.57.5875>. arXiv:hep-ph/9709411
209. J.F. Kamenik, C. Smith, FCNC portals to the dark sector. *JHEP* **03**, 090 (2012). [https://doi.org/10.1007/JHEP03\(2012\)090](https://doi.org/10.1007/JHEP03(2012)090). arXiv:1111.6402
210. F. Björkeröth, E.J. Chun, S.F. King, Flavourful axion phenomenology. *JHEP* **08**, 117 (2018). [https://doi.org/10.1007/JHEP08\(2018\)117](https://doi.org/10.1007/JHEP08(2018)117). arXiv:1806.00660
211. J. Martin Camalich, M. Pospelov, P.N.H. Vuong, R. Ziegler, J. Zupan, Quark flavor phenomenology of the QCD axion. *Phys. Rev. D* **102**, 015023 (2020). <https://doi.org/10.1103/PhysRevD.102.015023>. arXiv:2002.04623
212. M. Bauer, M. Neubert, S. Renner, M. Schnubel, A. Thamm, Flavor probes of axion-like particles. *JHEP* **09**, 056 (2022). [https://doi.org/10.1007/JHEP09\(2022\)056](https://doi.org/10.1007/JHEP09(2022)056). arXiv:2110.10698
213. E. Goudzovski et al., New physics searches at kaon and hyperon factories. *Rep. Prog. Phys.* **86**, 016201 (2023). <https://doi.org/10.1088/1361-6633/ac9cee>. arXiv:2201.07805
214. J. Beacham et al., Physics beyond colliders at CERN: beyond the standard model working group report. *J. Phys. G* **47**, 010501 (2020). <https://doi.org/10.1088/1361-6471/ab4cd2>. arXiv:1901.09966
215. P. Harris, P. Schuster, J. Zupan, Snowmass White Paper: new flavors and rich structures in dark sectors, in *Snowmass 2021* (2022). arXiv:2207.08990
216. S. Gori et al., Dark sector physics at high-intensity experiments. arXiv:2209.04671
217. P. Ballett, M. Hostert, S. Pascoli, Dark neutrinos and a three portal connection to the standard model. *Phys. Rev. D* **101**, 115025 (2020). <https://doi.org/10.1103/PhysRevD.101.115025>. arXiv:1903.07589
218. A. Atre, T. Han, S. Pascoli, B. Zhang, The search for heavy Majorana neutrinos. *JHEP* **05**, 030 (2009). <https://doi.org/10.1088/1126-6708/2009/05/030>. arXiv:0901.3589
219. G. Krnjaic, G. Marques-Tavares, D. Redigolo, K. Tobioka, Probing muophilic force carriers and dark matter at kaon factories. *Phys. Rev. Lett.* **124**, 041802 (2020). <https://doi.org/10.1103/PhysRevLett.124.041802>. arXiv:1902.07715
220. NA62 Collaboration, Search for a feebly interacting particle X in the decay $K^+ \rightarrow \pi^+X$. *JHEP* **03**, 058 (2021). [https://doi.org/10.1007/JHEP03\(2021\)058](https://doi.org/10.1007/JHEP03(2021)058). arXiv:2011.11329
221. NA62 Collaboration, Search for π^0 decays to invisible particles. *JHEP* **02**, 201 (2021). [https://doi.org/10.1007/JHEP02\(2021\)201](https://doi.org/10.1007/JHEP02(2021)201). arXiv:2010.07644
222. NA62 Collaboration, Search for heavy neutral lepton production in K^+ decays to positrons. *Phys. Lett. B* **807**, 135599 (2020). <https://doi.org/10.1016/j.physletb.2020.135599>. arXiv:2005.09575
223. NA62 Collaboration, Search for K^+ decays to a muon and invisible particles. *Phys. Lett. B* **816**, 136259 (2021). <https://doi.org/10.1016/j.physletb.2021.136259>. arXiv:2101.12304
224. A.M. Abdullahi et al., The present and future status of heavy neutral leptons. *J. Phys. G* **50**, 020501 (2023). <https://doi.org/10.1088/1361-6471/ac98f9>. arXiv:2203.08039
225. PIENU Collaboration, Improved search for heavy neutrinos in the decay $\pi \rightarrow e\nu$. *Phys. Rev. D* **97**, 072012 (2018). <https://doi.org/10.1103/PhysRevD.97.072012>. arXiv:1712.03275
226. J.-L. Tastet, E. Goudzovski, I. Timiryasov, O. Ruchayskiy, Projected NA62 sensitivity to heavy neutral lepton production in $K^+ \rightarrow \pi^0 + N$ decays. *Phys. Rev. D* **104**, 055005 (2021). <https://doi.org/10.1103/PhysRevD.104.055005>. arXiv:2008.11654
227. NA48/2 Collaboration, Search for the dark photon in π^0 decays. *Phys. Lett. B* **746**, 178 (2015). <https://doi.org/10.1016/j.physletb.2015.04.068>. arXiv:1504.00607
228. NA62 Collaboration, Searches for lepton number violating K^+ decays. *Phys. Lett. B* **797**, 134794 (2019). <https://doi.org/10.1016/j.physletb.2019.07.041>. arXiv:1905.07770
229. NA62 Collaboration, Search for lepton number and flavor violation in K^+ and π^0 decays. *Phys. Rev. Lett.* **127**, 131802 (2021). <https://doi.org/10.1103/PhysRevLett.127.131802>. arXiv:2105.06759
230. NA62 Collaboration, Searches for lepton number violating $K^+ \rightarrow \pi^-(\pi^0)e^+e^+$ decays. *Phys. Lett. B* **830**,

- 137172 (2022). <https://doi.org/10.1016/j.physletb.2022.137172>. arXiv:2202.00331
231. NA62 Collaboration, A search for the $K^+ \rightarrow \mu^- \nu e^+ e^+$ decay. Phys. Lett. B **838**, 137679 (2023). <https://doi.org/10.1016/j.physletb.2023.137679>. arXiv:2211.04818
232. NA62 Collaboration, Search for K^+ decays into the $\pi^+ e^+ e^- e^+ e^-$ final state. Phys. Lett. B **846**, 138193 (2023). <https://doi.org/10.1016/j.physletb.2023.138193>. arXiv:2307.04579
233. R. Röntsch, M. Schulze, Constraining couplings of top quarks to the Z boson in $t\bar{t} + Z$ production at the LHC. JHEP **07**, 091 (2014). [https://doi.org/10.1007/JHEP09\(2015\)132](https://doi.org/10.1007/JHEP09(2015)132). arXiv:1404.1005
234. J. Brod, A. Greljo, E. Stamou, P. Uttayarat, Probing anomalous $t\bar{t}Z$ interactions with rare meson decays. JHEP **02**, 141 (2015). [https://doi.org/10.1007/JHEP02\(2015\)141](https://doi.org/10.1007/JHEP02(2015)141). arXiv:1408.0792
235. W. Buchmüller, D. Wyler, Effective Lagrangian analysis of new interactions and flavor conservation. Nucl. Phys. B **268**, 621 (1986). [https://doi.org/10.1016/0550-3213\(86\)90262-2](https://doi.org/10.1016/0550-3213(86)90262-2)
236. B. Grzadkowski, M. Iskrzyński, M. Misiak, J. Rosiek, Dimension-six terms in the standard model Lagrangian. JHEP **10**, 085 (2010). [https://doi.org/10.1007/JHEP10\(2010\)085](https://doi.org/10.1007/JHEP10(2010)085). arXiv:1008.4884
237. F. del Aguila, M. Pérez-Victoria, J. Santiago, Observable contributions of new exotic quarks to quark mixing. JHEP **09**, 011 (2000). <https://doi.org/10.1088/1126-6708/2000/09/011>. arXiv:hep-ph/0007316
238. ATLAS Collaboration, Measurement of t -channel production of single top quarks and antiquarks in pp collisions at 13 TeV using the full ATLAS Run 2 dataset (2023). <http://cds.cern.ch/record/2860644>
239. CMS Collaboration, Measurement of CKM matrix elements in single top quark t -channel production in proton–proton collisions at $\sqrt{s} = 13$ TeV. Phys. Lett. B **808**, 135609 (2020). <https://doi.org/10.1016/j.physletb.2020.135609>. arXiv:2004.12181
240. F.F. Deppisch, K. Fridell, J. Harz, Constraining lepton number violating interactions in rare kaon decays. JHEP **12**, 186 (2020). [https://doi.org/10.1007/JHEP12\(2020\)186](https://doi.org/10.1007/JHEP12(2020)186). arXiv:2009.04494
241. M. Gorbahn, U. Moldanazarova, K.H. Sieja, E. Stamou, M. Tabet, The anatomy of $K^+ \rightarrow \pi^+ \nu \bar{\nu}$ distributions. arXiv:2312.06494
242. M. Gorbahn, U. Moldanazarova, K.H. Sieja, E. Stamou, M. Tabet (in preparation)
243. R. Barbieri, G. Isidori, A. Pattori, F. Senia, Anomalies in B -decays and $U(2)$ flavour symmetry. Eur. Phys. J. C **76**, 67 (2016). <https://doi.org/10.1140/epjc/s10052-016-3905-3>. arXiv:1512.01560
244. A. Crivellin, C. Greub, D. Müller, F. Saturnino, Importance of loop effects in explaining the accumulated evidence for new physics in B decays with a vector leptoquark. Phys. Rev. Lett. **122**, 011805 (2019). <https://doi.org/10.1103/PhysRevLett.122.011805>. arXiv:1807.02068
245. X.-G. He, X.-D. Ma, G. Valencia, FCNC B and K meson decays with light bosonic Dark Matter. JHEP **03**, 037 (2023). [https://doi.org/10.1007/JHEP03\(2023\)037](https://doi.org/10.1007/JHEP03(2023)037). arXiv:2209.05223
246. V. Cirigliano, J. Jenkins, M. Gonzalez-Alonso, Semileptonic decays of light quarks beyond the Standard Model. Nucl. Phys. B **830**, 95 (2010). <https://doi.org/10.1016/j.nuclphysb.2009.12.020>. arXiv:0908.1754
247. M. González-Alonso, J. Martin Camalich, Global effective-field-theory analysis of new-physics effects in (semi)leptonic kaon decays. JHEP **12**, 052 (2016). [https://doi.org/10.1007/JHEP12\(2016\)052](https://doi.org/10.1007/JHEP12(2016)052). arXiv:1605.07114
248. V. Cirigliano, W. Dekens, J. de Vries, E. Mereghetti, T. Tong, Anomalies in global SMEFT analyses: a case study of first-row CKM unitarity. JHEP **03**, 033 (2024). [https://doi.org/10.1007/JHEP03\(2024\)033](https://doi.org/10.1007/JHEP03(2024)033). arXiv:2311.00021
249. Kaons@CERN (2023). <https://indico.cern.ch/event/1300660/>